

Effect of Membrane Weight on Vibrations of Air-Inflated Dams

by

Tony Duane Fagan

Thesis submitted to the Faculty of the
Virginia Polytechnic Institute and State University
in partial fulfillment of the requirements for the degree of
Master of Science
in
Civil Engineering

APPROVED:

Raymond H. Plaut, Chairman

Siegfried M. Holzer

Kamal B. Rojiani

March, 1987

Blacksburg, Virginia

Effect of Membrane Weight on Vibrations of Air-Inflated Dams

by

Tony Duane Fagan

Raymond H. Plaut, Chairman

Civil Engineering

(ABSTRACT)

Inflatable dams are flexible membrane structures, pressurized with either air, water, or both, which have been used in recent years as a means of temporarily impounding water. A number of procedures have been developed to investigate the static behavior of the dams, but the dynamic behavior has been largely neglected. The few studies that have been done on dynamic behavior have used the simplifying assumption that the weight of the membrane was negligible.

In this study, equations of equilibrium and equations of motion were derived for an air-inflated dam impounding no water, but loaded with its own membrane weight. It was assumed that the effect of membrane extensibility is negligible in the analysis. Derivatives required in the equations of motion were approximated using finite difference equations. Computer programs were written to find solutions for the eigenvalues and eigenvectors of the equations of motion. The computer program plotted the mode shapes of vibration associated with the four lowest eigenvalues, as well as the static shape of the dam. The eigenvalues obtained were the square of the frequencies of the system, so the effects of a series of membrane weights on the frequencies of dams of various base lengths could be analyzed.

Acknowledgements

I would like to thank Dr. Plaut for his willingness to help with difficult situations encountered in the research done in this project, and for his encouragement rendered to me throughout my graduate studies. Thanks also go to the National Science Foundation for their grant which made much of this study possible. Finally, I would like to thank Dr. Holzer and Dr. Rojiani for serving on my thesis committee.

Table of Contents

Chapter 1. Introduction	1
Chapter 2. Literature Review	3
2.1 Introduction	3
2.2 Anwar's Analysis	4
Static Analysis	4
Hydrodynamic Analysis	8
2.2 Binnie's Analysis	11
2.3 Parbery's Work	12
2.4 Watson's Work	17
2.5 Other Contributions	18
Chapter 3. The Static Analysis	21
3.1 Introduction	21
3.2 Derivation of the Static Equations	22
3.3 Solution of the Static Equations	27

Chapter 4. Analysis of the Dynamic Behavior	30
4.1 Introduction	30
4.2 The Dynamic Equations	31
4.3 Defining the Study Cases	35
4.4 Numerical Results	38
Chapter 5. Conclusions and Recommendations	54
5.1 Summary and Conclusions	54
5.2 Recommendations for Future Studies	56
Bibliography	57
Appendix A. The Equations of Motion	59
A.1. The Static Equations	59
A.2. Derivation of the Dynamic Equations	60
A.3 Approximation of Derivatives by Finite Differences	77
Approximations of the Derivatives of the Initial Angles	78
Approximations of the Derivatives of the Tangential Displacements	80
A.4 The Equations of Motion in Computer Form	83
Appendix B. The STATIC Computer Program	88
Appendix C. The ALPHA Program	95
Appendix D. The DYNAMIC Program	98
Vita	105

List of Illustrations

Figure 1.	Anwar's Diagram for an Air-Inflated Dam under Static Loading [1]	5
Figure 2.	Anwar's Results for Computed and Experimental Shapes [1]	7
Figure 3.	Anwar's Diagram for the Hydrodynamic Analysis [1]	9
Figure 4.	Diagram of an Air-Inflated Dam for the Static Case [21]	14
Figure 5.	Parbery's Computed Displacements Due to Weight [21]	16
Figure 6.	Cross-Section of an Air-Inflated Dam under Static Conditions	23
Figure 7.	Free Body Diagram of an Element of the Cross-Section	24
Figure 8.	Static Shapes for $P/q = 0.0$ and $P/q = 0.02$ for $B/S' = 0.40$	40
Figure 9.	Mode Shapes of Vibration for $B/S' = 0.40$ with $P/q = 0.0$	42
Figure 10.	Mode Shapes of Vibration for $B/S' = 0.40$ with $P/q = 0.001$	43
Figure 11.	Base Length versus Frequency for $P/q = 0.005$	47
Figure 12.	Base versus Frequency for $P/q = 0.0$ for a Range of Base Lengths	48
Figure 13.	Weight versus Frequency for the First Mode of Vibration	49
Figure 14.	Weight versus Frequency for the Second Mode of Vibration	50
Figure 15.	Weight versus Frequency for the Third Mode of Vibration	51
Figure 16.	Weight versus Frequency for the Fourth Mode of Vibration	52
Figure 17.	An Element of the Cross-Section with Dynamic Loading	61
Figure 18.	Original and Elongated Elements Used in Strain Relationship	64

List of Tables

Table 1. Base Length, Weight, and Tension for the Static Conditions	39
Table 2. Derivatives of the Initial Angle for $B/S' = 0.40$ with $P/q = 0.0$	41
Table 3. Eigenvectors for $B/S' = 0.40$ with $P/q = 0.0$	44
Table 4. Eigenvectors for $B/S' = 0.40$ with $P/q = 0.001$	45

Chapter 1. Introduction

Methods of temporarily impounding water have become increasingly important in recent years. In many areas, it is not uncommon to experience very limited stream flow during the majority of the year, while for short periods, excessive runoff exists. By capturing some of the flow, it is possible to store a portion of the temporary excess to be used in later dry periods. Temporary impounding or diversion of floodwaters is also of great importance, since with proper management of the situation, it is often possible to save lives, as well as property. Large dams made of concrete or earth are used for such purposes in many areas, but the use of such structures is often limited by economics and by the large amount of land required to accommodate the stored volume of water. Smaller structures such as dikes, levies, and sandbag dams have been used for the same purposes, but with varying degrees of effectiveness. All of these structures are basically permanent, with the exception of the sandbag, which is also the least efficient method. However, in 1956, a new type of structure capable of impounding water was introduced by N. M. Imbertson [22].

The structure consists of an inflated tube, constructed of a rubber coated, high strength fabric, which is firmly anchored to a reinforced concrete foundation. Inflation of the tube, often called an inflatable dam, is accomplished by using either air, water, or a combination of the two. Since the fabric has negligible bending stiffness, it is basically a membrane structure. The shape

taken by the structure to reach equilibrium varies according to the loading conditions, and changes as the loadings change. The method of inflation also affects the structure's shape.

Since the inflatable dam was introduced, it has been adapted to function in many capacities. Among the most important uses are controlling flood flow conditions, increasing the storage capacity of existing dams, and storing water for irrigation during dry months. They have also been used for recreational purposes, as locks for small boats, and as a means of preventing tidal water from contaminating fresh water with salt.

In general, the inflatable dam has been found to be very durable; however, some problems do exist. Several dams have collapsed, and it is believed that vibrations in the structure may have contributed in some of the occurrences. The static behavior of inflatable dams has been investigated and reported, but the dynamic analysis has been limited to a few investigations which neglected the membrane weight. In this thesis, the importance of the weight of the membrane as it affects the frequencies and modes of vibration of an air-inflated dam will be investigated. The case considered will include no external head, but Shepherd et al. [24] have shown that this is an important part of the overall analysis, since the dam will sometimes be tested under such conditions. It is believed that the knowledge of the effect of the weight on the mode shapes and on the frequencies of vibration will be of interest to future investigators of inflatable dams who consider the effect of external head on dynamic cases.

Chapter 2. Literature Review

2.1 Introduction

The inflatable dam was invented and patented in 1956 by Norman M. Imbertson as a way to impound water during periods of low flow, while allowing easy runoff during heavier flow conditions which could cause flooding [22]. It is basically used as a holding device for water under hydrostatic conditions [1], for such uses as flood control, increasing storage capacity at existing dams, tidal control to prevent salinity in coastal water supplies, and for recreation and wildlife management purposes. However, the collapse of the flexible, water-inflated dams at the Mangla Dam Project, Pakistan, in 1967 [4], and of the water-and-air-inflated Belmore Fabridam at the Belmore River, Australia, in 1969 [23], proved that new methods of analyzing inflatable dams were needed. The hydrodynamic conditions causing the collapse of these structures showed that such effects could cause major problems, so a dynamic analysis was needed.

2.2 Anwar's Analysis

Shortly before the collapse of the inflatable dam at the Mangla Dam Project, H. O. Anwar, the Principal Scientific Officer at the Hydraulics Research Station, Wallingford, Berks, England, reported the results of work completed at his installation [1]. He was the first to present techniques of hydrostatic analysis for both air and water inflated dams. His work also included the hydrodynamic analysis of an air-filled dam experiencing flow over its crest, and experimental work was conducted to check the accuracy of the formulated equations.

Static Analysis

For both the hydrostatic and the hydrodynamic analyses, Anwar assumed that the weight of the material was negligible and that the membrane was inextensible. Then, for the static case, it was assumed that the internal pressure on the dam was proportional to the total upstream depth,

$$p_i = \alpha \rho g H$$

where α is the proportionality factor, ρg is the specific weight of the water, and the other terms are as illustrated in Figure 1 on page 5. For the air-inflated dam, Anwar had shown that the downstream face would be a semicircular arc, so he used this property to find the horizontal force, T , acting on the dam, per unit width:

$$T = \frac{1}{2} \alpha \rho g H^2$$

Equations for the horizontal and the vertical component of the force at an arbitrary point, P , were found to be:

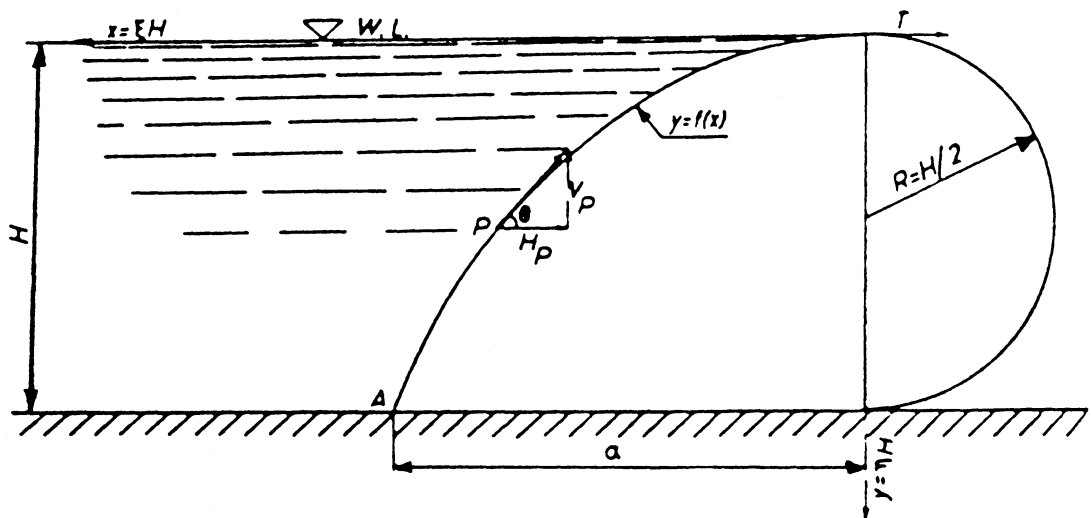


Figure 1. Anwar's Diagram for an Air-Inflated Dam under Static Loading [1]

$$H_p = \frac{1}{2}\alpha\rho gH^2 + \frac{1}{2}\rho gy^2 - \alpha\rho gHy$$

and

$$V_p = \rho g \int f(x) dx - \alpha\rho gHx$$

where $f(x)$ is an analytical function describing the shape of the dam. The two components of the force at a point can be related using the trigonometric function, tangent, such that

$$\tan \theta = y' = \frac{V_p}{H_p} = \frac{-2\int f(x) dx - 2\alpha Hx}{\alpha H^2 + y^2 - 2\alpha Hy}$$

This function can be differentiated with respect to x , and $y = f(x)$ can be used as the shape function, so the equation reduces to

$$(y^2 - 2\alpha Hy + \alpha H^2)y'' + 2(y - \alpha H)(y')^2 + 2(y - \alpha H)y = 0$$

with the boundary conditions $y(0) = y'(0) = 0$, since Anwar used the top of the dam as the origin of his coordinate system. After nondimensionalizing by using the upstream head level, H , and applying the boundary conditions, the resulting equation for the position of the x - coordinate of any point is:

$$\xi = \sqrt{2\alpha} \left\{ 2\hat{E}\left(\sqrt{\frac{\alpha}{2}}\right) - \hat{F}\left(\sqrt{\frac{\alpha}{2}}\right) - E\left[\arccos\left(\frac{\eta}{\alpha} - 1\right), \sqrt{\frac{\alpha}{2}}\right] + \frac{1}{2}F\left[\arccos\left(\frac{\eta}{\alpha} - 1\right), \sqrt{\frac{\alpha}{2}}\right] \right\} \quad [2 - 1]$$

where ξ and η are nondimensional values of the x and y coordinates of a point, and E and F are elliptic integrals of the second and first kind, respectively. The circumflex marks represent complete integrals. Anwar stated that Eq. [2-1] had been evaluated with different proportionality factors, and it was discovered that the lowest value for which a solution was possible was $\alpha = 1/2$. He presented results for $\alpha = 1/2$ and $\alpha = 1$, along with experimentally measured values, for the upstream side

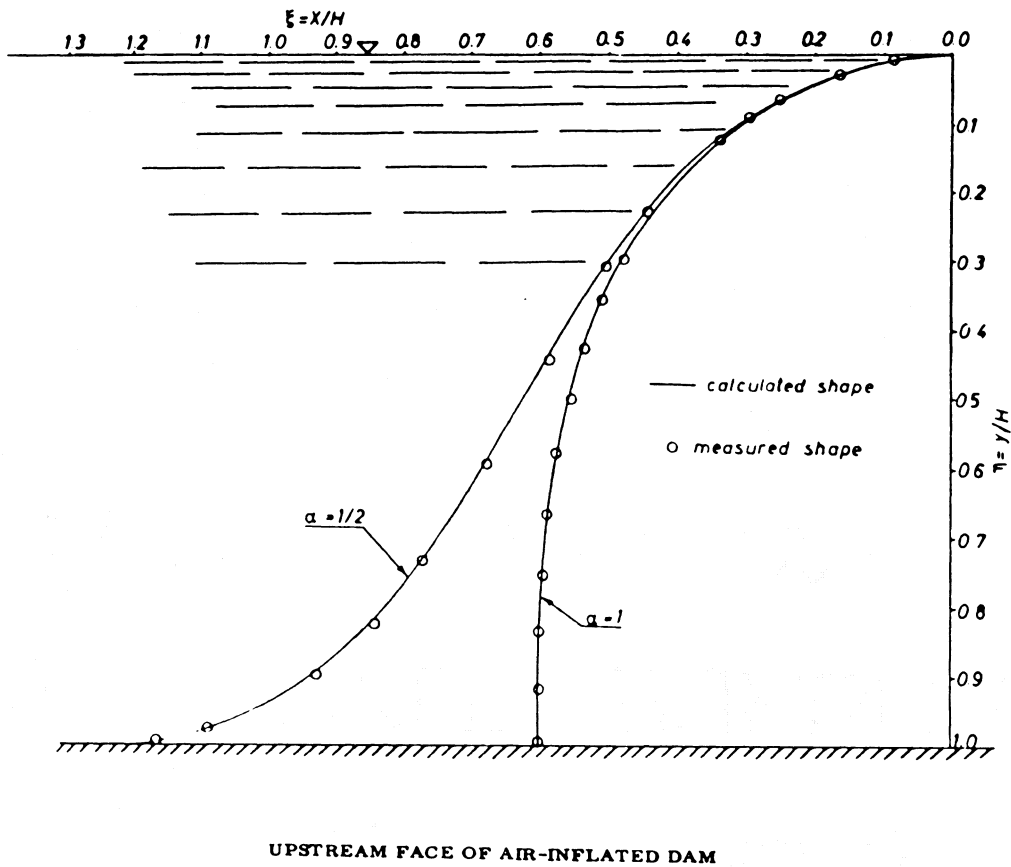


Figure 2. Anwar's Results for Computed and Experimental Shapes [1]

of the dam, as is shown in Figure 2 on page 7. The base length varied according to the value used as the proportionality constant.

Hydrodynamic Analysis

Anwar simplified the analysis by assuming flow over the crest to act as if flowing over a fully aerated nappe, thus allowing the downstream side of the dam to be fully exposed to atmospheric pressure. He assumed the internal pressure to be proportional to the total upstream depth, $(h + H)$, yielding:

$$p_i = \alpha \rho g (h + H)$$

The terms used in the analysis are illustrated for the dynamic case in Figure 3 on page 9. Using a procedure similar to that used for the static analysis, the horizontal force, T , acting at the crest of the dam, for a unit width, is

$$T = \frac{1}{2} \alpha \rho g (h + H) H$$

The horizontal component of the force, H_p , acting at any point P , can be shown to be

$$H_p = \frac{1}{2} \alpha \rho g (h + H) H + \rho g \left[Xy - \int_0^X \varphi(X) dX - xy + \int_0^x f(x) dx \right] - \alpha \rho g (h + H) y$$

The vertical component of the force is given by

$$V_p = \rho g \left[\int_0^x g(x) dx + \int_0^x f(x) dx \right] - \alpha \rho g (h + H) x$$

The tangent of the angle of the components can be found as with the static analysis, and after the equation is differentiated with respect to x , it becomes:

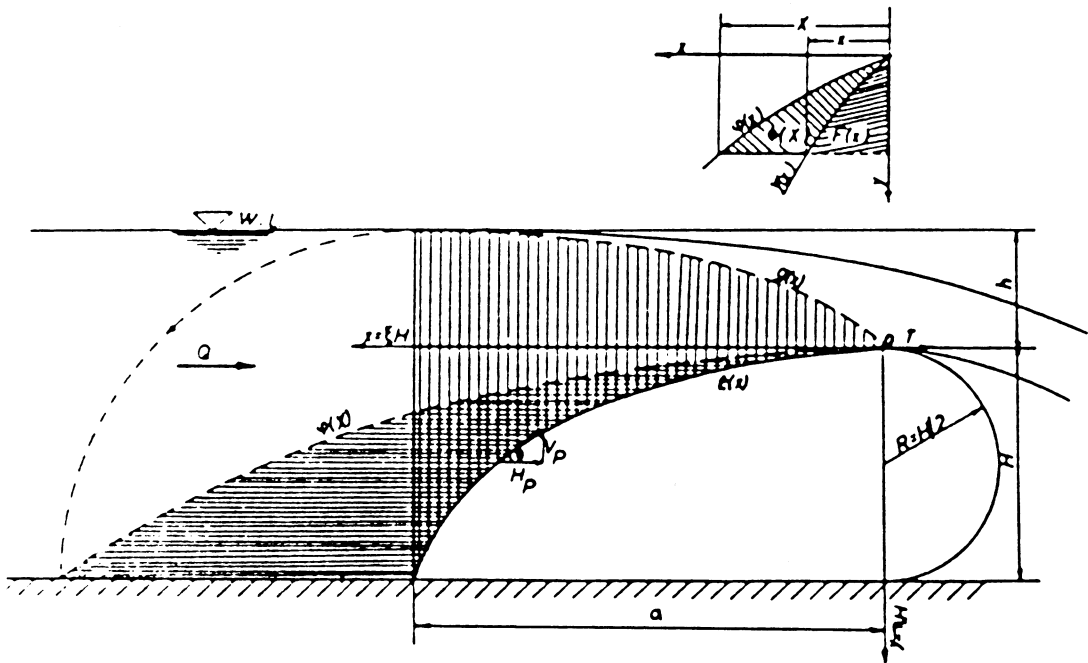


Figure 3. Anwar's Diagram for the Hydrodynamic Analysis [1]

$$\begin{aligned}
& \left[\frac{\alpha}{2}(h + H)H + Xy - \int_0^X \varphi(X)dX - xy + \int_0^x ydx - \alpha(h + H)y \right] y'' \\
& + \left[X'y + Xy' - \frac{d}{dx} \int_0^X \varphi(X)dX - xy' - \alpha(h + H)y' \right] y' \\
& = - [g(x) + y - \alpha(h + H)]
\end{aligned} \tag{2-2}$$

in which $y(x)$ describes the dam, and $g(x)$ and $\varphi(X)$ are unknown functions describing the pressure and horizontal force distribution, respectively. Since Eq. [2-2] contains two unknown functions, Anwar proposed the use of an approximate method to obtain a solution. A power series in x using only the first term was tried and found to yield unacceptable results, so Anwar retained the first two terms of each approximation, and used the boundary conditions

$$y'(0) = 0$$

$$g'(0) = 0$$

$$\varphi'(0) = 0$$

$$y(a) = H$$

$$g(a) = h$$

$$\varphi(a + h + H) = H$$

to determine the six coefficients required. Substituting the power series approximations into Eq. [2-2], and making the resulting equation dimensionless, yields:

$$\begin{aligned}
& \left[X'\eta + X\eta' - \frac{X'X^2}{(1 + \sigma + \beta)^2} - \xi\eta' - \alpha(\sigma + 1)\eta' \right] \eta' \\
& + \left[\frac{\alpha}{2}(\sigma + 1) + X\eta - \frac{X^3}{3(1 + \sigma + \beta)^2} - \xi\eta + \frac{1}{3} \left(\frac{1}{\beta} \right)^2 \xi^3 - \alpha(\sigma + 1)\eta \right] \eta'' \\
& + \left[2\gamma\xi - \frac{\gamma}{\beta}\xi^2 + \eta - \alpha(\sigma + 1) \right] = 0
\end{aligned} \tag{2-3}$$

where $\sigma = h/H$, $\beta = a/H$, $\gamma = h/a$, $\xi = x/H$, $\eta = y/H$, and $X = \xi + 2\gamma\xi - (\frac{\gamma}{\beta})\xi^2 + \eta$. Primes denote derivatives with respect to ξ .

Anwar used a computer to solve the equation numerically, then compared the results to those obtained experimentally. He concluded that overall agreement between the two sets of results was satisfactory. A three-term power series approximation was tested and shown to give results slightly different from those obtained in the two-term approximation, but the difference was small enough that Anwar concluded that a parabolic (two-term) approximation gave reasonable results.

Although Anwar's analysis allows one to obtain the shape of the structure under dynamic flow conditions, it does nothing to account for changes in the shape of the structure due to oscillations. He noted the presence of skin vibrations in the air-inflated dam when the nondimensional overflow coefficient, σ , was greater than 0.25. A lower internal pressure, ($\alpha = 1/2$), produced greater vibrations than did a higher pressure, ($\alpha = 1$), so higher inflation pressures seem to add to stability. In addition, Anwar stated that observations indicated that a flexible dam was not suitable for high overflows, due to the fact that the dam is more prone to vibrations at such flows.

2.2 Binnie's Analysis

Using the problems experienced in laboratory experiments on air-inflated dams reported by Anwar, and the actual collapse conditions of the water-and-air-inflated weir at Mangla [4], A. M. Binnie [3] decided to completely ignore the air-inflated dam, and to concentrate on the water-inflated dam with impounded head reaching the top of the dam. Since Anwar had ignored the effects of the base length and the perimeter, allowing them to be variables dependent on the internal pressure, Binnie derived relationships between these factors, the internal pressure, and the height of the dam. The derivation presented by Binnie differs from that of Anwar, but their conclusions on the shape of the water-inflated dam are the same. Although his analysis in the form presented

is not applicable to the study of air inflated dams, it did point out that problems existed in Anwar's method of analysis, and that more work was needed on the subject.

2.3 Parbery's Work

R. D. Parbery's first published work on inflatable dams presented the derivation of the differential equations of equilibrium for the membrane structure [20]. Since Parbery was interested in the most general case possible, he stated that the shape of the dam was a function of the water levels on each side (upstream and downstream) of the dam, as well as the internal water depth and air pressure. Then, in order to further generalize the derivation, he assumed the membrane to have a constant weight, w , per unit area, and that it obeyed an elastic relationship of the form $\epsilon = g(\sigma)$. His derivation of the static equation is almost identical to that which will be presented in Chapter 3, although he also included the effects of the stretching of the membrane. He related the stretched element length, dS^x , to the unstretched element length, dS , by the equation

$$\frac{dS^x}{dS} = 1 + g(\sigma) = f(\sigma)$$

where $\sigma = T/t$, T is the tension per unit width, and t is the thickness of the membrane. Although the terminology is slightly different, his three basic static equations are the same as those which will be presented in Chapter 3, except that he also includes the term f as a multiplier of each equation to account for possible stretching of the membrane. In addition, the initial boundary conditions presented by Parbery are the same as those to be used in Chapter 3, so they will not be shown here. With S as the independent variable, there were two unknowns, ϕ and T_0 , at each point on the membrane, in addition to the location variables, x and y . Since the equations presented were nonlinear, Parbery suggested the use of an iterative solution technique for the system, utilizing a fourth order Runge-Kutta method, with initial estimates of ϕ and T_0 , which were then refined using

the Newton-Raphson method. The values would continue to be refined, and new iterations made until the boundary conditions were met. Problems arise in the analysis of nearly full dams due to the fact that two solutions may be obtained for certain values of upstream water head, and because the membrane may lay flat at the downstream anchor point. Parbery suggested that a particular upstream initial angle be fixed, and that the tension and upstream head be chosen to fill the boundary conditions by using the Newton-Raphson method. For the condition of a horizontal strip of the membrane at the downstream point, the boundary conditions were modified according to the flat length of the membrane. The relationship between the upstream head, H , and the initial tension in the membrane, T_0 , was then found by taking forces in the horizontal direction, and imposing the equilibrium condition for the static shape. Parbery's equation for the relationship assumes a nearly full dam with the downstream slope laid flat for some distance. Figure 4 on page 14 is used, considering pressure prisms acting on the upstream and downstream sides of the dam, with the internal pressure dropping out. The horizontal tension component of the upstream side is $T_0 \cos \varphi(0)$, while at the downstream side, the resulting horizontal tension force is $T_0 \cos \varphi(L)$, yielding:

$$\frac{1}{2}\gamma H^2 - \frac{1}{2}\gamma D^2 - T_0[\cos \varphi(0) + \cos \varphi(L)] = 0$$

Assuming the membrane is laid flat for some distance on the downstream side, the angle $\varphi(L) = 0$, so the relationship reduces to that shown by Parbery,

$$\frac{1}{2}\gamma H^2 = T_0[1 + \cos \varphi(0)] + \frac{1}{2}\gamma D^2$$

from which the depth of the upstream head may be found to be:

$$H = \left\{ \frac{2}{\gamma} T_0 [1 + \cos \varphi(0)] + D^2 \right\}^{1/2}$$

Parbery compared the finite element analysis of static behavior developed by Harrison [9] to his own continuous method, and found that the finite element method was a second-order ap-

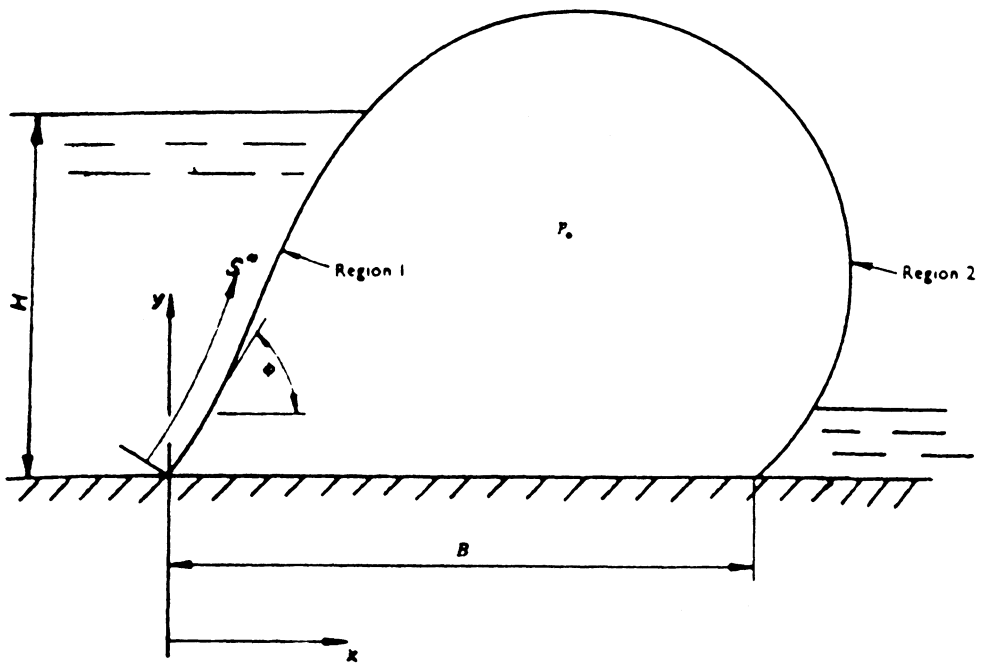


Figure 4. Diagram of an Air-Inflated Dam for the Static Case [21]

proximation of the equations of equilibrium. Using the data from examples in Harrison's work, Parbery used his own method to show that the results of the two methods were very similar for the case of the water-inflated dam, although a considerable difference was obtained between the methods for the case of a water-and-air-filled dam. Parbery concluded that for those cases giving two solutions to the problem, the physically unstable case would 'collapse', with the overflow discharge causing the upstream head to drop to the level of the stable solution. Finally, Parbery stated that higher inflation pressures caused the dam to be stiffer, making multiple solutions less likely.

Parbery's second paper examined the static form of the air-inflated dam [21]. Using the equations of equilibrium derived in his previous paper, along with the matching initial boundary conditions, he assumed that an air-inflated dam would not lie flat on its downstream side. With these tools, he proceeded to analyze the effects of inflation pressure, impounded head, and perimeter length, along with the membrane weight and elasticity. Increased pressure made the dam stiffer, and allowed an increase in maximum impounded head, but this also increased the membrane tension. Longer perimeters experienced less deformation for a given pressure and upstream head, but this also resulted in an increase in the tension in the membrane. For long perimeter lengths, when the internal pressure and impounded head were constant, the problem of dual solutions for the equations was evident, but by shortening the perimeter length, this problem was eliminated.

Parbery stated that membrane weight causes some change in the shape of the dam, and can cause a change in the stretched length due to the fact that the tension at a point is

$$T = T_0 + wy$$

where w is the weight of the membrane. When he compared the profiles for several membranes weighing between 0 and 4.5 lb/sq ft, he decided that the effect of weight on the profile was negligible, due to the fact that displacements due to weight were very small compared to the overall dimensions of the dam. Parbery's displacements due to weight for the static shape are plotted in Figure 5 on page 16, for weights from 1.5 lb/sq ft to 4.5 lb/sq ft. The curves shown illustrate the displacements for various weights from the shape obtained for the weightless condition. The displacement due to extensibility was also checked, and found to be two orders of magnitude less than

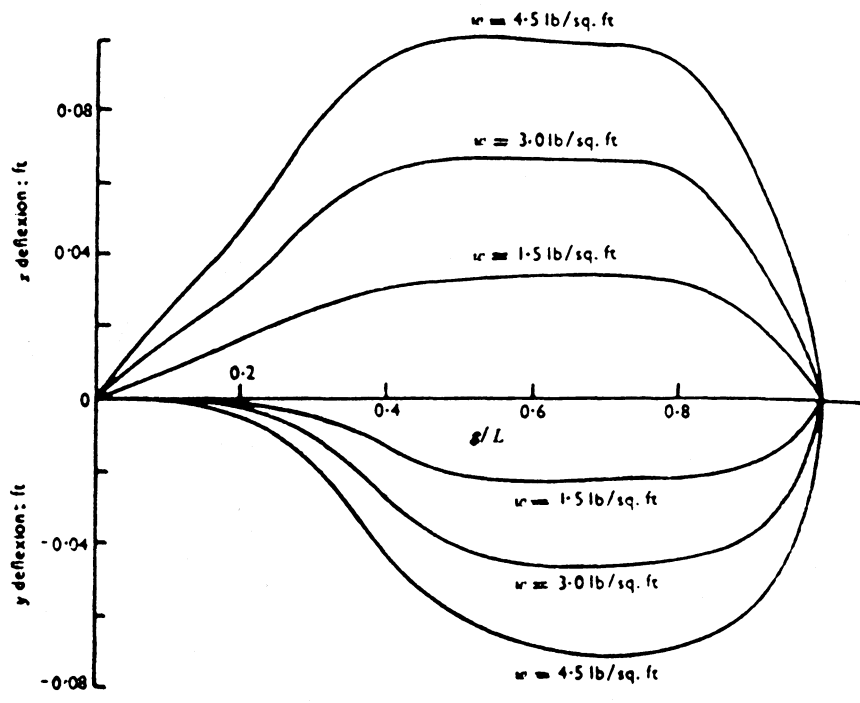


Figure 5. Parbery's Computed Displacements Due to Weight [21]

that due to membrane weight, so Parbery neglected these effects in his subsequent solution. The effect of neglecting these variables makes the tension constant around the perimeter, along with eliminating the strain in the membrane.

After dropping the membrane weight and the extensibility term from his equations of equilibrium, Parbery proceeded to make the equations nondimensional, using the base length as the generalized length term, rather than the head, so various solutions could be compared. Using elliptic integrals of the first and second kind, he derived a set of equations which define the static shape of the dam for given values of the initial angle, $\varphi(0)$, and the initial tension. He again suggested the Newton-Raphson method as a possible way of obtaining the initial values. Parbery stated that the use of the elliptical integrals gives a significant savings in computation time when compared to the numerical integration of the differential equations of equilibrium. In conclusion, he noted that the air-inflated dam could achieve a stable configuration when the air pressure was less than the upstream head.

It should be noted that Parbery's work dealt only with the static condition, and that the effect of the assumption of the weightlessness of the membrane on the dynamic action of the dam was unknown. His work did prove that membrane weight and elasticity made little difference in the static analysis, therefore showing that Anwar's initial assumptions had been justified.

2.4 Watson's Work

R. Watson derived new sets of equations defining the shapes of dams under several hydrostatic inflation conditions [27]. Although never stated, he assumed the membrane to be weightless and inextensible. For dams inflated with air, he used his equations to show that there are four stages of inflation, and also to develop diagrams relating various properties of the dams. Since they deal only with static behavior, his equations are of little interest in this analysis, except

to note that elliptic integrals were again involved in the solution, and that the results verified the static shapes obtained by Anwar and Binnie for the special cases presented in their works.

2.5 Other Contributions

A number of other researchers have investigated various aspects of the behavior of inflatable dams. Baker et al. [2] reported the results of experimental work conducted on flexible dam models based on the design of the inflatable weir at the Mangla Dam, Pakistan. The investigators reported the presence of vibrations and large fluctuations in the tension when the depth of flow over the dam was large. They proposed several methods of reducing or eliminating the vibrations, including the attachment of a flexible "trip wire" or rod near the crest of the dam to cause the flow to separate from the downstream face of the dam, allowing the dam to "ventilate" itself. Anwar's [1] later experiments also showed that the trip rod could cause a considerable reduction in the vibration, but only if the dam was well ventilated and if the depth of flow over the dam was not extremely large. Harrison [9] reported that Stodulka and Marr achieved similar results on the effectiveness of the trip rod in model tests at Sydney University in 1970. Binnie's study of the collapse of the Mangla weir proposed that the downstream tailwater pressure and the oscillation of the bags could have caused resonance in the system, which would have contributed to the instability of the structure. The Mangla dams were not equipped with trip rods, although the depth of flow over the structures at the times of collapse would have probably limited their usefulness for their design purpose.

H. B. Harrison also introduced a finite element method for the solution of the static properties of inflatable dams. His analysis included the effect of weight, and allowed the upstream head to vary, but not to exceed the height of the dam. Either water or water-and-air could be used as the means of inflation for the dam. For the water-and-air inflated case, it was required that the internal water level equal the downstream head. Therefore, for the special case where the down-

stream head was zero, the water-and-air case would reduce to the air-inflated case. Since the method involved the solution of $3N-2$ simultaneous equations, where N is the number of elements defining the dam perimeter, Harrison wrote a computer program which he used to obtain results for various test cases. His results predicted that dams inflated with air would become stable at a much lower pressure than those inflated with water, and that the resulting tension would also be much smaller. However, he stated that the risk of explosive failure in air inflated dams was much larger than that in dams inflated with water only, and he concluded by saying that in design, the factor of safety for air-inflated dams would need to be much larger than that for water-inflated dams.

The discussion by van Beesten [4] of Binnie's study of the Mangla collapse reported the presence of deep "V" notches near the ends of models of the Mangla weir, which were tested at the Nandipur field laboratory of the Irrigation Research Institute. The unsteady flow through the "V" notches caused variations in the pressure in the bags, and created vibrations caused by the surging action of the free water surface in water-and-air-inflated dam models. The presence of "V" notches in air-inflated dams has been noted by Marshall [18], and by the manufacturer's literature [22].

Researchers investigating the behavior of inflatable membrane structures have contributed to the knowledge of the mechanics of inflatable dams. Irvine [15] stated that the dam is assumed to be long, so that the generators of the perimeter are straight. This is a general assumption used in many of the theories of long membrane structures [16,19,25]. It allows a three-dimensional problem to be modeled in two-dimensions, since it eliminates complications caused by the end conditions. However, van Beesten observed that significant longitudinal surging had occurred in models tested at Nandipur, which suggests that a two dimensional analysis of dynamic behavior may be inadequate for water-and-air-inflated dams. Binnie et al. [4] concluded that if the dam were compartmentalized, the individual sections might reduce longitudinal movements of water in such structures.

A significant amount of research into the static and dynamic behaviors of air-supported cylindrical membranes has been done by Firt [7], who effectively eliminated the effects of weight by assuming static loads in the direction radial to the deformed membrane, and by replacing static loads on circular arcs with a constant mean value. This was because Firt considered the internal

air pressure to be so much larger than the membrane weight, that the weight was relatively insignificant.

Finally, it should be noted that a number of other researchers studying membrane structures, and inflatable dams in particular, have concluded that the membrane may be assumed to be both weightless and inextensible [1,11,15,16,17,19,25,26]. It has also been shown that Parbery's analysis included both parameters in the derivation of the equations of equilibrium for the air-inflated dam, but that both were found to have negligible effect on the static behavior of the structure, and were eliminated. Although there is general agreement among most researchers about the effect of weight on static behavior, the manner in which membrane weight affects the dynamic behavior of the flexible dam inflated by air pressure apparently was not studied until now.

Chapter 3. The Static Analysis

3.1 Introduction

It has been shown that a number of researchers have previously investigated the static behavior of inflatable dams under a variety of inflation conditions and external loadings. Often, in order to simplify the analysis, it is assumed that the membrane material is weightless and inextensible [1,15,21]. For the case considered, there are no external loadings applied to the air-inflated membrane. The internal pressure and the self-weight of the membrane are the only forces applied to the structure. A set of differential equations will be derived for the static conditions of the dam, and a differential equation solver will be used to determine solutions of the equations.

3.2 Derivation of the Static Equations

In order to obtain the static equations, a cross-sectional shape of the air-inflated membrane, loaded only with its own weight, is examined as shown in Figure 6 on page 23. The section taken is assumed to be in the central portion of a long dam, so that the end effects will not contribute significantly to the static analysis [7,15]. An element of the section can be taken as a free body diagram, showing all forces, dimensions, and angles of importance, as in Figure 7 on page 24. The variables illustrated are the differential element length, dS ; the tension at the beginning of the element, T_1 ; the rate of change in tension along the element, dT_1/dS ; the weight of the membrane material per unit area of the dam, P ; the internal gauge air pressure, q ; the initial angle of the membrane element, ψ_0 ; and the change in the angle through the element, $d\psi_0$. The $x - y$ coordinate system is defined by the horizontal x -axis and the vertical y -axis. It is important to note that the equation for the tension at the end of the element is a Taylor series with only the linear terms retained. Higher order terms could be included, but this is not necessary, since they would drop out when the element length is allowed to approach zero.

Equations of equilibrium are used to obtain the first two static equations of the structure. First, forces are summed in the normal direction with respect to the curvature of the element. The resulting equation is set equal to zero, giving:

$$\left[T_1 + \left(\frac{dT_1}{dS} \right) dS \right] \sin d\psi_0 + qdS - P \cos \psi_0 dS = 0 \quad [3 - 1]$$

Next, it is specified that dS and $d\psi_0$ must be small, as would be appropriate for a differential element; therefore, $\sin d\psi_0$ is approximately equal to $d\psi_0$. After dividing by dS , and letting dS approach zero, Eq. [3-1] can be rearranged to obtain:

$$\frac{d\psi_0}{dS} = \frac{-q + P \cos \psi_0}{T_1} \quad [3 - 2]$$

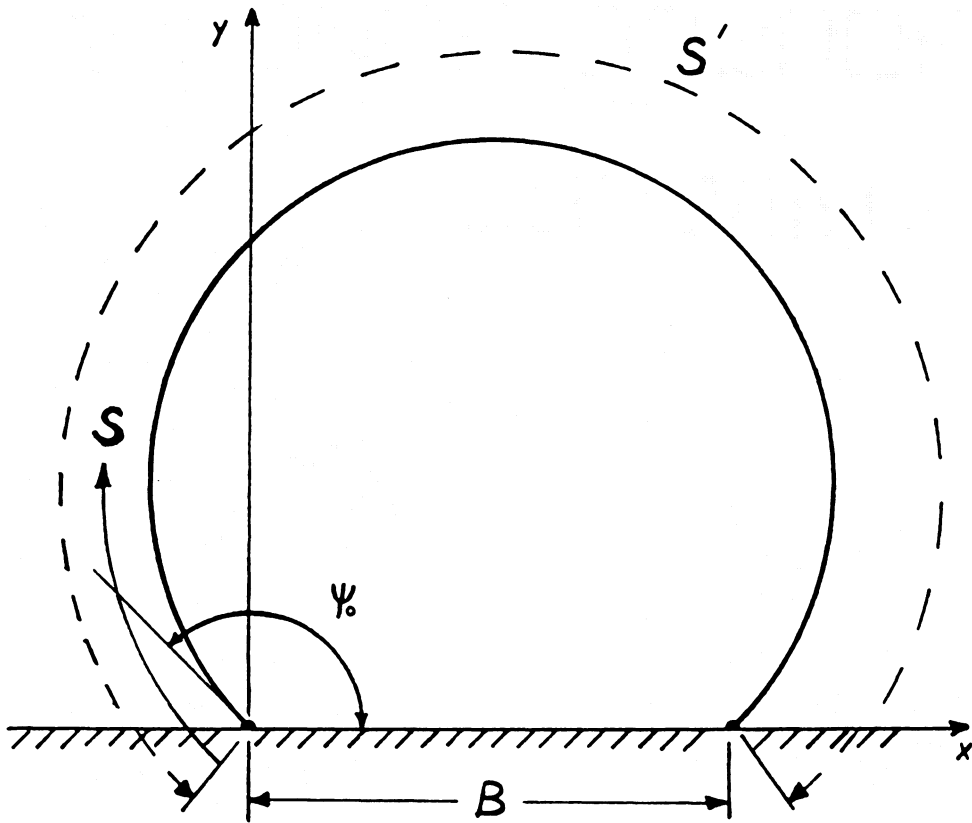


Figure 6. Cross-Section of an Air-Inflated Dam under Static Conditions

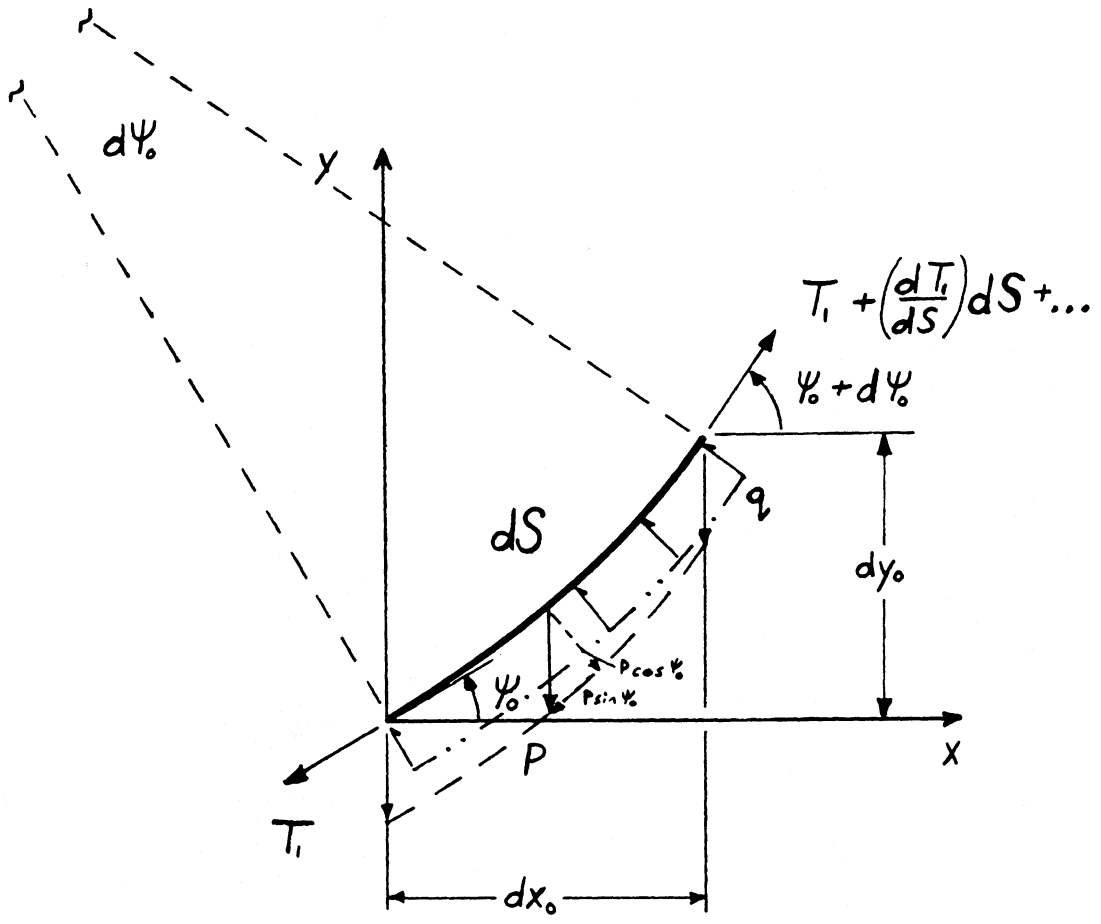


Figure 7. Free Body Diagram of an Element of the Cross-Section

Forces are then summed in the tangential direction of the arc:

$$- T_1 + \left[T_1 + \left(\frac{dT_1}{dS} \right) dS \right] \cos d\psi_0 - P \sin \psi_0 dS = 0 \quad [3 - 3]$$

As before, $d\psi_0$ is considered to be small, so $\cos d\psi_0$ is approximately one. By making this approximation, and allowing dS to approach zero, the following equation results after combining terms:

$$\frac{dT_1}{dS} = P \sin \psi_0 \quad [3 - 4]$$

For a very small arc length, the element dS is approximately a straight line, so dS , dx_0 , and dy_0 form a right triangle with a base angle of ψ_0 . The definitions of sine and cosine give the following approximations:

$$\frac{dy_0}{dS} = \sin \psi_0 \quad [3 - 5]$$

$$\frac{dx_0}{dS} = \cos \psi_0 \quad [3 - 6]$$

Substituting Eq. [3-5] into Eq. [3-4], reducing, and rearranging, it can be seen that a simple differential equation results, if T_1 is now treated as a function of y_0 :

$$\frac{dT_1}{dy_0} = P \quad [3 - 7]$$

Integrating this equation yields:

$$T_1 = Py_0 + C \quad [3 - 8]$$

To evaluate the constant, C , the boundary conditions must be satisfied. At the base, where $y_0 = 0$, the initial tension in the element is $T_1 = T_0$, so by setting $y_0 = 0$ in Eq. [3-8], it is found that $C = T_0$. Equation [3-8] then becomes:

$$T_1 = Py_0 + T_0 \quad [3 - 9]$$

It is now possible to substitute Eq. [3-9] into Eq. [3-2], yielding:

$$\frac{d\psi_0}{dS} = \frac{-q + P \cos \psi_0}{Py_0 + T_0} \quad [3 - 10]$$

On examining equations [3-5], [3-6], and [3-10], it can be seen that there are three differential equations in S with the unknowns x_0 , y_0 , and ψ_0 . The set is a solvable system of equations.

The set can be simplified by making all terms in each equation nondimensional. The terms x_0 , y_0 , and S have units of length, P and q have units of force per length, and the tension is in terms of force. The angle ψ_0 is in units of radians, which is a nondimensional term. A generalized length term, ℓ , is introduced to be used in the nondimensionalizing process. By arranging the terms appropriately to eliminate all units, one can define:

$$\frac{x_0}{\ell} = x \quad [a]$$

$$\frac{y_0}{\ell} = y \quad [b]$$

$$\frac{S}{\ell} = s \quad [c]$$

$$\frac{P}{q} = p \quad [d]$$

$$\frac{T_0}{q\ell} = \bar{T}_0 \quad [e]$$

where x , y , s , p , and \bar{T}_0 are nondimensional terms to be used in equations [3-5], [3-6], and [3-10].

This yields the nondimensional equations:

$$\frac{dy}{ds} = \sin \psi_0 \quad [3 - 11]$$

$$\frac{dx}{ds} = \cos \psi_0 \quad [3 - 12]$$

$$\frac{d\psi_0}{ds} = \frac{-1 + p \cos \psi_0}{py + \bar{T}_0} \quad [3 - 13]$$

Similarly, it can be shown that Eq. [3-9] can be nondimensionalized to become:

$$\bar{T}_1 = py + \bar{T}_0 \quad [3 - 14]$$

where \bar{T}_1 is the nondimensional value of the tension in the membrane at any point, y .

3.3 Solution of the Static Equations

The three nondimensional equations of the static shape of the dam contain three unknowns that are dependent on the location on the dam cross-section. The unknowns, x , y , and ψ_0 , can be obtained by using a differential equation solver in conjunction with the known boundary conditions, if constant values of membrane weight, p , and initial tension, \bar{T}_0 , are used. From the shape of the dam and the assigned origin of the coordinate system, it is seen that the values of both x and y are zero at the initial point on the cross-section. This gives two boundary conditions, but a third is required if the system is to be solved, since there are three unknowns. At the end of the cross-section, the value of y must be zero, but there are many values of x at which this might occur. Therefore, it is required that y at the end of the cross-section equal zero at an assigned base length, B , from the initial starting point. The value, B , is transformed into a nondimensional value, b , by using the generalized length term, ℓ :

$$\frac{B}{\ell} = b \quad [3]$$

The finite difference method is used to solve the set of equations, [3.11] – [3.13]. A number of equally spaced points is chosen for consideration, and the derivatives are approximated at those points. Using these approximations, a differential equation solver can compute the values of the unknowns at each node.

To obtain the shape of the dam from the static equations, it is necessary to solve the simultaneous differential equations at each node, using the boundary conditions already discussed. Therefore, a standard, pre-programmed computer package for the solution of simultaneous differential equations can be used. The International Mathematics Subroutine Library [13], available through Virginia Tech's IBM 3084 processor complex on the VM1 mainframe system, contains several differential equation solvers, including DVERK, a routine which uses the Runge-Kutta-Verner fifth and sixth order solution method. However, the use of DVERK as the routine for solving the system of differential equations presents a problem. DVERK requires the use of initial boundary conditions, whereas in this case, only two of the three known boundary conditions occur at the initial point. A third initial boundary condition must be found which will satisfy the conditions at the end of the membrane. Since the unknowns x and y have already been assigned as boundary conditions for the initial point on the cross-section, only ψ_0 remains as a possible choice for the last initial condition. Fortunately, a computer algorithm called ZEROIN is available to help choose the correct starting angle. A possible range of angles is entered, and ZEROIN uses a bisection algorithm and an interpolation algorithm to compute the proper initial angle [8]. A computer program developed by Hsieh [12] incorporated the ZEROIN algorithm and DVERK together to solve a problem related to the one being discussed. The program was rewritten to suit the current problem, so it could be used to obtain the static shape of the dam. The modified program, SHAPE, written in the FORTRAN 77 computer language, is presented in Appendix B.

Maximum and minimum possible values of the initial angle are included in the program, along with the number of nodes used. The program computes the element size and reads the nondimensional value of initial tension and membrane weight. The boundary conditions at the first node are given as $x = 0$, $y = 0$, and $\psi_0 = \theta$, where θ is the value of the initial angle for the present iteration. In order to fulfill the known boundary condition, ($y = 0$ at the end of the cross-section

at the assigned base length, b), the distance from the actual end point to the required end point is computed for each iteration. The ZEROIN subroutine converges to the initial angle that gives the smallest possible error distance, and uses this as the last boundary condition for the solution of the static shape.

For the actual shape for a given case to be obtained, the error distance must be zero. Changing the range of ψ_0 's requires the program to use either more or fewer iterations to converge to the correct value of the initial ψ_0 , but does nothing to change the error distance. Since a particular membrane weight is a constant value, only the tension can effectively be changed to cause a difference in the error distance. The tension can be varied in successive runs of the program in order to find the value which gives an error distance of approximately zero. The zero error distance will only be found when the correct initial tension and initial angle are used.

Finally, it should be noted that the SHAPE program also includes a graphics subroutine which plots the shape of the dam for a given case. This allows the user to make a visual comparison of various cases, and demonstrates the weight's impact on the shape of the dam. The program also smoothes the values at each point, producing a symmetrically shaped cross-section, since there are no nonsymmetrical loads on the structure. It then prints the nodal values to an output file so that the data for a given static shape can be used as the initial conditions of the dam in the dynamic analysis.

Chapter 4. Analysis of the Dynamic Behavior

4.1 Introduction

In Chapter 3, equations were derived which define the equilibrium shape of the air-inflated dam for the case of self-weight loading. The boundary conditions, which allow the set of equations to be solved, were given, and the SHAPE program, including the DVERK and ZEROIN routines, were developed in order to solve the equations. For a particular case, the shape obtained from this procedure is the starting point from which an analysis of dynamic behavior may be attempted. Due to the length of the procedure, the complete derivations of the equations used in the analysis of the dynamic behavior are presented in Appendix A. Here, the method of obtaining a solution for the equations of motion will be discussed, as well as the results found for a series of sample problems.

4.2 The Dynamic Equations

The nondimensional equation of motion for the air-inflated dam loaded with its membrane-weight is derived in Appendix A as:

$$\begin{aligned}
 0 = & \bar{V}[-p\bar{A}\bar{B}\sin\psi_0 - 2p\bar{A}^3\cos\psi_0 - \bar{A}\bar{C}\bar{T}_1 + \bar{B}^2\bar{T}_1] \\
 & + \bar{V}'[\sin\psi_0(-5p\bar{A}^{-2}\bar{B}^2 + 2p\bar{A}^{-1}\bar{C} - 2p\bar{A}^2) + 2p\bar{B}\cos\psi_0 \\
 & \quad + 8\bar{A}^{-3}\bar{B}^3\bar{T}_1 - 7\bar{A}^{-2}\bar{B}\bar{C}\bar{T}_1 + \bar{A}^{-1}\bar{D}\bar{T}_1 - \bar{A}\bar{B}\bar{T}_1] \\
 & + \bar{V}''[5p\bar{A}^{-1}\bar{B}\sin\psi_0 - 2p\bar{A}\cos\psi_0 - 8\bar{A}^{-2}\bar{B}^2\bar{T}_1 + 3\bar{A}^{-1}\bar{C}\bar{T}_1 - \bar{A}^2\bar{T}_1] \\
 & + \bar{V}'''[-2p\sin\psi_0 + 4\bar{A}^{-1}\bar{B}\bar{T}_1] \\
 & + \bar{V}''''[-\bar{T}_1] \\
 & - \bar{\omega}^2\bar{V}'[-2\bar{A}^{-1}\bar{B}] \\
 & - \bar{\omega}^2\bar{V}''[1] \\
 & - \bar{\omega}^2\bar{V}[-\bar{A}^2]
 \end{aligned} \tag{4-1}$$

where \bar{V} and $\bar{V}' - \bar{V}''''$ are the amplitudes of the mode shape and its derivatives with respect to \bar{S} in the tangential direction of the cross-section; \bar{S} is the arc length; p is the value of the membrane weight; \bar{T}_1 is the tension at the point of interest; $\bar{\omega}$ is the frequency; and $\bar{A} - \bar{D}$ are the first through fourth order derivatives of ψ_0 with respect to \bar{S} . All of these values are nondimensional.

Derivatives of ψ_0 and \bar{V} with respect to \bar{S} are needed in the equation, so finite difference equations are used to approximate them. Although central difference equations can be used over most of the perimeter, near the ends lack of data requires one to use forward and backward differences for some derivatives, as discussed in Appendix A.

Since the finite difference equations for the derivatives of ψ_0 contain only the previously computed values of ψ_0 and the distance between the nodes on the cross-section, the approximations of these derivatives can be computed independently of the equation of motion. This is done utilizing the computer program ALPHA, presented as Appendix C. However, the equations for the derivatives of \bar{V} must be substituted into the equation of motion since the values of \bar{V} are un-

known. Therefore, upon substitution, node-specific equations are obtained. The general equation for any node i , before substitution, is:

$$0 = \bar{V}_i R1_i + \bar{V}_i' R2_i + \bar{V}_i'' R3_i + \bar{V}_i''' R4_i + \bar{V}_i'''' R5_i - \bar{\omega}^2 \bar{V}_i' R6_i - \bar{\omega}^2 \bar{V}_i'' R7_i - \bar{\omega}^2 \bar{V}_i R8_i$$

where

$$R1 = -p\bar{A}\bar{B} \sin \psi_0 - 2p\bar{A}^3 \cos \psi_0 - \bar{A}\bar{C}\bar{T}_1 + \bar{B}^2\bar{T}_1$$

$$R2 = \sin \psi_0 (-5p\bar{A}^{-2}\bar{B}^2 + 2p\bar{A}^{-1}\bar{C} - 2p\bar{A}^2) + 2p\bar{B} \cos \psi_0 + 8\bar{A}^{-3}\bar{B}^3\bar{T}_1 - 7\bar{A}^{-2}\bar{B}\bar{C}\bar{T}_1 + \bar{A}^{-1}\bar{D}\bar{T}_1 - \bar{A}\bar{B}\bar{T}_1$$

$$R3 = 5p\bar{A}^{-1}\bar{B} \sin \psi_0 - 2p\bar{A} \cos \psi_0 - 8\bar{A}^{-2}\bar{B}^2\bar{T}_1 + 3\bar{A}^{-1}\bar{C}\bar{T}_1 - \bar{A}^2\bar{T}_1$$

$$R4 = -2p \sin \psi_0 + 4\bar{A}^{-1}\bar{B}\bar{T}_1$$

$$R5 = -\bar{T}_1$$

$$R6 = -2\bar{A}^{-1}\bar{B}$$

$$R7 = 1$$

$$R8 = -\bar{A}^2$$

After substitution, for most interior nodes, the resulting equation of motion for a particular node i is:

$$\begin{aligned}
0 = & \left(-\frac{R4_i}{2h^3} + \frac{R5_i}{h^4} \right) v_{i-2} \\
& + \left(-\frac{R2_i}{2h} + \frac{R3_i}{h^2} + \frac{2R4_i}{2h^3} - \frac{4R5_i}{h^4} \right) v_{i-1} \\
& + \left(R1_i - \frac{2R3_i}{h^2} + \frac{6R5_i}{h^4} \right) v_i \\
& + \left(\frac{R2_i}{2h} + \frac{R3_i}{h^2} - \frac{2R4_i}{2h^3} - \frac{4R5_i}{h^4} \right) v_{i+1} \\
& + \left(\frac{R4_i}{2h^3} + \frac{R5_i}{h^4} \right) v_{i+2} \\
& - \bar{\omega}^2 \left(-\frac{R6_i}{2h} + \frac{R7_i}{h^2} \right) v_{i-1} \\
& - \bar{\omega}^2 \left(-\frac{2R7_i}{h^2} + R8_i \right) v_i \\
& - \bar{\omega}^2 \left(\frac{R6_i}{2h} + \frac{R7_i}{h^2} \right) v_{i+1}
\end{aligned} \tag{4-2}$$

Different equations are obtained at the two exterior nodes at each end of the cross-section, as shown in Appendix A. The equations contain the unknowns v_i at each node except the first and the last, where the values of v_1 and v_N are zero since these points are fixed, and $\bar{\omega}^2$. By placing the equations in matrix form, one obtains:

$$[A - \bar{\omega}^2 B][v_i] = 0$$

This is an eigenvalue problem, where

$$|A - \lambda B| = 0 \tag{4-3}$$

is the characteristic equation of the system, and λ , the eigenvalue, is equal to $\bar{\omega}^2$.

In order to solve Eq. [4-3], the DYNAMIC program uses the EISPACK subroutine library [6]. The subroutine RGG (Real General Generalized matrix) solves the characteristic equation for the eigenvalues of the system. It also computes the associated normalized eigenvectors, which correspond to the values of v_i at the nodes. Since the eigenvalues are obtained in no particular or-

der, the IMSL subroutine VSRTRD [14] is used to sort the eigenvalues from the smallest to the largest. The eigenvectors are placed in the same order as their corresponding eigenvalues.

Since the eigenvectors are normalized, the largest displacement assigned will be ± 1 . For this analysis, S' , the length of the perimeter of the cross-section, is chosen as the length by which terms are made nondimensional, since its value is larger than any other term involving length in the analysis. Then, one finds that $\bar{S}' = 1$, so a displacement of ± 1 is obviously too large. The displacements must be scaled down by some factor to be realistic. Ideally, a scale factor can be found that will preserve the length of the perimeter as 1, but actual displacements are not required, so any scale factor that gives a reasonable displacement when plotted will do. After some experimentation, scale factors of 1/20 and 1/50 were chosen for the first and second pairs of mode shapes, respectively.

The entries in the eigenvector correspond to the movement of the nodes in the tangential direction of the cross-section, but the movements of the nodes in the normal direction are still unknown. In the derivation of the equations of motion, one finds that

$$w = \left(\frac{d\psi_0}{dS} \right)^{-1} \frac{\partial v}{\partial S} = A^{-1} v_S$$

Since the values of A and v are known at each point, it is possible to again use finite differences to find the value of v_S in the computation of w . At the interior nodes, the value of w is:

$$w_i = A_i^{-1} \left(\frac{v_{i+1} - v_{i-1}}{2h} \right)$$

At nodes 2 and $N-1$, the values of w are

$$w_2 = A_2^{-1} \left(\frac{v_3}{2h} \right)$$

$$w_{N-1} = A_{N-1}^{-1} \left(- \frac{v_{N-2}}{2h} \right)$$

The nondimensional values of A , which have already been computed by the ALPHA program, can be used, and since both v and h are nondimensional terms, the resulting equations are nondimensional.

Before any plotting can occur, the displacements at each node in the v and w directions must be converted to displacements in the x and y directions. The displacements are from the static position, computed in the STATIC program. By examining Figure 17 in Appendix A, one can see that the coordinates of a node in the dynamic case, x_d and y_d , are:

$$x_{di} = x_i + v_i \cos \psi_{0i} - w_i \sin \psi_{0i}$$

$$y_{di} = y_i + v_i \sin \psi_{0i} + w_i \cos \psi_{0i}$$

Once the scaled displacements in the x and y directions are obtained, it is easy to plot the mode shape. The plotting program is the final part of the DYNAMIC program, which is presented in Appendix D.

4.3 Defining the Study Cases

The effect of the membrane-weight on the dynamic behavior of the dam can now be studied. In order to do so, a series of study cases with a constant base length to perimeter ratio and with various membrane weights will be examined. Then, other base-perimeter ratios will be examined for the same membrane-weight cases. The results of the various cases will be examined to determine if the weight of the membrane has a significant impact on the structure's behavior during vibration by comparing the study cases to the dynamic behavior exhibited in the weightless condition.

The equations of motion are nondimensional, so the value of any term is not a physical quantity. However, it is desirable that the nondimensional terms be fairly realistic. For example,

if one were to use a value of B/S' greater than one, there would be a problem. Terms involving length were made nondimensional by dividing by the perimeter length, so the largest value possible is $\bar{S}' = 1$. If B/S' is equal to \bar{S}' , the membrane lies flat over its entire surface, and if B/S' is greater than \bar{S}' , in addition to lying flat, it cannot even be connected to one of the end supports. Another example might be $P/q = 1$, which might correspond to $P = q = 4$ lbs/sq in. An internal pressure of 4 lb/sq in. is very reasonable, but an equivalent membrane weight would equal 576 pounds per square foot. Considering that a membrane might be a quarter of an inch thick, this proposed material would weigh 27,648 pounds per cubic foot! This is approximately 39 times the weight of an equivalent amount of lead. Therefore, it is obvious that care must be taken in choosing the values used in the analysis if the results are to have any meaning.

In order to choose typical values that might be used in the analysis, examples given by Harrison [9], Parbery [20,21], and Watson [27] were examined. The range of values given for the base to perimeter ratio was from a low of 0.12 to a high of 0.50. It was decided to examine three cases in this range, for ratios of 1/2.5, 1/3, and 1/4.

A wide range of weight to internal pressure ratios was desired, in order to be able to determine the effects of increasing levels of weight on the membrane. The weightless case was also chosen so that the computed values for the cases involving weight could be compared to the weightless condition. The values chosen were: 0.0, 0.001, 0.005, 0.010, 0.020, 0.030, and 0.040. For an internal pressure of 4 psi, the largest value corresponds to a material weighing about 23 pounds per square foot. This value is much larger than what might be considered reasonable, but it was retained in order to obtain results for a wider range of values, to help determine the effects of continuing to increase the weight. Higher values of 0.05 and 0.10 were tested, but were found to give unreasonable results for the number of nodes considered.

The number of nodes chosen for the analysis also contributes to the accuracy of the solution obtained. Initially, twenty-one nodes were used, but this number was found to give poor results when the shapes were plotted. In addition, for the weightless dam, it was found that the shape of the static case was a portion of a circle. The first derivative of the initial angle ψ_0 should be the curvature of the shape. For a circle, the curvature is constant, so higher order derivatives

of ψ_0 should be zero. When twenty-one nodes were used, the higher order derivatives computed by the ALPHA program were small, but were not considered to be close enough to zero. Therefore, the number of nodes was increased to forty-one. The resulting plots were much clearer, and the derivatives for the weightless case were very close to zero, so this number of nodes was used. The results of the weightless case were compared to those of Hsieh [12], and found to be identical for the same number of nodes.

The choice of forty-one nodes on the cross-section gives thirty-nine points capable of being displaced, since the node at each end must be anchored. This yields thirty-nine simultaneous equations in the problem, with thirty-nine eigenvalues to be computed. For each eigenvalue, there is a corresponding eigenvector, which contains the nodal displacements in the tangential direction to the membrane. Thirty-nine modes of vibration could be computed and plotted if desired. However, the mode shapes associated with larger eigenvalues require more energy to be achieved than do those shapes associated with smaller eigenvalues. Since structures will take their dynamic shape according to the amount of energy in the system, shapes associated with smaller eigenvalues will generally occur. If the amount of energy involved in the vibration increases, mode shapes associated with larger eigenvalues might be achieved. With this knowledge, it is expected that the most common mode of vibration assumed will be that associated with the lowest eigenvalue. Therefore, it was decided that for purposes of this study, only the modes of vibration associated with the four smallest eigenvalues would be plotted.

Once the problems to be studied had been chosen, it was desired to validate the accuracy of the equations. Since Firt [7] and Hsieh [12] had evaluated a semi-circular shape for the weightless membrane, it was decided to compare the results obtained from the DYNAMIC program with their sets of results. The first four eigenvalues obtained by this analysis, after being divided by π , the angle of the arc of the semi-circle, were found to be 1.70, 5.92, 12.92, 21.42, which were similar to those of Hsieh, whose values were 1.70, 5.96, 13.05, and 21.74. They differed slightly more with those of Firt, whose results were 1.71, 5.97, 13.07, and 21.86. The similarity in results seems to validate the numerical procedure presented for lower eigenvalues, although the increasing discrepancy in the values brings into question their usefulness for higher eigenvalues. Of course, if a larger

number of nodes had been used, a higher degree of agreement might have been achieved for the results.

4.4 Numerical Results

Once the cases were defined, the STATIC program was used to obtain the static shape of the cross-section of the dam for each case being studied. The resulting values for the nondimensional weight and tension for each of the three base lengths are given in Table 1 on page 39. The tension was found to decrease both as the weight increased, and as the base length became smaller. The shapes computed for weights of 0.0 and 0.02 are given in Figure 8 on page 40, for a base length to perimeter ratio of 0.40. It can be seen from the diagram that the weight has little influence on the shape for a reasonable range of values of membrane weight, as concluded by Parbery [20,21] and others [1,11,15]. A check of the coordinates of the cross-section for the weightless case confirmed that the shape was a portion of a circle. The derivatives of ψ_0 with respect to \bar{S} were calculated using the ALPHA program. The resulting derivatives of the weightless case showed that the first derivative was constant, and that the higher order derivatives were close to zero, as shown in Table 2 on page 41.

The DYNAMIC program was used to obtain a solution for each of the twenty-one cases being studied. In examining the plotted mode shapes, it quickly became obvious that each of the first four modes of vibration had a basic shape for the range of nondimensional base lengths and weights used. However, the basic shape of each mode was occasionally changed to a second shape, which seemed to contradict the first form. Since the structure may move in either the positive or negative direction of the eigenvalue, the second shape was actually the negative of the first. This conclusion was confirmed by looking at the cases with weights of 0.0 and 0.001 for the base length of 0.40. The mode shapes for these two cases are shown in Figure 9 on page 42 and Figure 10 on page 43. The first and fourth mode shapes are different, although the change in weight was very

<u>B/S</u>	<u>P/Q</u>	<u>T</u>
0.250	0.000	0.2020548
	0.001	0.2016627
	0.005	0.2000972
	0.010	0.1981460
	0.020	0.1942635
	0.030	0.1904083
	0.040	0.1865816
0.333	0.000	0.2194068
	0.001	0.2189936
	0.005	0.2173397
	0.010	0.2152770
	0.020	0.2111671
	0.030	0.2070787
	0.040	0.2030129
0.400	0.000	0.2352559
	0.001	0.2348247
	0.005	0.2331017
	0.010	0.2309517
	0.020	0.2266646
	0.030	0.2223953
	0.040	0.2181443

Table 1. Base Length, Weight, and Tension for the Static Conditions

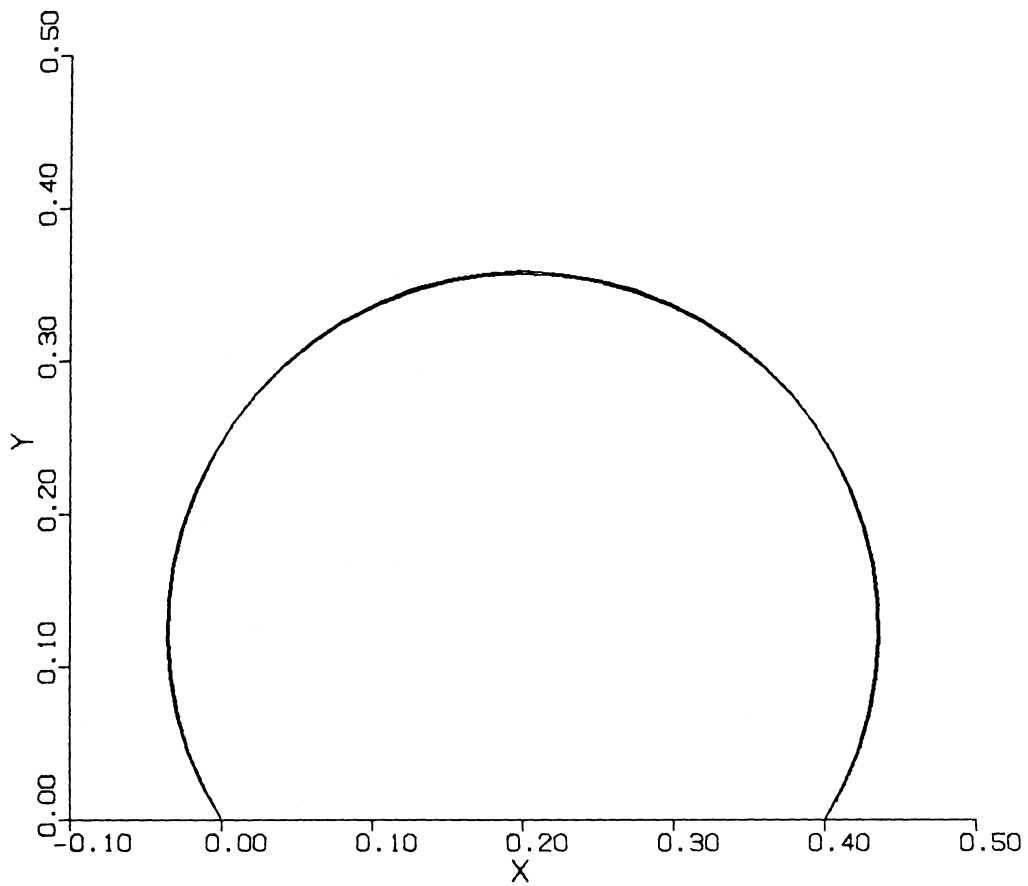


Figure 8. Static Shapes for $P/q = 0.0$ and $P/q = 0.02$ for $B/S' = 0.40$

A	B	C	D
-4.250690471780	0.000000000000	-0.000000006395	0.000000766818
-4.250690471782	-0.000000000160	0.000000003190	0.000000766818
-4.250690471782	0.000000000160	0.000000003205	-0.000000765681
-4.250690471780	0.000000000000	-0.000000003190	0.000000254090
-4.250690471780	0.000000000000	-0.000000000007	0.000000000568
-4.250690471780	0.000000000000	-0.000000003205	-0.000000256364
-4.250690471782	-0.000000000160	0.000000003205	0.000000769091
-4.250690471782	0.000000000160	0.000000003205	-0.000000769091
-4.250690471780	0.000000000000	-0.000000003197	0.000000256932
-4.250690471780	0.000000000000	0.000000000000	0.000000000000
-4.250690471780	0.000000000000	-0.000000003197	-0.000000255227
-4.250690471782	-0.000000000160	0.000000003205	0.000000768523
-4.250690471782	0.000000000160	0.000000003197	-0.000000767351
-4.250690471780	0.000000000000	-0.000000003204	0.000000256293
-4.250690471780	0.000000000000	-0.000000000003	0.000000000213
-4.250690471780	0.000000000000	-0.000000003201	-0.000000255653
-4.250690471782	-0.000000000160	0.000000003200	0.000000767422
-4.250690471782	0.000000000160	0.000000003201	-0.000000768274
-4.250690471780	0.000000000000	-0.000000003200	0.000000255902
-4.250690471780	0.000000000000	-0.000000000001	0.000000000000
-4.250690471780	0.000000000000	-0.000000003200	-0.000000255902
-4.250690471782	-0.000000000160	0.000000003201	0.000000768274
-4.250690471782	0.000000000160	0.000000003200	-0.000000768452
-4.250690471780	0.000000000000	-0.000000003201	0.000000255618
-4.250690471780	0.000000000000	-0.000000000003	-0.000000000462
-4.250690471780	0.000000000000	-0.000000003204	-0.000000256328
-4.250690471782	-0.000000000160	0.000000003197	0.000000767351
-4.250690471782	0.000000000160	0.000000003206	-0.000000768097
-4.250690471780	0.000000000000	-0.000000003195	0.000000255582
-4.250690471780	0.000000000000	-0.000000000001	0.000000000071
-4.250690471780	0.000000000000	-0.000000003204	-0.000000256399
-4.250690471782	-0.000000000160	0.000000003205	0.000000769091
-4.250690471782	0.000000000160	0.000000003205	-0.000000769091
-4.250690471780	0.000000000000	-0.000000003205	0.000000256364
-4.250690471780	0.000000000000	-0.000000000007	-0.000000000568
-4.250690471780	0.000000000000	-0.000000003190	-0.000000254090
-4.250690471782	-0.000000000160	0.000000003205	0.000000765681
-4.250690471782	0.000000000160	0.000000003190	-0.000000766818
-4.250690471780	0.000000000000	-0.000000006395	-0.000000766818

Table 2. Derivatives of the Initial Angle for $B/S' = 0.40$ with $P/q = 0.0$

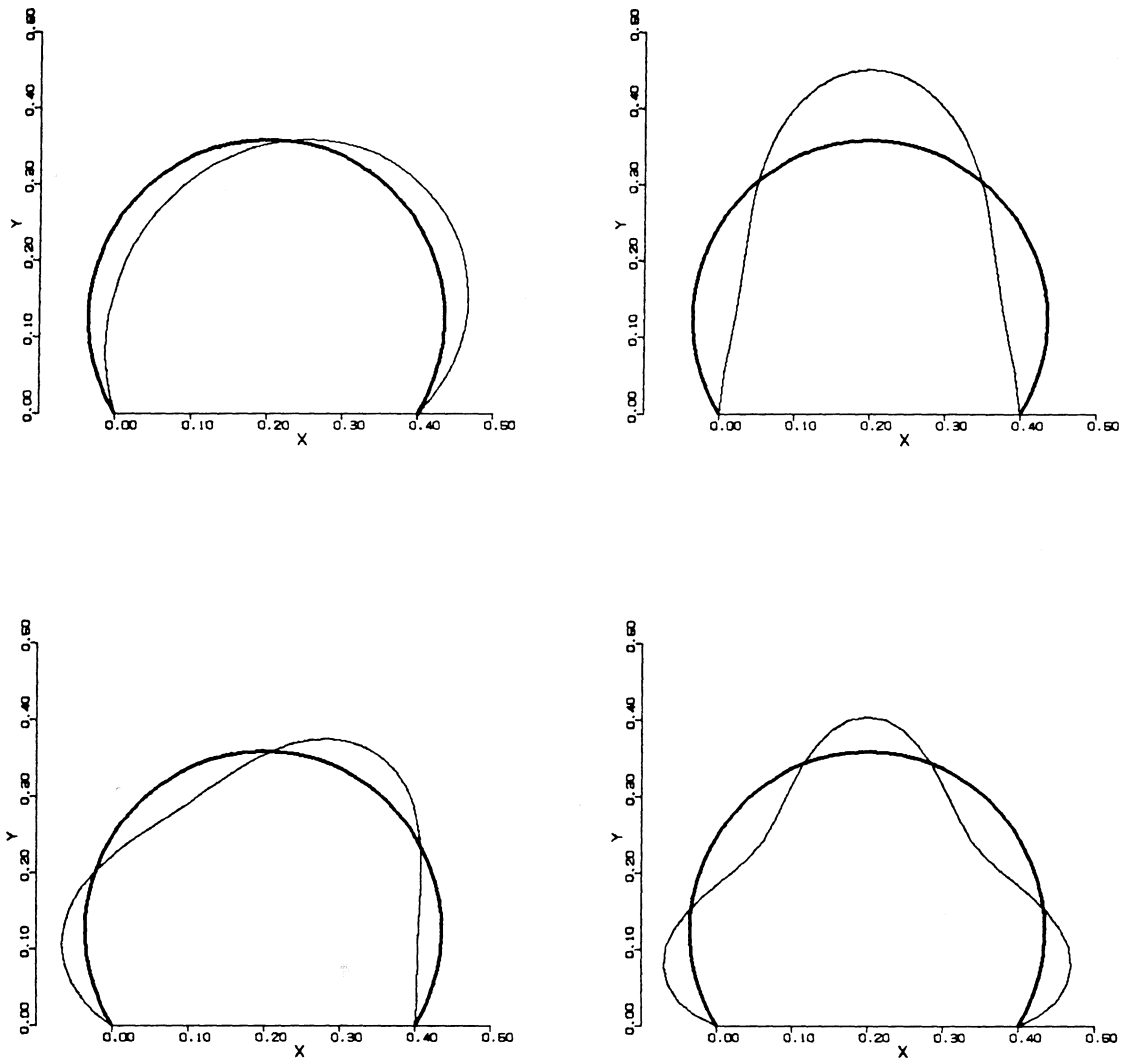


Figure 9. Mode Shapes of Vibration for $B/S' = 0.40$ with $P/q = 0.0$

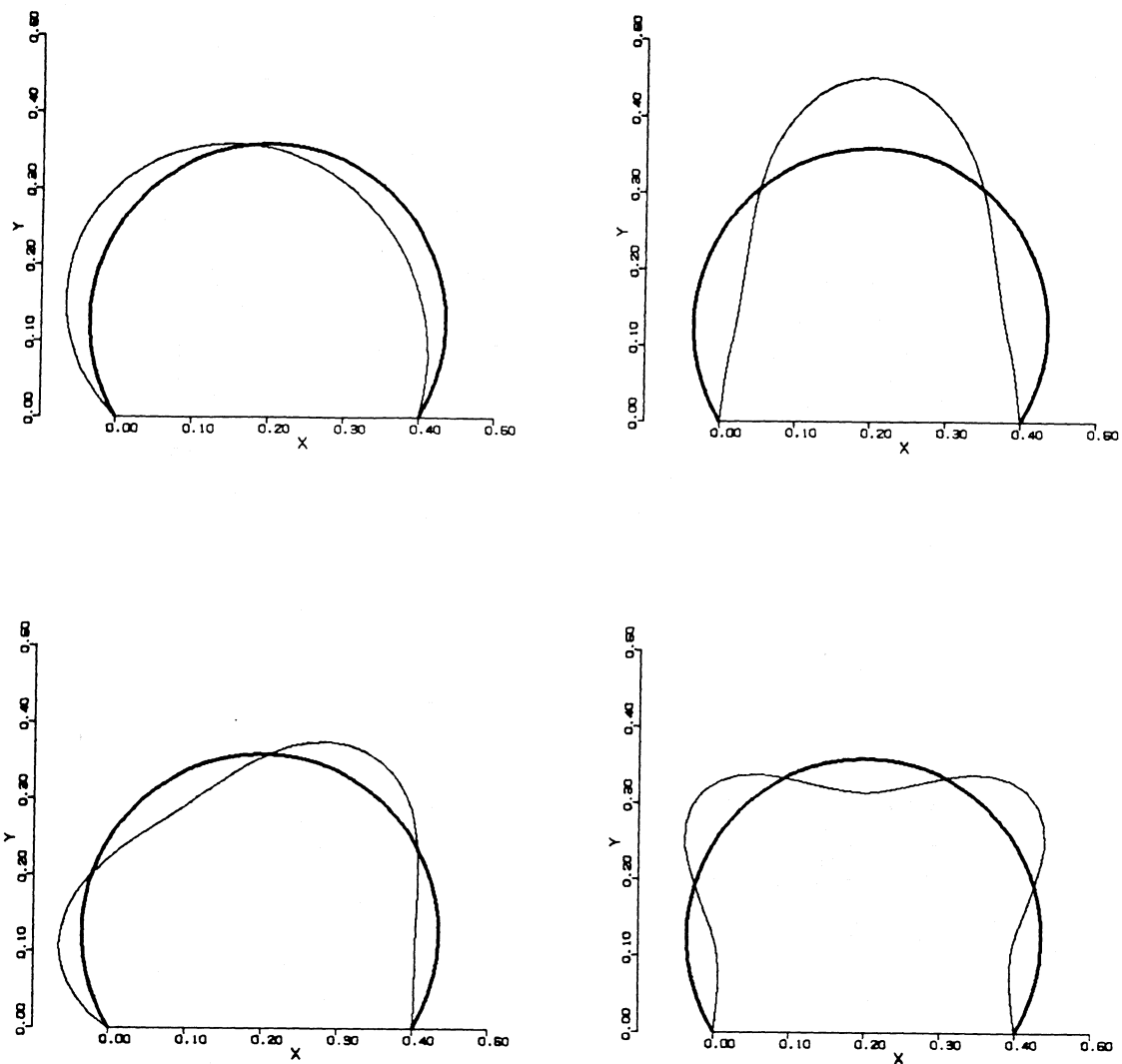


Figure 10. Mode Shapes of Vibration for $B/S' = 0.40$ with $P/q = 0.001$

EIGENVECTORS (FIRST THROUGH FOURTH MODES)

0.00705746	0.01971111	-0.03242357	-0.05104321
0.02747136	0.07454700	-0.12130120	-0.18697659
0.06025850	0.15882734	-0.25373408	-0.37942832
0.10422881	0.26573097	-0.41342212	-0.59279549
0.15800749	0.38759266	-0.58207538	-0.78922371
0.22006093	0.51624037	-0.74100632	-0.93391373
0.28872595	0.64335734	-0.87276109	-1.00000000
0.36224174	0.76085210	-0.96264406	-0.97230760
0.43878389	0.86121906	-1.00000000	-0.84945289
0.51649970	0.93787285	-0.97913919	-0.64398886
0.59354428	0.98544082	-0.89982320	-0.38057418
0.66811651	1.00000000	-0.76726780	-0.09242547
0.73849426	0.97924742	-0.59166254	0.18344334
0.80306811	0.92259588	-0.38724970	0.41151858
0.86037287	0.83119049	-0.17104446	0.56286880
0.90911639	0.70784536	0.03868993	0.61928942
0.94820492	0.55690310	0.22407638	0.57592145
0.97676460	0.38402372	0.36922207	0.44197229
0.99415868	0.19591257	0.46163843	0.23943673
1.00000000	0.00000000	0.49335649	0.00000000
0.99415868	-0.19591257	0.46163843	-0.23943673
0.97676460	-0.38402372	0.36922207	-0.44197229
0.94820492	-0.55690310	0.22407638	-0.57592145
0.90911639	-0.70784536	0.03868993	-0.61928942
0.86037287	-0.83119049	-0.17104446	-0.56286880
0.80306811	-0.92259588	-0.38724970	-0.41151858
0.73849426	-0.97924742	-0.59166254	-0.18344334
0.66811651	-1.00000000	-0.76726780	0.09242547
0.59354428	-0.98544082	-0.89982320	0.38057418
0.51649970	-0.93787285	-0.97913919	0.64398886
0.43878389	-0.86121906	-1.00000000	0.84945289
0.36224174	-0.76085210	-0.96264406	0.97230760
0.28872595	-0.64335734	-0.87276109	1.00000000
0.22006093	-0.51624037	-0.74100632	0.93391373
0.15800749	-0.38759266	-0.58207538	0.78922371
0.10422881	-0.26573097	-0.41342212	0.59279549
0.06025850	-0.15882734	-0.25373408	0.37942832
0.02747136	-0.07454700	-0.12130120	0.18697659
0.00705746	-0.01971111	-0.03242357	0.05104321

Table 3. Eigenvectors for $B/S' = 0.40$ with $P/q = 0.0$

EIGENVECTORS (FIRST THROUGH FOURTH MODES)

-0.00707992	0.01977027	-0.03250889	0.05116322
-0.02755095	0.07474473	-0.12157408	0.18733804
-0.06041879	0.15920236	-0.25422277	0.38002349
-0.10448211	0.26628343	-0.41408693	0.59350746
-0.15835536	0.38828971	-0.58282503	0.78987095
-0.22049530	0.51702454	-0.74172154	0.93430744
-0.28923079	0.64415676	-0.87332108	1.00000000
-0.36279511	0.76159140	-0.96295146	0.97186306
-0.43936024	0.86182974	-1.00000000	0.84861854
-0.51707228	0.93830214	-0.97882999	0.64291347
-0.59408744	0.98565807	-0.89925622	0.37946493
-0.66860783	1.00000000	-0.76653800	0.09149768
-0.73891628	0.97905053	-0.59089097	-0.18401840
-0.80340964	0.92224494	-0.38656153	-0.41165458
-0.86062974	0.83074510	-0.17054650	-0.56258409
-0.90929165	0.70737420	0.03892815	-0.61870078
-0.94830846	0.55647530	0.22403463	-0.57521354
-0.97681224	0.38370025	0.36893247	-0.44135068
-0.99417083	0.19573877	0.46117909	-0.23907603
-1.00000000	0.00000000	0.49283686	0.00000000
-0.99417083	-0.19573877	0.46117909	0.23907603
-0.97681224	-0.38370025	0.36893247	0.44135068
-0.94830846	-0.55647530	0.22403463	0.57521354
-0.90929165	-0.70737420	0.03892815	0.61870078
-0.86062974	-0.83074510	-0.17054650	0.56258409
-0.80340964	-0.92224494	-0.38656153	0.41165458
-0.73891628	-0.97905053	-0.59089097	0.18401840
-0.66860783	-1.00000000	-0.76653800	-0.09149768
-0.59408744	-0.98565807	-0.89925622	-0.37946493
-0.51707228	-0.93830214	-0.97882999	-0.64291347
-0.43936024	-0.86182974	-1.00000000	-0.84861854
-0.36279511	-0.76159140	-0.96295146	-0.97186306
-0.28923079	-0.64415676	-0.87332108	-1.00000000
-0.22049530	-0.51702454	-0.74172154	-0.93430744
-0.15835536	-0.38828971	-0.58282503	-0.78987095
-0.10448211	-0.26628343	-0.41408693	-0.59350746
-0.06041879	-0.15920236	-0.25422277	-0.38002349
-0.02755095	-0.07474473	-0.12157408	-0.18733804
-0.00707992	-0.01977027	-0.03250889	-0.05116322

Table 4. Eigenvectors for $B/S' = 0.40$ with $P/q = 0.001$

small. A comparison of the eigenvectors of these modes, shown in Table 3 and Table 4, shows that although the numerical values are very similar, the signs are opposite. A check of a few values of one mode showed that if the signs were changed for one eigenvector, the coordinates associated with the other eigenvector would result, as was expected.

The relationship between the eigenvalue and the frequency is recalled as $\lambda = \omega^2$. For the range of base lengths studied, it was found that the relationship between the nondimensional base length and frequency was almost linear, as can be seen from Figure 11 on page 47. The curve for any particular mode shape studied was not significantly affected by an increase in weight. Since this was so, it was decided to consider a few additional base lengths to determine whether the relationship remained linear as the base length increased. The semi-circular case, corresponding to a base length of $2/\pi$, and cases with base lengths of 0.8, 0.85, and 0.9 were examined for $P/q = 0.0$ and $P/q = 0.020$. When the results of the weightless case were plotted, it could be seen that the relationship between the base length and the frequency became increasingly nonlinear as the base length increased, as shown in Figure 12 on page 48. The results of the case where $P/q = 0.020$ were found to be almost identical to those of the weightless case, although the frequency for a given base length was slightly less than that of the corresponding base length for the weightless case. Therefore, it can be concluded that a change in the base length to perimeter ratio will have a more significant effect on the frequency than will an increase in membrane weight, for a realistic range of weights.

By checking the results for the various cases, it was found that the frequency of the system decreased as the weight increased, and for the range of lengths used, increased as the base to perimeter length increased. When larger base lengths were examined for the weightless case, the frequency continued to increase as the base length increased. For each of the first four modes of vibration, figures showing the relationship between the nondimensional weight and the frequency were plotted. By examining the plots, presented as Figure 13 on page 49, Figure 14 on page 50, Figure 15 on page 51, and Figure 16 on page 52, it can be seen that over the range of weights shown, the relationship is almost linear. A mathematical check showed this to be true, with the slope of the curve of the relationship generally becoming only slightly less negative as the weight

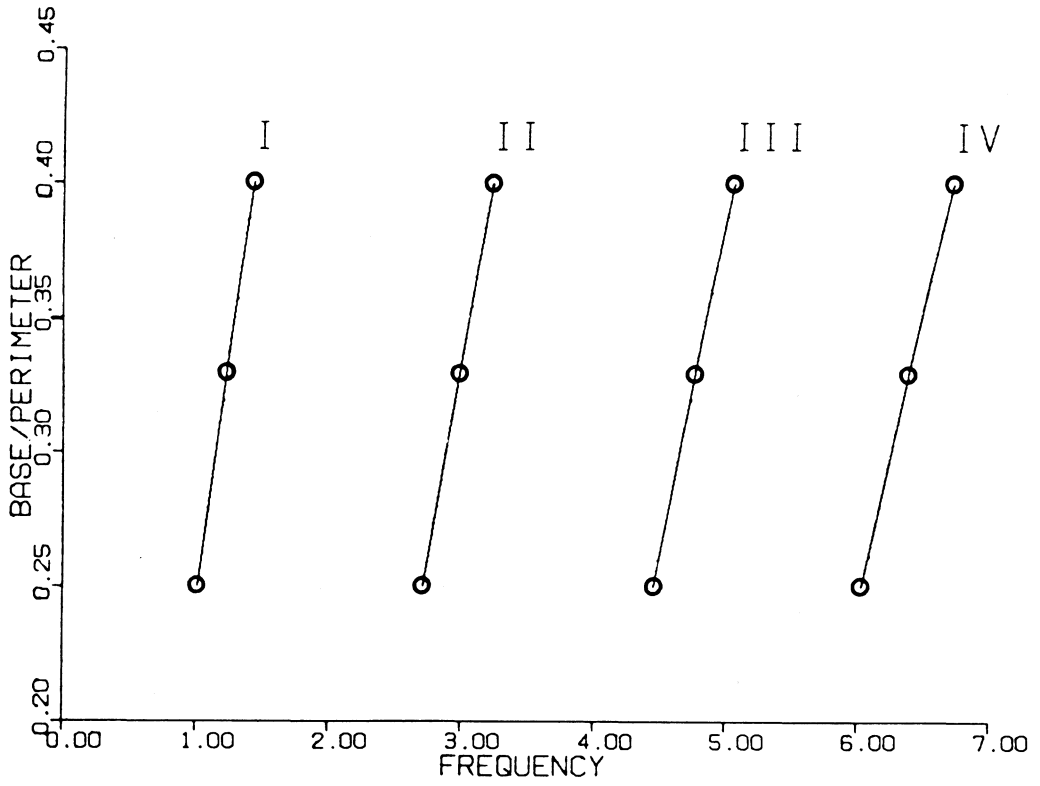


Figure 11. Base Length versus Frequency for $P/q = 0.005$

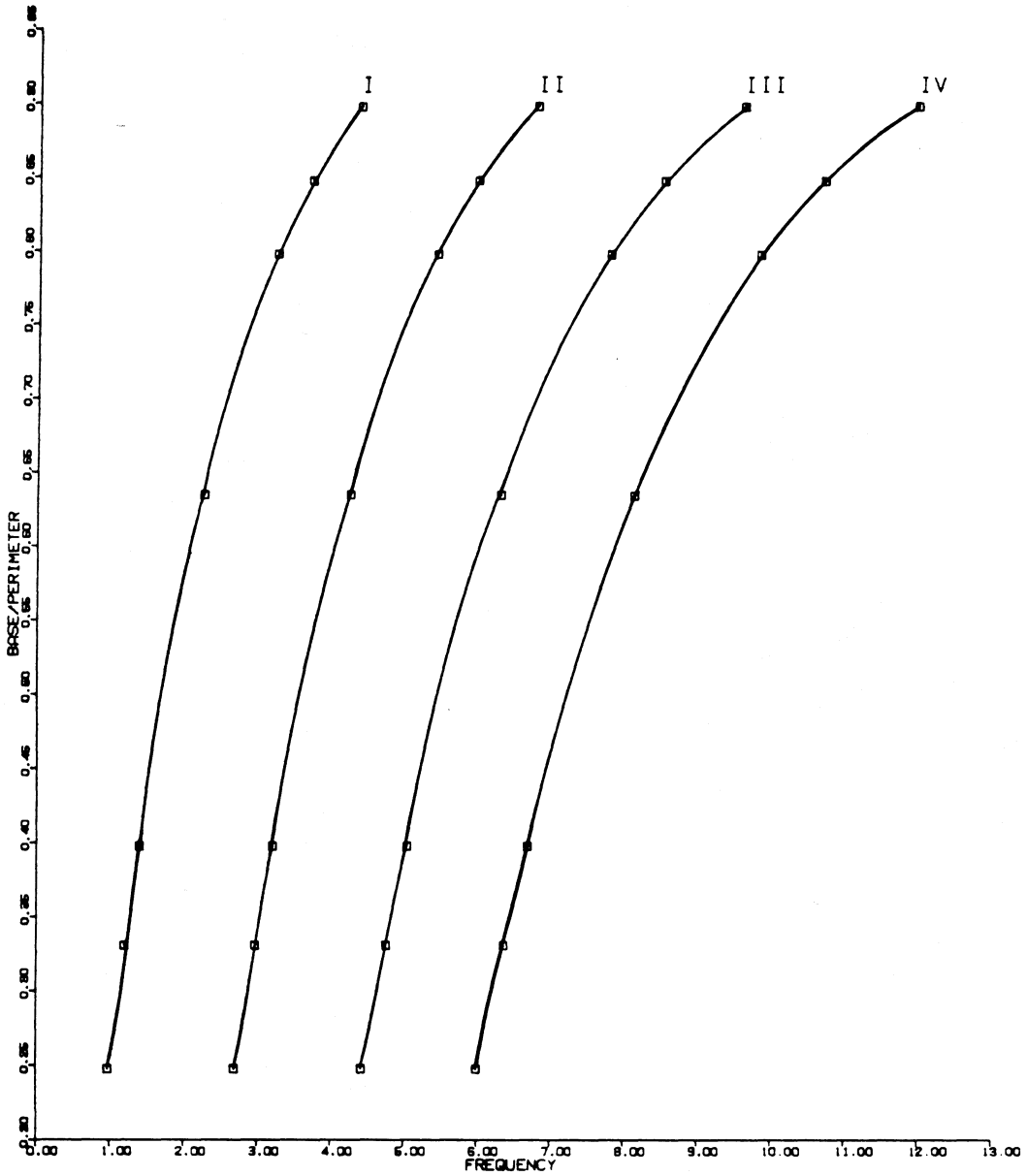


Figure 12. Base versus Frequency for $P/q = 0.0$ for a Range of Base Lengths

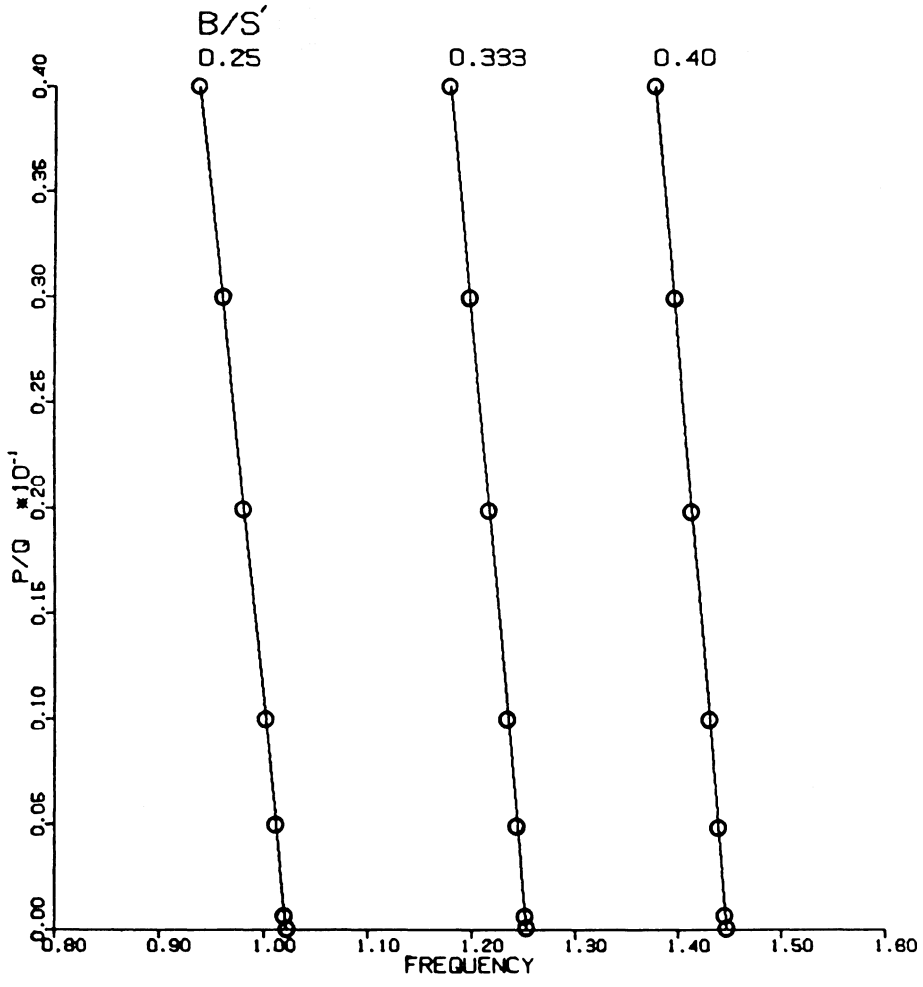


Figure 13. Weight versus Frequency for the First Mode of Vibration

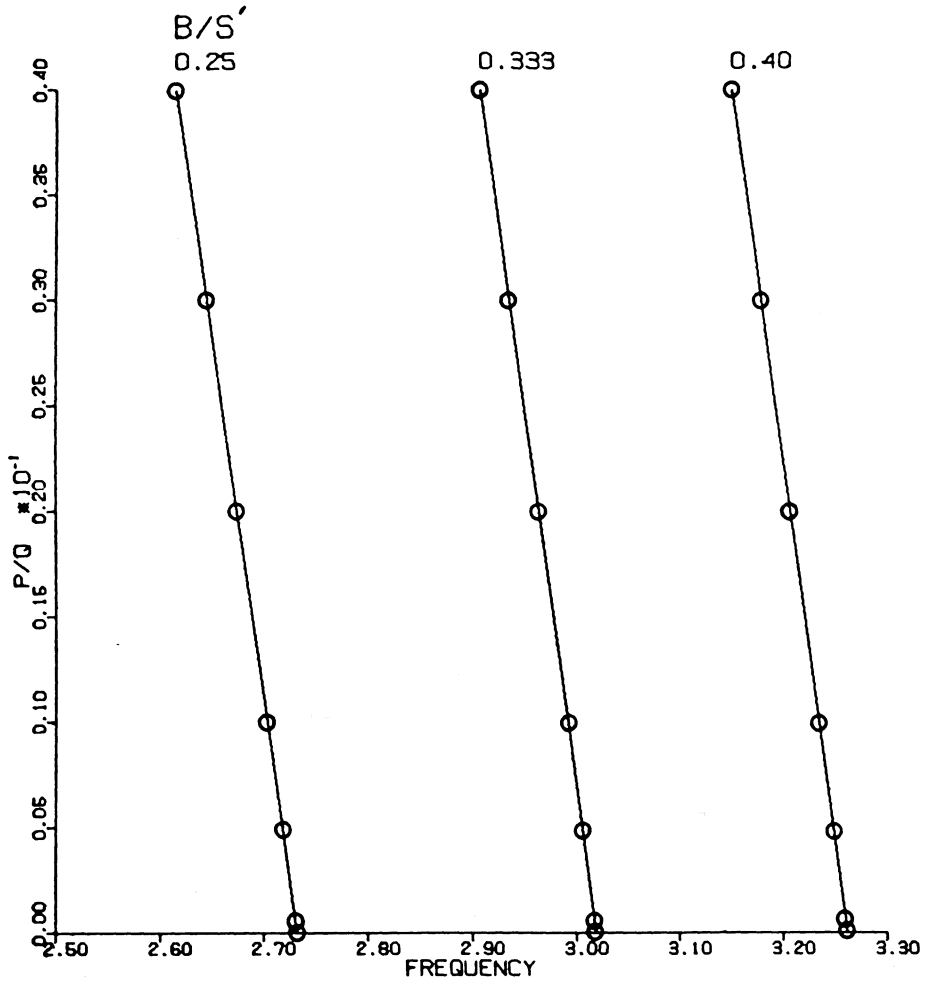


Figure 14. Weight versus Frequency for the Second Mode of Vibration

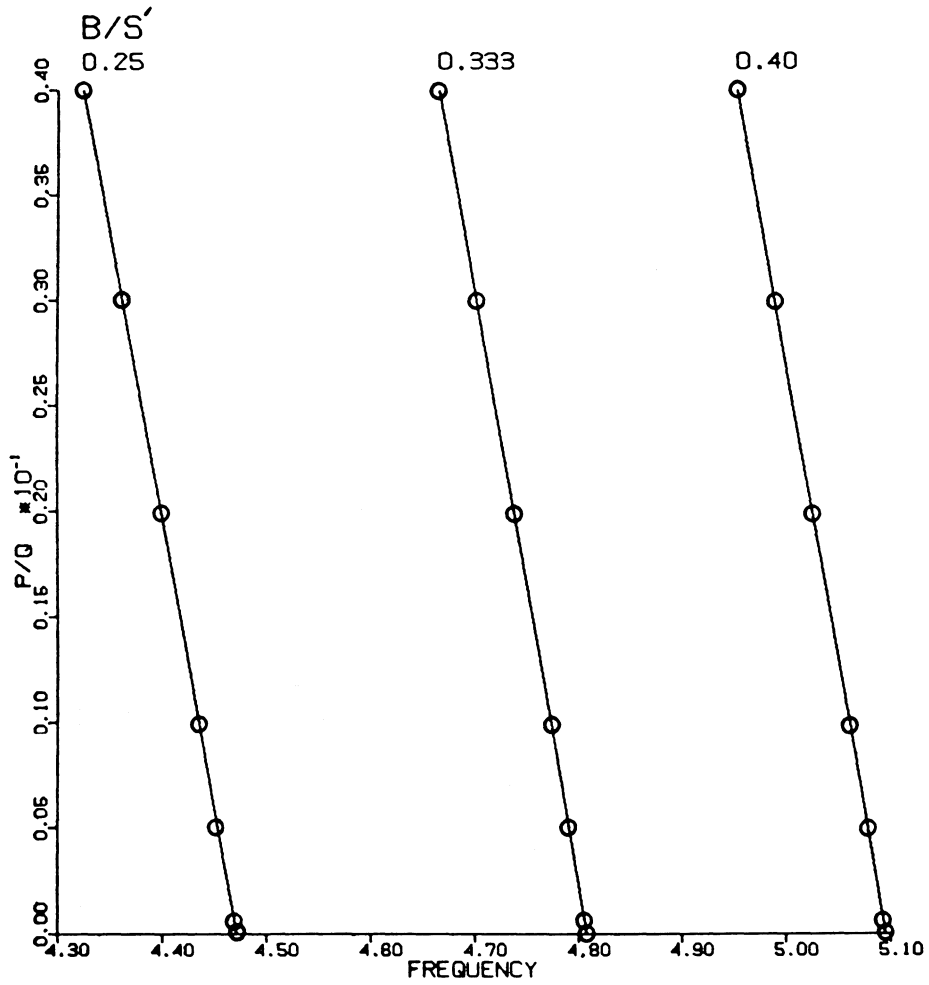


Figure 15. Weight versus Frequency for the Third Mode of Vibration

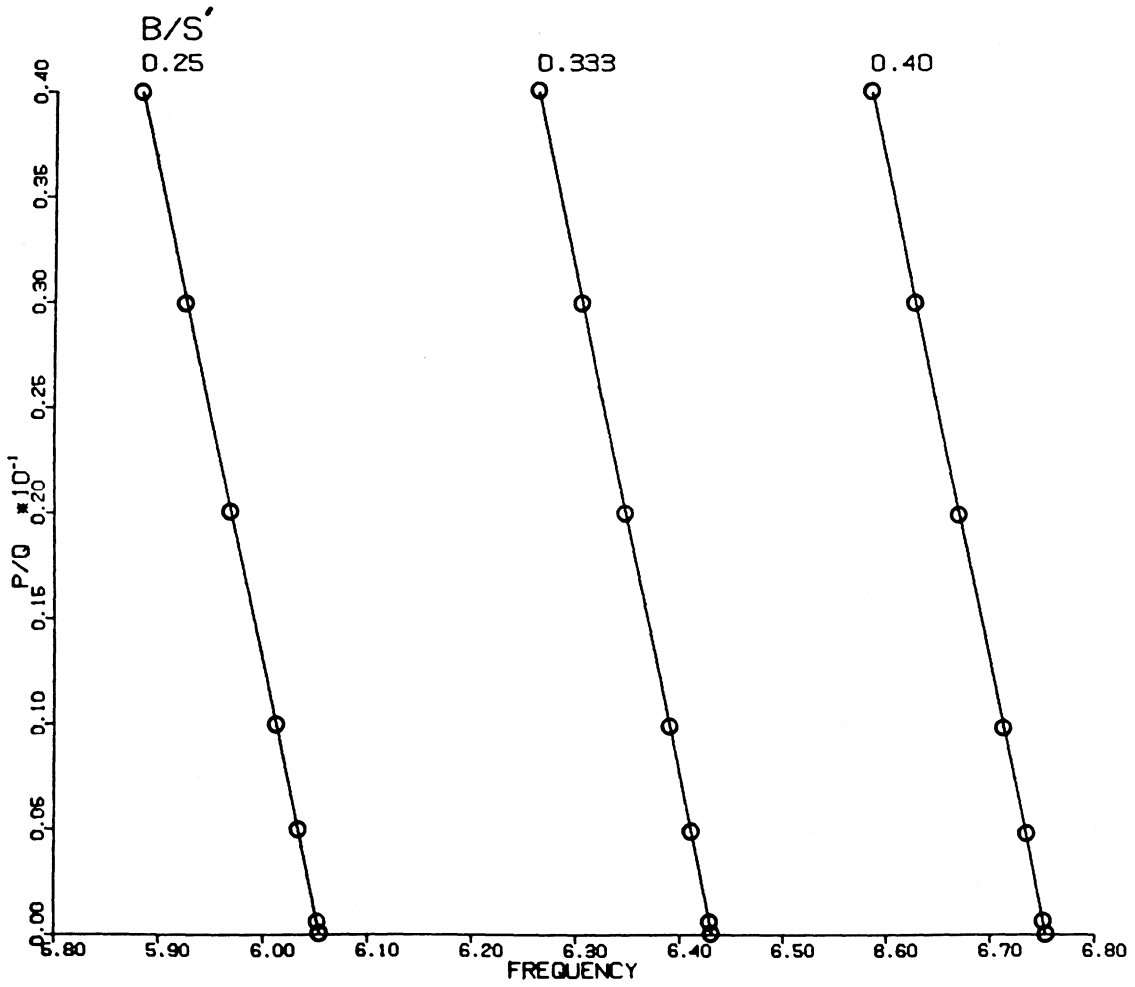


Figure 16. Weight versus Frequency for the Fourth Mode of Vibration

increased. It was also found that the slopes of the curves of the respective constant base to perimeter lengths became less negative with higher modes of vibration. It should be noted that the frequency, plotted on the abscissa, is illustrated over a limited range in order to utilize the same scale for all four diagrams, while making the figures as large as possible.

Chapter 5. Conclusions and Recommendations

5.1 Summary and Conclusions

In summary, a number of observations and conclusions have been made in this work on the effect of membrane weight on vibrations of an air-inflated dam. The conclusions reached in this study will be summarized below, and recommendations for future research on the subject will be made.

Assuming the effect of membrane extensibility to be negligible, it was found that the weight of the membrane does not have a significant effect on the static form of the air-inflated dam, which confirms the general conclusion of Parbery and others. The results of the static case showed that the membrane tension increased as the base to perimeter length ratio increased, which also agrees with the findings of Parbery. It was found that an increase in the weight of the membrane led to a reduction in the tension in the fabric. It was also found that the static forms of the weightless cases were always a portion of circle, with the base acting as a chord cutting the circle. With only the internal pressure, considered constant throughout the height of the structure, acting normal to the membrane surface at all points, the circular shape obtained is understandable.

For the analysis using the equations of motion derived in this study, the DYNAMIC program was developed, tested, and used. The eigenvalues obtained for the weightless, semicircular membrane structure were found to be only slightly different than those found by Firt and by Hsieh for the same structure. The deviations in the values computed, in comparison to those previously found, increased with larger eigenvalues. However, the shapes generally taken during vibration correspond to the lower eigenvalues, since less energy is required to achieve such forms, so the procedure developed here is believed to be acceptable for the most commonly occurring shapes. In addition, it is felt that the accuracy of the solutions obtained by this procedure can be improved by using a larger number of nodes on the cross-section of the structure, although the degree of improvement may be small.

The relationship between the base to perimeter length ratio and the frequency was checked for a realistic range of weights for constant modes of vibration. For base lengths between 0.25 and about 0.60, the relationship was almost linear, although at larger base lengths, the frequencies increased more rapidly with equivalent increases in the base length. Testing a series of weights for base lengths between 0.25 and 0.40 showed that an increase in weight had little effect on the frequency.

Finally, in a check of the weight to frequency relationship for base lengths of 0.25, 0.333, and 0.40, it was found that for a constant base length, an increase in weight led to a reduction in the frequencies. For the range of weights tested, the relationship between the weight and the frequency was almost linear for each of the four modes of vibration studied. It was seen from Figure 13 through Figure 16 that a major reduction in weight would have much less effect on the frequency than would an increase in the base length, which confirms the previous result.

With the results obtained in this study, it can be concluded that the effect of membrane weight on the vibration of flexible dams inflated by air pressure is minor. Furthermore, it is felt that if weight were neglected, the results obtained from the equations of motion would be conservative, since membrane weight causes a reduction in both tension and frequency when compared to the weightless case.

5.2 Recommendations for Future Studies

The conclusion of this study points to a number of possible avenues of future research. The effect of the weight on the higher order modes of vibration could be investigated, although it is believed that the same general results obtained for the lower modes would also be found for the higher modes. If such an investigation is conducted, the computer programs developed in this study might be utilized, although some improvements in their structure would be appropriate. The STATIC program uses the ZEROIN routine as a shooting method to find the initial angle at each node on the cross-section, but the initial tension must still be found by a trial and error procedure. The use of a shooting method to obtain the initial tension would not be extremely complicated, if the present file were imbedded inside the loop used for the method. The ZEROIN routine might be used again, or some other method tried, such as Parbery's suggestion of the use of the Newton-Raphson method.

Since the case studied considered only loadings of internal air pressure and weight, future research into the effects of weight on the vibration of the air-inflated dam might consider additional loading conditions, such as external water pressure acting on the upstream face, downstream face, or both faces of the structure, and the effect of overflow coupled with that of weight. The introduction of water, with its increase in pressure with greater depth, would present a complication in the analysis. Finally, it would be desirable to rederive the equations of motion for the structure, retaining all the nonlinear terms in v and w which were eliminated in this study. The results obtained from such equations might be compared to those obtained in this study, to determine the effect of the nonlinear terms.

Bibliography

1. Anwar, H. O., "Inflatable Dams," *Journal of the Hydraulics Division, ASCE*, Vol. 93, May, 1967, pp. 99-119.
2. Baker, P. J., Buxton, D. H., and Worster, R. C., "Model Tests on a Proposed Flexible Fabric Dam for the Mangla Project, Pakistan, Parts I and II," *British Hydromechanics Research Association Reports 803 and 827*, 1965.
3. Binnie, A. M., "The Theory of Flexible Dams Inflated by Water Pressure," *Journal of Hydraulic Research*, Vol. 11, 1973, pp. 61-68.
4. Binnie, G. M., Thomas, A. R., and Gwyther, J. R., "Inflatable Weir Used during Construction of Mangla Dam," *Proceedings of the Institution of Civil Engineers, Part 1: Design and Construction*, Vol. 54, 1973, pp. 625-639; Discussion by C. van Beesten, Vol. 56, 1974, pp. 189-191.
5. Crandall, S. H., *Engineering Analysis, A Survey of Numerical Procedures*, McGraw-Hill Book Company, New York, 1956, pp. 154-160, 243-249.
6. Eigensystem Subroutine Package (EISPACK), *Package F312 RGG, Real General Generalized Eigenproblem Solution Routine*, Argonne National Laboratory, Applied Mathematics Division, Argonne, Illinois, 1975.
7. Firt, V., *Statics, Formfinding and Dynamics of Air-Supported Membrane Structures*, Martinus Nijhoff Publishers, The Hague, 1983.
8. Forsythe, G. E., Malcolm, M. A., and Moler, C. B., *Computer Methods for Mathematical Computations*, Prentice-Hall, Englewood Cliffs, New Jersey, 1977, pp. 156-166.
9. Harrison, H. B., "The Analysis and Behavior of Inflatable Membrane Dams Under Static Loading," *Proceedings of the Institution of Civil Engineers*, Vol. 45, 1970, pp. 661-676; Closure, Vol. 48, 1971, pp. 137-139.
10. Henrych, J., *The Dynamics of Arches and Frames*, Elsevier Scientific Publishing Company, Amsterdam, 1981, pp. 21-27.

11. Hitch, N. M., and Narayanan, R., "Flexible Dams Inflated by Water," *Journal of Hydraulic Engineering*, Vol. 109, 1983, pp. 1044-1048.
12. Hsieh, J. C., Ph.D dissertation, in progress, Virginia Polytechnic Institute and State University, Blacksburg, Virginia.
13. International Mathematical and Statistical Libraries, Inc., *DVERK Differential Equation Solver Routine*, Houston, Texas, 1982.
14. International Mathematical and Statistical Libraries, Inc., *VSRTD Sorting Routine*, Houston, Texas, 1980.
15. Irvine, H. M., *Cable Structures*, The MIT Press, Cambridge, Massachusetts, 1981, pp. 31-38.
16. Maaskant, R., and Roorda, J., "Stability of Air-Supported Structures," *Journal of Engineering Mechanics*, Vol. 111, 1985, pp. 1487-1501.
17. Malcolm, D. J., and Glockner, P. G., "Collapse by Ponding of Air-Supported Spherical Caps," *Journal of the Structural Division, ASCE*, Vol. 107, 1981, pp. 1731-1742.
18. Marshall, E. R., "Some Technical and Economic Evaluations of an Inflatable Dam as an Emergency Flood Control System," M.S. Thesis, Virginia Polytechnic Institute and State University, Blacksburg, Virginia, 1984.
19. Namias, V., "Load-Supporting Fluid-Filled Cylindrical Membranes," *Journal of Applied Mechanics*, Vol. 51, 1985, pp. 1-6.
20. Parbery, R. D., "A Continuous Method of Analysis for the Inflatable Dam," *Proceedings of the Institution of Civil Engineers, Part 2*, Vol. 61, 1976, pp. 725-736.
21. Parbery, R. D., "Factors Affecting the Membrane Dam Inflated by Air Pressure," *Proceedings of the Institution of Civil Engineers, Part 2*, Vol. 65, 1978, pp. 645-654.
22. "Presenting the Imbertson Fabridam," Firestone Coated Fabrics Company, Akron, Ohio, 1968.
23. "Report of an Investigation into the Failure of an Inflatable Dam," University of Sidney, Civil Engineering Laboratories, Investigation Report No. S89, May, 1969.
24. Shepherd, E. M., McKay, F. A., and Hodgen, V. T., "The Fabridam Extension on Koombooloomba Dam of the Tully Falls Hydro-Electric Power Project," *Journal of the Institution of Engineers, Australia*, Vol. 41, 1969, pp. 1-7.
25. Szyszkowski, W., and Glockner, P. G., "Finite Deformation and Stability Behavior of Cylindrical Membranes Subjected to Symmetric Line Loads," *International Journal of Non-Linear Mechanics*, Vol. 20, 1985, pp. 177-198.
26. Wang, C. Y., and Watson, L. T., "The Fluid-Filled Cylindrical Membrane Container," *Journal of Engineering Mathematics*, Vol. 15, 1981, pp. 81-88.
27. Watson, R., "A Note on the Shapes of Flexible Dams," *Journal of Hydraulic Research*, Vol. 23, 1985, pp. 179-194.

Appendix A. The Equations of Motion

A.1. The Static Equations

It was shown in Chapters 3 and 4 that the equations for the static shape of the dam are needed to establish initial conditions for a particular case when the dynamic analysis is performed. A set of differential equations for the static shape were derived in Chapter 3, and are repeated below, in their dimensional form, for easy reference in the following derivations:

$$\frac{dT_1}{dS} = P \sin \psi_0 \quad [3 - 4]$$

$$\frac{dy_0}{dS} = \sin \psi_0 \quad [3 - 5]$$

$$\frac{dx_0}{dS} = \cos \psi_0 \quad [3 - 6]$$

$$T_1 = Py_0 + T_0 \quad [3 - 9]$$

$$\frac{d\psi_0}{dS} = \frac{-q + P \cos \psi_0}{Py_0 + T_0} \quad [3 - 10]$$

A.2. Derivation of the Dynamic Equations

An element of the membrane is illustrated in Figure 17 on page 61. It is very similar to Figure 7 on page 24, except that the components of movement, v and w , are shown in their positive directions. It should also be noted that the equation of motion requires a mass term. The mass per unit length of the membrane will be denoted μ .

An equation of motion can be derived in each of the two defined directions of motion, in order to obtain the dynamic equations for the system. If motion in the tangential direction is considered, the following equation results:

$$\mu dS \frac{\partial^2 v}{\partial t^2} = -T + \left(T + \frac{\partial T}{\partial S} dS + \dots \right) \cos d\psi - P \sin \psi dS$$

where μdS is the mass, $\partial^2 v / \partial t^2$ is the acceleration, and the terms to the right of the equal sign are forces acting on the cross-section in the tangential direction. If $d\psi$ is very small, then $\cos d\psi \cong 1$.

Simplifying the equation and rearranging terms yields:

$$\mu \frac{\partial^2 v}{\partial t^2} = \frac{\partial T}{\partial S} - P \sin \psi \quad [A - 1]$$

Considering motion in the normal direction, it is found that:

$$\mu dS \frac{\partial^2 w}{\partial t^2} = \left(T + \frac{\partial T}{\partial S} dS + \dots \right) \sin d\psi - P \cos \psi dS + q dS$$

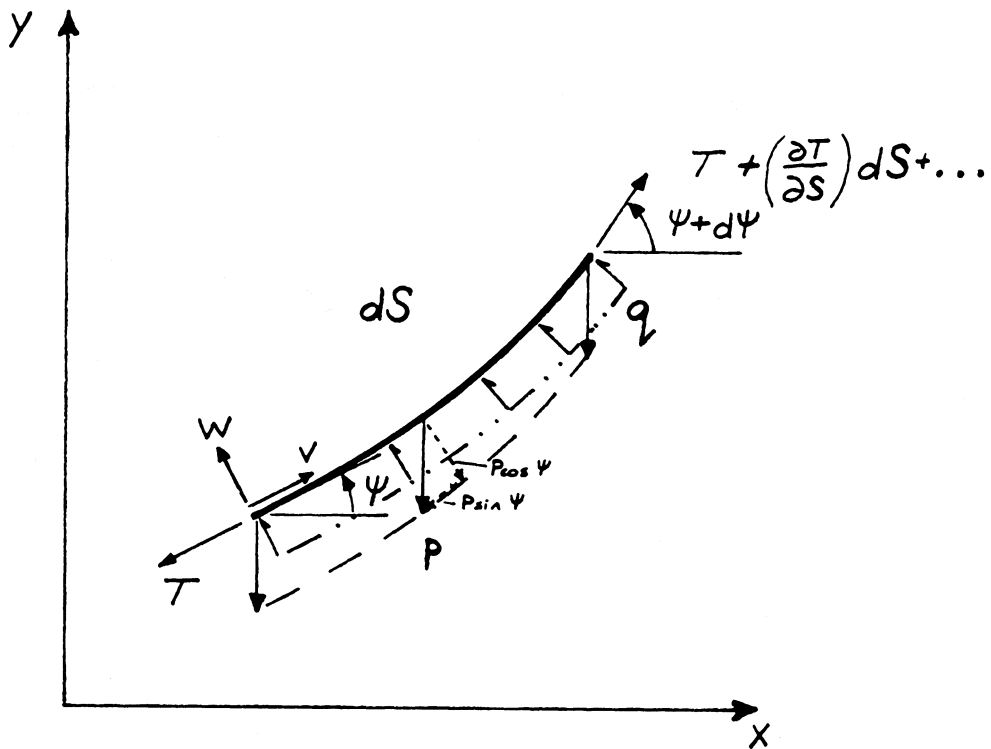


Figure 17. An Element of the Cross-Section with Dynamic Loading

As before, $d\psi$ is considered to be small, yielding $\sin d\psi \cong d\psi$. Substituting, dividing by dS , and letting $dS \rightarrow 0$, the previous equation can be rearranged to become:

$$\mu \frac{\partial^2 w}{\partial t^2} = T \frac{\partial \psi}{\partial S} - P \cos \psi + q \quad [A - 2]$$

Equation [A-2] can be rearranged to give:

$$T \frac{\partial \psi}{\partial S} = \mu \frac{\partial^2 w}{\partial t^2} + P \cos \psi - q$$

or,

$$T = \left(\frac{\partial \psi}{\partial S} \right)^{-1} \left(\mu \frac{\partial^2 w}{\partial t^2} + P \cos \psi - q \right)$$

This can be differentiated with respect to S to yield:

$$\begin{aligned} \frac{\partial T}{\partial S} = & - \left(\frac{\partial \psi}{\partial S} \right)^{-2} \left(\frac{\partial^2 \psi}{\partial S^2} \right) \left[\mu \frac{\partial^2 w}{\partial t^2} + P \cos \psi - q \right] \\ & + \left(\frac{\partial \psi}{\partial S} \right)^{-1} \left[\mu \frac{\partial^3 w}{\partial S \partial t^2} - P \frac{\partial \psi}{\partial S} \sin \psi - \frac{\partial q}{\partial S} \right] \end{aligned}$$

Substituting this equation into Eq. [A-1] gives:

$$\begin{aligned} \mu \frac{\partial^2 v}{\partial t^2} = & - \left(\frac{\partial \psi}{\partial S} \right)^{-2} \left(\frac{\partial^2 \psi}{\partial S^2} \right) \left[\mu \frac{\partial^2 w}{\partial t^2} + P \cos \psi - q \right] \\ & + \left(\frac{\partial \psi}{\partial S} \right)^{-1} \left[\mu \frac{\partial^3 w}{\partial S \partial t^2} - P \frac{\partial \psi}{\partial S} \sin \psi - \frac{\partial q}{\partial S} \right] - P \sin \psi \end{aligned}$$

If this equation is multiplied by $(\partial \psi / \partial S)^2$, and similar terms are combined, the following equation is obtained:

$$\begin{aligned} \mu \frac{\partial^2 v}{\partial t^2} \left(\frac{\partial \psi}{\partial S} \right)^2 = & -\mu \frac{\partial^2 w}{\partial t^2} \frac{\partial^2 \psi}{\partial S^2} - P \frac{\partial^2 \psi}{\partial S^2} \cos \psi + q \frac{\partial^2 \psi}{\partial S^2} + \mu \frac{\partial \psi}{\partial S} \frac{\partial^3 w}{\partial S \partial t^2} \\ & - 2P \left(\frac{\partial \psi}{\partial S} \right)^2 \sin \psi - \frac{\partial \psi}{\partial S} \frac{\partial q}{\partial S} \end{aligned} \quad [A - 3]$$

The relationship between $\partial\psi/\partial S$ and $d\psi_0/dS$ can be found using derivations presented by Henrych [10]. The curvature of the deformed shape (dynamic case) can be found by adding the change in curvature to the curvature of the original shape (static case). Using the terminology of this study, Henrych's equation for the change in curvature is:

$$\Delta K = \frac{1}{Q} \left[\frac{\partial^2 w}{\partial S^2} + \left(\frac{d\psi_0}{dS} \right)^2 w + \frac{d^2 \psi_0}{dS^2} v \right]$$

where $Q = 1 + \frac{\partial v}{\partial S} - \frac{d\psi_0}{dS} w$. For a linear analysis, the last two terms of Q may be neglected. With the original curvature defined as $K_1 = d\psi_0/dS$ and the resulting curvature defined as $K_2 = \partial\psi/\partial S$, the relationship between the curvature at the two stages is $K_2 = K_1 + \Delta K$, or:

$$\frac{\partial \psi}{\partial S} = \frac{d\psi_0}{dS} + \frac{\partial^2 w}{\partial S^2} + \left(\frac{d\psi_0}{dS} \right)^2 w + \frac{d^2 \psi_0}{dS^2} v \quad [A - 4]$$

It is possible to integrate Eq. [A-4] to obtain:

$$\psi = \psi_0 + \frac{\partial w}{\partial S} + \int \left[\left(\frac{d\psi_0}{dS} \right)^2 w + \frac{d^2 \psi_0}{dS^2} v \right] dS$$

Since the second half of the equation is more difficult to integrate, a way to reduce the equation is sought.

The definition of strain, $\varepsilon = \frac{\Delta \ell}{\ell}$, can be used to obtain one displacement in terms of the other. The original and elongated elements, N and M , respectively, are illustrated in Figure 18 on page 64. The length of N is found to be:

$$N = \lim_{dR \rightarrow 0} \frac{R + (R + dR)}{2} d\psi = \frac{2R}{2} = R d\psi$$

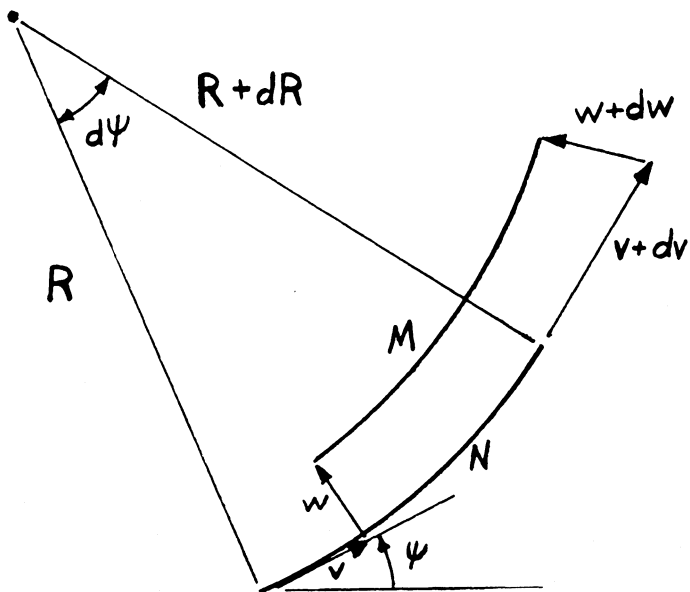


Figure 18. Original and Elongated Elements Used in Strain Relationship

Similarly, M 's length is discovered to be:

$$\begin{aligned} M &= (R - w)d\psi + \left(\frac{v + dv}{R + dR}\right)(R + dR - w - dw) - \left(\frac{v}{R}\right)(R - w) \\ &= Rd\psi - wd\psi + \left(\frac{vR + Rdv - vw - wdv - vdw - dvdw}{R + dR}\right) - v + \frac{vw}{R} \end{aligned}$$

In general, it can be assumed that the radius of the arc is much larger than the change in radius which occurs in the length, N , so $R \cong R + dR$. Making this approximation, and simplifying the resulting equation, the length of M becomes:

$$M = Rd\psi - wd\psi + dv - \frac{wdv}{R} - \frac{vdw}{R} - \frac{dvdw}{R}$$

It is also probable that the displacement in the normal direction will be small in comparison to the length of the radius of the element. By making this assumption, it is possible to neglect the last three terms in the preceding equation, which reduces to:

$$M = Rd\psi - wd\psi + dv$$

In terms of M and N , the strain equation is

$$\varepsilon = \frac{M - N}{N}$$

From the derivation of the static equations of the system, it is recalled that it was assumed that the membrane material was inextensible. A material that does not extend under stress experiences no strain, so according to the assumption, $\varepsilon = 0$. When the components are substituted into the strain equation, the following results are obtained:

$$0 = \frac{Rd\psi - wd\psi + dv - Rd\psi}{Rd\psi} = \frac{1}{R} \left(\frac{dv}{d\psi} - w \right)$$

Multiplying by R , the equation can be rearranged to find:

$$w = \frac{dv}{d\psi}$$

The chain rule for derivatives can be used to put w in a different form:

$$w = \frac{\partial v}{\partial \psi} = \frac{\partial v}{\partial S} \frac{\partial S}{\partial \psi}$$

This is easily transformed into:

$$w = \left(\frac{\partial \psi}{\partial S} \right)^{-1} \frac{\partial v}{\partial S}$$

Since the nonlinear terms are relatively insignificant, if only the linear terms of Eq. [A-4] are retained, and substituted into the above equation, it is found that:

$$w = \left(\frac{d\psi_0}{dS} \right)^{-1} \frac{\partial v}{\partial S} \quad [A - 5]$$

Also, using Eq. [A-5] in the integration of Eq. [A-4], one obtains:

$$\psi = \psi_0 + \frac{\partial w}{\partial S} + \frac{d\psi_0}{dS} v \quad [A - 6]$$

In order to simplify the equations, a simplified notation will be adopted for the derivatives of ψ with respect to S , as shown below:

$$A = \psi_{0S} = \frac{d\psi_0}{dS}$$

$$B = \psi_{0SS} = \frac{d^2\psi_0}{dS^2}$$

$$C = \psi_{0SSS} = \frac{d^3\psi_0}{dS^3}$$

$$D = \Psi_{0SSSS} = \frac{d^4 \Psi_0}{dS^4}$$

In addition, derivatives of v and w will be denoted by the appropriate letter with as many sub S 's as the order of the derivative. Finally, derivatives with respect to time will be denoted by the appropriate letter with the number of sub t 's equaling the number of the order of the derivative. These substitutions will reduce the length of the equations, and make them look less formidable, while retaining their meaning.

Although all components of Eq. [A-3] have been obtained, substitution will be easier if each component is put in the same form as in the equation. Since the terms v and w are considered to be small, nonlinear combinations of these terms are eliminated prior to the combination of components, since the nonlinear forms will be negligible. Therefore, it is found that:

$$\begin{aligned} \left(\frac{\partial \Psi}{\partial S}\right)^2 = & A^2 + 2A \frac{\partial^2 w}{\partial S^2} + 2A^3 w + 2ABv + \left(\frac{\partial^2 w}{\partial S^2}\right)^2 + 2 \frac{\partial^2 w}{\partial S^2} A^2 w \\ & + 2 \frac{\partial^2 w}{\partial S^2} Bv + A^4 w^2 + 2A^2 Bvw + B^2 v^2 \end{aligned}$$

Eliminating the nonlinear terms involving v and w , the equation reduces to:

$$\left(\frac{\partial \Psi}{\partial S}\right)^2 = A^2 + 2Aw_{SS} + 2A^3 w + 2ABv$$

Then one can write

$$\left(\frac{\partial^2 v}{\partial t^2}\right) \left(\frac{\partial \Psi}{\partial S}\right)^2 = A^2 \frac{\partial^2 v}{\partial t^2} + 2A \frac{\partial^2 w}{\partial S^2} \frac{\partial^2 v}{\partial t^2} + 2A^3 w \frac{\partial^2 v}{\partial t^2} + 2ABv \frac{\partial^2 v}{\partial t^2}$$

When nonlinear terms are dropped, the resulting equation is:

$$\left(\frac{\partial^2 v}{\partial t^2}\right) \left(\frac{\partial \Psi}{\partial S}\right)^2 = A^2 v_{tt}$$

Using the simplified notation, the first derivative of Eq. [A-4] is:

$$\frac{\partial^2 \psi}{\partial S^2} = B + w_{SSS} + 2ABw + A^2 w_S + Cv + Bv_S$$

The final components of Eq. [A-3] to be obtained are $\cos \psi$ and $\sin \psi$. If ψ is arbitrarily set equal to $\alpha + \beta$, then the trigonometric identities,

$$\cos(\alpha + \beta) = \cos \alpha \cos \beta - \sin \alpha \sin \beta$$

$$\sin(\alpha + \beta) = \sin \alpha \cos \beta + \cos \alpha \sin \beta$$

can be used. If ψ , from Eq. [A-6], is divided as $\alpha = \psi_0$ and $\beta = \partial w / \partial S + (d\psi_0 / dS)v$, then β will be small since both of its components are small, so $\cos \beta \cong 1$ and $\sin \beta \cong \beta$. Therefore, the geometric identities reduce to the following forms in the simplified notation:

$$\cos \psi \cong \cos \psi_0 - (w_S + Av) \sin \psi_0$$

$$\sin \psi \cong \sin \psi_0 + (w_S + Av) \cos \psi_0$$

The components of Eq. [A-3] can now be substituted, yielding:

$$\begin{aligned} \mu A^2 v_{tt} = & -\mu w_{tt}(B + w_{SSS} + 2ABw + A^2 w_S + Cv + Bv_S) - PB \cos \psi_0 \\ & - Pw_{SSS} \cos \psi_0 - 2ABPw \cos \psi_0 - PA^2 w_S \cos \psi_0 - PCv \cos \psi_0 \\ & - PBv_S \cos \psi_0 + PB(w_S + Av) \sin \psi_0 + Pw_{SSS}(w_S + Av) \sin \psi_0 \\ & + 2PABw(w_S + Av) \sin \psi_0 + PA^2 w_S(w_S + Av) \sin \psi_0 + PCv(w_S + Av) \sin \psi_0 \\ & + PBv_S(w_S + Av) \sin \psi_0 + qB + qw_{SSS} + 2ABqw + A^2 qw_S + Cqv + Bqv_S \\ & + \mu Aw_{Stt} + \mu w_{SS} w_{Stt} + \mu A^2 w w_{Stt} + \mu Bv w_{Stt} \\ & - 2PA^2 \sin \psi_0 - 4PAw_{SS} \sin \psi_0 - 4PA^3 w \sin \psi_0 - 4PABv \sin \psi_0 \\ & - 2PA^2(w_S + Av) \cos \psi_0 - 4PAw_{SS}(w_S + Av) \cos \psi_0 - 4PA^3 w(w_S + Av) \cos \psi_0 \\ & - 4PABv(w_S + Av) \cos \psi_0 - Aq_S - w_{SS}q_S - A^2 wq_S - Bvq_S \end{aligned}$$

When the equation is examined, it is found to have a number of nonlinear terms containing v , w , or both. If these terms are eliminated, the equation reduces to:

$$\begin{aligned}
\mu A^2 v_{tt} = & -\mu B w_{tt} - PB \cos \psi_0 - P w_{SSS} \cos \psi_0 - 2PABw \cos \psi_0 \\
& - PA^2 w_S \cos \psi_0 - PCv \cos \psi_0 - PBv_S \cos \psi_0 + PBw_S \sin \psi_0 \\
& + PABv \sin \psi_0 + qB + qw_{SSS} + 2ABqw + A^2 qw_S + Cqv \\
& + Bqv_S + \mu Aw_{Stt} - 2PA^2 \sin \psi_0 - 4PAw_{SS} \sin \psi_0 \\
& - 4PA^3 w \sin \psi_0 - 4PABv \sin \psi_0 - 2PA^2 w_S \cos \psi_0 - 2PA^3 v \cos \psi_0 \\
& - Aq_S - w_{SS}q_S - A^2 wq_S - Bvq_S
\end{aligned} \tag{A-7}$$

It is noted that several terms in Eq. [A-7] do not contain either v or w . These terms can be gathered into one term, γ :

$$\gamma = -PB \cos \psi_0 + qB - 2PA^2 \sin \psi_0 - Aq_S \tag{A-8}$$

It is possible to eliminate q from the equation by using static Equations [3-9] and [3-10], which combine to give:

$$\frac{d\psi_0}{dS} = \frac{-q + P \cos \psi_0}{T_1}$$

This can be rearranged to give

$$q = P \cos \psi_0 - AT_1 \tag{A-9}$$

and the first derivative of q with respect to S is found to be

$$q_S = -PA \sin \psi_0 - BT_1 - A \frac{dT_1}{dS}$$

From Eq. [3-4], it is seen that dT_1/dS can be placed in terms of $P \sin \psi_0$, so Eq. [A-9] becomes:

$$q_S = -2PA \sin \psi_0 - BT_1 \tag{A-10}$$

Substituting Equations [A-9] and [A-10] into Eq. [A-8] yields:

$$\gamma = -PB \cos \psi_0 + PB \cos \psi_0 - ABT_1 - 2PA^2 \sin \psi_0 - (-2PA^2 \sin \psi_0 - ABT_1)$$

When similar terms are combined, it is found that all terms are eliminated, or $\gamma = 0$, so all terms in Eq. [A-7] not involving either v or w can be dropped from the equation. This was to be expected, since if v and w are zero, there is no movement of the cross-section of the dam, so all other terms must add up to zero.

The q terms in Eq. [A-7] can be eliminated by substituting in Equations [A-9] and [A-10]:

$$\begin{aligned} \mu A^2 v_{tt} = & -\mu B w_{tt} - P w_{SSS} \cos \psi_0 - 2PABw \cos \psi_0 - PA^2 w_S \cos \psi_0 \\ & - PCv \cos \psi_0 - PBv_S \cos \psi_0 + PBw_S \sin \psi_0 + PABv \sin \psi_0 \\ & + P w_{SSS} \cos \psi_0 - AT_1 w_{SSS} + 2PABw \cos \psi_0 - 2A^2 BT_1 w \\ & + PA^2 w_S \cos \psi_0 - A^3 T_1 w_S + PCv \cos \psi_0 - ACT_1 v + PBv_S \cos \psi_0 \\ & - ABT_1 v_S + \mu A w_{Stt} - 4PAw_{SS} \sin \psi_0 - 4PA^3 w \sin \psi_0 - 4PABv \sin \psi_0 \\ & - 2PA^2 w_S \cos \psi_0 - 2PA^3 v \cos \psi_0 + 2PAw_{SS} \sin \psi_0 + BT_1 w_{SS} \\ & + 2PA^3 w \sin \psi_0 + A^2 BT_1 w + 2PABv \sin \psi_0 + B^2 T_1 v \end{aligned}$$

When similar terms are combined, the equation reduces to the following:

$$\begin{aligned} \mu A^2 v_{tt} = & -\mu B w_{tt} + PBw_S \sin \psi_0 - AT_1 w_{SSS} - A^2 BT_1 w - A^3 T_1 w_S \\ & - ACT_1 v - ABT_1 v_S + \mu A w_{Stt} - 2PAw_{SS} \sin \psi_0 - 2PA^3 w \sin \psi_0 \quad [A - 11] \\ & - PABv \sin \psi_0 - 2PA^2 w_S \cos \psi_0 - 2PA^3 v \cos \psi_0 + BT_1 w_{SS} + B^2 T_1 v \end{aligned}$$

The relationship between v and w was shown in Eq. [A-5]. In the simplified notation, this equation becomes:

$$w = A^{-1} v_S$$

Since all three terms are functions of S , and both v and w are functions of t , it is possible to take derivatives with respect to these variables to obtain w in terms of v in order to substitute into Eq. [A-11] to eliminate the w terms. When the appropriate derivatives are taken, the following equations in simplified notation result:

$$w_S = -A^{-2}Bv_S + A^{-1}v_{SS}$$

$$w_{SS} = 2A^{-3}B^2v_S - A^{-2}Cv_S - 2A^{-2}Bv_{SS} + A^{-1}v_{SSS}$$

$$w_{SSS} = -6A^{-4}B^3v_S + 6A^{-3}BCv_S + 6A^{-3}B^2v_{SS} - A^{-2}Dv_S - 3A^{-2}Cv_{SS} \\ - 3A^{-2}Bv_{SSS} + A^{-1}v_{SSSS}$$

$$w_{tt} = A^{-1}v_{Stt}$$

$$w_{Stt} = -A^{-2}Bv_{Stt} + A^{-1}v_{SSStt}$$

After substituting these equations and combining similar terms, Eq. [A-11] becomes:

$$\begin{aligned} \mu A^2 v_{tt} = & -2\mu A^{-1}Bv_{Stt} - 5PA^{-2}B^2v_S \sin \psi_0 + 5PA^{-1}Bv_{SS} \sin \psi_0 \\ & + 8A^{-3}B^3T_1v_S - 7A^{-2}BCT_1v_S - 8A^{-2}B^2T_1v_{SS} + A^{-1}DT_1v_S \\ & + 3A^{-1}CT_1v_{SS} + 4A^{-1}BT_1v_{SSS} - T_1v_{SSSS} - A^2T_1v_{SS} - ACT_1v \\ & - ABT_1v_S + \mu v_{SSStt} + 2PA^{-1}Cv_S \sin \psi_0 - 2Pv_{SSS} \sin \psi_0 - 2PA^2v_S \sin \psi_0 \\ & - PABv \sin \psi_0 + 2PBv_S \cos \psi_0 - 2PAv_{SS} \cos \psi_0 - 2PA^3v \cos \psi_0 + B^2T_1v \end{aligned} \quad [A - 12]$$

Since the w terms have been eliminated in Eq. [A-12], the equation can be simplified by combining terms according to the order of the derivatives of v . The resulting equation is:

$$\begin{aligned} 0 = v[& -PAB \sin \psi_0 - 2PA^3 \cos \psi_0 - ACT_1 + B^2T_1] \\ & + v_S[\sin \psi_0(-5PA^{-2}B^2 + 2PA^{-1}C - 2PA^2) \\ & + 2PB \cos \psi_0 + 8A^{-3}B^3T_1 - 7A^{-2}BCT_1 + A^{-1}DT_1 - ABT_1] \\ & + v_{SS}[5PA^{-1}B \sin \psi_0 - 2PA \cos \psi_0 - 8A^{-2}B^2T_1 + 3A^{-1}CT_1 - A^2T_1] \\ & + v_{SSS}[-2P \sin \psi_0 + 4A^{-1}BT_1] \\ & + v_{SSSS}[-T_1] \\ & + v_{Stt}[-2\mu A^{-1}B] \\ & + v_{SSStt}[\mu] \\ & + v_{tt}[-\mu A^2] \end{aligned} \quad [A - 13]$$

It should be recalled that the equations of equilibrium used in the derivation of the dynamic equations were in their dimensional form, and additional equations obtained using the equation of motion also contain dimensional values. It is desirable to nondimensionalize the equations, so the same procedure used for the static equations will be followed. The nondimensional terms used are repeated below:

$$\frac{x_0}{\ell} = x \quad [A - a]$$

$$\frac{y_0}{\ell} = y \quad [A - b]$$

$$\frac{S}{\ell} = \bar{S} \quad [A - c]$$

$$\frac{P}{q} = p \quad [A - d]$$

$$\frac{T_1}{q\ell} = \bar{T}_1 \quad [A - e]$$

where x , y , \bar{S} , p , and \bar{T}_1 are nondimensional terms, and ℓ is a generalized length term. The additional terms v and t can be made nondimensional by:

$$\frac{v}{\ell} = \bar{v} \quad [A - f]$$

$$\beta t = \bar{t} \quad [A - g]$$

where β is a nondimensionalizing constant for time.

Using these equations, it is possible to place derivatives with respect to S in their nondimensional form as:

$$A = \frac{d\psi_0}{dS} = \frac{1}{\ell} \frac{d\psi_0}{d\bar{S}} = \frac{1}{\ell} \bar{A}$$

$$B = \frac{d^2 \psi_0}{dS^2} = \frac{1}{\ell^2} \frac{d^2 \psi_0}{d\bar{S}^2} = \frac{1}{\ell^2} \bar{B}$$

$$C = \frac{d^3 \psi_0}{dS^3} = \frac{1}{\ell^3} \frac{d^3 \psi_0}{d\bar{S}^3} = \frac{1}{\ell^3} \bar{C}$$

$$D = \frac{d^4 \psi_0}{dS^4} = \frac{1}{\ell^4} \frac{d^4 \psi_0}{d\bar{S}^4} = \frac{1}{\ell^4} \bar{D}$$

$$v_S = \frac{\partial v}{\partial S} = \frac{\ell}{\ell} \frac{\partial \bar{v}}{\partial \bar{S}} = \bar{v}_{\bar{S}}$$

$$v_{SS} = \frac{\partial^2 v}{\partial S^2} = \frac{\ell}{\ell^2} \frac{\partial^2 \bar{v}}{\partial \bar{S}^2} = \frac{1}{\ell} \bar{v}_{\bar{S}\bar{S}}$$

$$v_{SSS} = \frac{\partial^3 v}{\partial S^3} = \frac{\ell}{\ell^3} \frac{\partial^3 \bar{v}}{\partial \bar{S}^3} = \frac{1}{\ell^2} \bar{v}_{\bar{S}\bar{S}\bar{S}}$$

$$v_{SSSS} = \frac{\partial^4 v}{\partial S^4} = \frac{\ell}{\ell^4} \frac{\partial^4 \bar{v}}{\partial \bar{S}^4} = \frac{1}{\ell^3} \bar{v}_{\bar{S}\bar{S}\bar{S}\bar{S}}$$

$$v_{S\bar{t}\bar{t}} = \frac{\partial^3 v}{\partial S \partial \bar{t}^2} = \frac{\ell}{\ell} \beta^2 \frac{\partial^3 \bar{v}}{\partial \bar{S} \partial \bar{t}^2} = \beta^2 \bar{v}_{\bar{S}\bar{t}\bar{t}}$$

$$v_{SS\bar{t}\bar{t}} = \frac{\partial^4 v}{\partial S^2 \partial \bar{t}^2} = \frac{\ell}{\ell^2} \beta^2 \frac{\partial^4 \bar{v}}{\partial \bar{S}^2 \partial \bar{t}^2} = \frac{\beta^2}{\ell} \bar{v}_{\bar{S}\bar{S}\bar{t}\bar{t}}$$

$$v_{\bar{t}\bar{t}} = \frac{\partial^2 v}{\partial \bar{t}^2} = \ell \beta^2 \frac{\partial^2 \bar{v}}{\partial \bar{t}^2} = \ell \beta^2 \bar{v}_{\bar{t}\bar{t}}$$

It is noted that in Eq. [A-g], β , a nondimensionalizing term for time, was introduced. Although it is necessary for the term to have units of $[1/t]$, the terms involved inside β to obtain the necessary units are unknown. Since β appears in several of the nondimensionalized derivatives, it is possible to substitute for each of the dimensional quantities in Eq. [A-13] in order to obtain the

required terms in β necessary to make the equation non-dimensional. This is illustrated below, with only the dimensional terms retained:

$$\begin{aligned}
 0 = & (\ell)(q)(1/\ell)(1/\ell^2) \\
 & + (1)(q)(\ell^2)(1/\ell^4) \\
 & + (1/\ell^2)(q)(\ell)(1/\ell) \\
 & + (1/\ell^2)(q) \\
 & + (1/\ell^3)(q\ell) \\
 & + \beta^2\mu(\ell)(1/\ell^2) \\
 & + (\beta^2/\ell)\mu \\
 & + \ell\beta^2\mu(1/\ell^2)
 \end{aligned}$$

Only the first set of dimensional terms for each derivative is shown above, since it is evident that every term in the multiplier of a derivative must have equivalent dimensions. The above dimensional equality can easily be reduced to show that the first five terms have dimensions of q/ℓ^2 , and the last three have dimensions of $\beta^2\mu/\ell$. If the equality is divided by q/ℓ^2 , so that it is eliminated from the first five terms, the last three terms then contain:

$$\frac{\beta^2\mu}{\ell} \left(\frac{1}{q/\ell^2} \right) = \beta^2 \frac{\mu\ell}{q}$$

This can be rearranged to obtain the non-dimensional equality,

$$\beta^2 = \frac{q}{\mu\ell}$$

or,

$$\beta = \sqrt{\frac{q}{\mu\ell}}$$

The nondimensional value has now been obtained for each dimensional term in Eq. [A-13]. Substituting these values into the equation yields:

$$\begin{aligned}
0 = & \bar{v} \left[-\frac{pq\bar{A}\bar{B}}{\ell^2} \sin \psi_0 - \frac{2pq\bar{A}^3}{\ell^2} \cos \psi_0 - \frac{q\bar{A}\bar{C}\bar{T}_1}{\ell^2} + \frac{q\bar{B}^2\bar{T}_1}{\ell^2} \right] \\
& + \bar{v}_{\bar{S}} \left[\sin \psi_0 \left(-\frac{5pq\bar{A}^{-2}\bar{B}^2}{\ell^2} + \frac{2pq\bar{A}^{-1}\bar{C}}{\ell^2} - \frac{2pq\bar{A}^2}{\ell^2} \right) \right. \\
& \quad \left. + \frac{2pq\bar{B}}{\ell^2} \cos \psi_0 + \frac{8q\bar{A}^{-3}\bar{B}^3\bar{T}_1}{\ell^2} - \frac{7q\bar{A}^{-2}\bar{B}\bar{C}\bar{T}_1}{\ell^2} + \frac{q\bar{A}^{-1}\bar{D}\bar{T}_1}{\ell^2} - \frac{q\bar{A}\bar{B}\bar{T}_1}{\ell^2} \right] \\
& + \bar{v}_{\bar{S}\bar{S}} \left[\frac{5pq\bar{A}^{-1}\bar{B}}{\ell^2} \sin \psi_0 - \frac{2pq\bar{A}}{\ell^2} \cos \psi_0 - \frac{8q\bar{A}^{-2}\bar{B}^2\bar{T}_1}{\ell^2} + \frac{3q\bar{A}^{-1}\bar{C}\bar{T}_1}{\ell^2} - \frac{q\bar{A}^2\bar{T}_1}{\ell^2} \right] \\
& + \bar{v}_{\bar{S}\bar{S}\bar{S}} \left[-\frac{2pq}{\ell^2} \sin \psi_0 + \frac{4q\bar{A}^{-1}\bar{B}\bar{T}_1}{\ell^2} \right] \\
& + \bar{v}_{\bar{S}\bar{S}\bar{S}\bar{S}} \left[-\frac{q}{\ell^2} \bar{T}_1 \right] \\
& + \bar{v}_{\bar{S}\bar{t}\bar{t}} \left[-\frac{2q}{\mu\ell} \mu\ell\bar{A}^{-1} \frac{\bar{B}}{\ell^2} \right] \\
& + \bar{v}_{\bar{S}\bar{S}\bar{t}\bar{t}} \left[\frac{q}{\mu\ell} \frac{1}{\ell} \mu \right] \\
& + \bar{v}_{\bar{t}\bar{t}} \left[-\ell \frac{q}{\mu\ell} \mu \frac{\bar{A}^2}{\ell^2} \right]
\end{aligned}$$

It is possible to reduce this equation by canceling terms, and dividing the equation by q/ℓ^2 , in order to give:

$$\begin{aligned}
0 = & \bar{v} [-p\bar{A}\bar{B} \sin \psi_0 - 2p\bar{A}^3 \cos \psi_0 - \bar{A}\bar{C}\bar{T}_1 + \bar{B}^2\bar{T}_1] \\
& + \bar{v}_{\bar{S}} [\sin \psi_0 (-5p\bar{A}^{-2}\bar{B}^2 + 2p\bar{A}^{-1}\bar{C} - 2p\bar{A}^2) \\
& \quad + 2p\bar{B} \cos \psi_0 + 8\bar{A}^{-3}\bar{B}^3\bar{T}_1 - 7\bar{A}^{-2}\bar{B}\bar{C}\bar{T}_1 + \bar{A}^{-1}\bar{D}\bar{T}_1 - \bar{A}\bar{B}\bar{T}_1] \\
& + \bar{v}_{\bar{S}\bar{S}} [5p\bar{A}^{-1}\bar{B} \sin \psi_0 - 2p\bar{A} \cos \psi_0 - 8\bar{A}^{-2}\bar{B}^2\bar{T}_1 + 3\bar{A}^{-1}\bar{C}\bar{T}_1 - \bar{A}^2\bar{T}_1] \\
& + \bar{v}_{\bar{S}\bar{S}\bar{S}} [-2p \sin \psi_0 + 4\bar{A}^{-1}\bar{B}\bar{T}_1] \tag{A - 14} \\
& + \bar{v}_{\bar{S}\bar{S}\bar{S}\bar{S}} [-\bar{T}_1] \\
& + \bar{v}_{\bar{S}\bar{t}\bar{t}} [-2\bar{A}^{-1}\bar{B}] \\
& + \bar{v}_{\bar{S}\bar{S}\bar{t}\bar{t}} [1] \\
& + \bar{v}_{\bar{t}\bar{t}} [-\bar{A}^2]
\end{aligned}$$

It should be remembered that the v terms in the preceding equation are functions of \bar{S} and \bar{t} . In eigenvalue analysis it is possible to separate the terms, by the form:

$$f(x,t) = \Phi(x)f(t)$$

where $\Phi(x)$ is the amplitude of the mode shape at x , and $f(t)$ is a time-dependent term. At any position, x , the mode shape has a constant value, although the displacement will vary due to the time-dependent term. For the case of interest, it is possible to divide v as follows:

$$v(S,t) = V(S) \cos \omega t \quad [A - 15]$$

where ω is the circular frequency, with units of $[1/t]$. Therefore, an additional nondimensional term must be introduced, in order to eliminate the units of time. This is done by:

$$\frac{\omega}{\beta} = \bar{\omega}$$

where $\bar{\omega}$ is the nondimensional value of the frequency, and β is the constant used to make time nondimensional as previously defined. Substituting the nondimensional quantities into Eq. [A-15], and reducing, yields:

$$\bar{v}(\bar{S}, \bar{t}) = \bar{V}(\bar{S}) \cos \bar{\omega} \bar{t}$$

Derivatives can be taken with respect to \bar{S} and to \bar{t} to give:

$$\bar{v}_{\bar{S}} = \bar{V}' \cos \bar{\omega} \bar{t}$$

$$\bar{v}_{\bar{S}\bar{S}} = \bar{V}'' \cos \bar{\omega} \bar{t}$$

$$\bar{v}_{\bar{S}\bar{S}\bar{S}} = \bar{V}''' \cos \bar{\omega} \bar{t}$$

$$\bar{v}_{\bar{S}\bar{S}\bar{S}\bar{S}} = \bar{V}'''' \cos \bar{\omega} \bar{t}$$

$$\bar{v}_{\bar{S}\bar{t}\bar{t}} = -\bar{\omega}^2 \bar{V}' \cos \bar{\omega} \bar{t}$$

$$\bar{v}_{SStt} = -\bar{\omega}^2 \bar{V}'' \cos \bar{\omega} \bar{t}$$

$$\bar{v}_{tt} = -\bar{\omega}^2 \bar{V} \cos \bar{\omega} \bar{t}$$

When these equations are placed into Eq. [A-14], and then divided by $\cos \bar{\omega} \bar{t}$, the result is the non-dimensional equation of motion for the inflatable dam, with constant internal pressure, carrying its own self-weight:

$$\begin{aligned}
0 = & \bar{V} [-p\bar{A}\bar{B} \sin \psi_0 - 2p\bar{A}^3 \cos \psi_0 - \bar{A}\bar{C}\bar{T}_1 + \bar{B}^2\bar{T}_1] \\
& + \bar{V}' [\sin \psi_0 (-5p\bar{A}^{-2}\bar{B}^2 + 2p\bar{A}^{-1}\bar{C} - 2p\bar{A}^2) + 2p\bar{B} \cos \psi_0 \\
& \quad + 8\bar{A}^{-3}\bar{B}^3\bar{T}_1 - 7\bar{A}^{-2}\bar{B}\bar{C}\bar{T}_1 + \bar{A}^{-1}\bar{D}\bar{T}_1 - \bar{A}\bar{B}\bar{T}_1] \\
& + \bar{V}'' [5p\bar{A}^{-1}\bar{B} \sin \psi_0 - 2p\bar{A} \cos \psi_0 - 8\bar{A}^{-2}\bar{B}^2\bar{T}_1 + 3\bar{A}^{-1}\bar{C}\bar{T}_1 - \bar{A}^2\bar{T}_1] \\
& + \bar{V}''' [-2p \sin \psi_0 + 4\bar{A}^{-1}\bar{B}\bar{T}_1] \qquad \qquad \qquad [A - 16] \\
& + \bar{V}'''' [-\bar{T}_1] \\
& - \bar{\omega}^2 \bar{V}' [-2\bar{A}^{-1}\bar{B}] \\
& - \bar{\omega}^2 \bar{V}'' [1] \\
& - \bar{\omega}^2 \bar{V} [-\bar{A}^2]
\end{aligned}$$

A.3 Approximation of Derivatives by Finite Differences

The equation of motion of the dam contains derivatives of both ψ_0 and \bar{V} with respect to \bar{S} , that must be satisfied at each point on the cross-section. Since information is needed at a discrete number of points on the membrane, a procedure to obtain the derivatives at the nodes is needed. It can be shown that the derivatives of a continuous system can be approximated by using finite difference techniques at each point of interest on the cross-section. Crandall [5] gives the first through fourth order derivative approximations, which after being rearranged, are represented as:

$$\left(\frac{d\psi}{dx}\right)_j = \frac{1}{2h}(\psi_{j+1} - \psi_{j-1}) + O(h^2)$$

$$\left(\frac{d^2\psi}{dx^2}\right)_j = \frac{1}{h^2}(\psi_{j+1} - 2\psi_j + \psi_{j-1}) + O(h^2)$$

$$\left(\frac{d^3\psi}{dx^3}\right)_j = \frac{1}{2h^3}(\psi_{j+2} - 2\psi_{j+1} + 2\psi_{j-1} - \psi_{j-2}) + O(h^2)$$

$$\left(\frac{d^4\psi}{dx^4}\right)_j = \frac{1}{h^4}(\psi_{j+2} - 4\psi_{j+1} + 6\psi_j - 4\psi_{j-1} + \psi_{j-2}) + O(h^2)$$

where $O(h^2)$ is a remainder term of order h^2 , and ψ_j is the value of ψ at node j . This term represents the error involved in using only the first portion of the equation to approximate the actual value of the appropriate derivative. By making the value of h small, the remainder term becomes very small due to h^2 , which is then multiplied by the appropriate constant terms to make the equation exact. The remainder term is usually small compared to the rest of the equation, so neglecting it does not significantly change the value of the derivative. By dropping the remainder terms, any of the above equations may be confirmed by taking appropriate differences of lower order difference equations. Some use will be made of forward and backward differences, due to the lack of data beyond the end points of the cross-section.

Approximations of the Derivatives of the Initial Angles

The equation of motion of the dam cross-section includes the first through fourth order derivatives of ψ_0 with respect to \bar{S} , represented as \bar{A} , \bar{B} , \bar{C} , and \bar{D} respectively. Through the central portion of the cross-section, the following approximations for the derivatives at any node i are valid:

$$\bar{A}_i = \frac{1}{2h}(\psi_{0i+1} - \psi_{0i-1})$$

$$\bar{B}_i = \frac{1}{h^2}(\psi_{0i+1} - 2\psi_{0i} + \psi_{0i-1})$$

$$\bar{C}_i = \frac{1}{2h^3}(\psi_{0i+2} - 2\psi_{0i+1} + 2\psi_{0i-1} - \psi_{0i-2})$$

$$\bar{D}_i = \frac{1}{h^4}(\psi_{0i+2} - 4\psi_{0i+1} + 6\psi_{0i} - 4\psi_{0i-1} + \psi_{0i-2})$$

where ψ_0 is the value of the base angle at the node indicated, and h is the uniform distance between nodes on the cross-section.

It should be noted that the preceding equations were said to be valid only in the central portion of the cross-section. Examination of the terms \bar{C} and \bar{D} shows that both terms require the use of ψ_{0i-2} and ψ_{0i+2} . It must be remembered that both the first and last nodes on the cross-section denoted by $i = 1$ and $i = N$, respectively, are anchored, and therefore, do not move, so the equation of motion must be used only between node 2 and node N-1. At the first point of concern on the cross-section, node $i = 2$, the angle at node 0 is required in the approximation of the third and fourth order derivatives. This is outside the realm of knowledge of the structure, as a look at the STATIC program will reveal, so a different approach must be taken at this node, as well as at node N-1, where a similar problem is encountered. The approximations for the derivatives at that point require the angle at node N + 1, which is also outside the area of the problem. At node 2, the first forward difference of the second difference and of the third difference will yield the third difference and the fourth difference equations, respectively, at the point:

$$\begin{aligned} \bar{C}_2 &= \frac{1}{h} \left[\left(\frac{\psi_{04} - 2\psi_{03} + \psi_{02}}{h^2} \right) - \left(\frac{\psi_{03} - 2\psi_{02} + \psi_{01}}{h^2} \right) \right] \\ &= \frac{1}{h^3}(\psi_{04} - 3\psi_{03} + 3\psi_{02} - \psi_{01}) \end{aligned}$$

$$\begin{aligned}\bar{D}_2 &= \frac{1}{h} \left[\left(\frac{\psi_{05} - 3\psi_{04} + 3\psi_{03} - \psi_{02}}{h^3} \right) - \left(\frac{\psi_{04} - 3\psi_{03} + 3\psi_{02} - \psi_{01}}{h^3} \right) \right] \\ &= \frac{1}{h^4} (\psi_{05} - 4\psi_{04} + 6\psi_{03} - 4\psi_{02} + \psi_{01})\end{aligned}$$

In a similar manner, the first backward difference of the second difference and of the third difference can be used to obtain the approximations of the third and fourth order derivatives at node N-1, which, after reduction, yield:

$$\bar{C}_{N-1} = \frac{1}{h^3} (\psi_{0N} - 3\psi_{0N-1} + 3\psi_{0N-2} - \psi_{0N-3})$$

$$\bar{D}_{N-1} = \frac{1}{h^4} (\psi_{0N} - 4\psi_{0N-1} + 6\psi_{0N-2} - 4\psi_{0N-3} + \psi_{0N-4})$$

A computer program, written in the FORTRAN programming language, was developed to calculate the values of the derivatives at each point from node 2 to node N-1, using the finite difference approximations shown above. The program, ALPHA, is presented as Appendix C.

Approximations of the Derivatives of the Tangential Displacements

The derivatives of \bar{V} will be obtained in a manner similar to that used to find those of ψ_0 . The major difference is that the boundary conditions at the ends of the cross-section are known for \bar{V} , while nothing was known about the conditions involving ψ_0 . At the end nodes, 1 and N, it is evident that v and w must be zero, since the end supports do not move. This means that the first and last nodes are not used in the equation of motion, so only nodes 2 through N-1 must be examined. Examination of the finite difference approximations for the third and fourth order derivatives shows that the value at node 0 is needed at point 2, and the value at node N+1 is required at point N-1. Since these are the only points with problems, the use of forward and backward differences could again be used, but the boundary conditions allow a more accurate approximation

to be made. Using the boundary conditions given for the static condition, it is known that the displacement at node 1 is zero. From Eq. [A-5], it is known that either $(d\psi_0/dS)^{-1}$ or $\partial v/\partial S$ must be zero. The first term is obtained from the finite difference equations and will have some value, so the term $\partial v/\partial S$ must then be zero. Therefore, denoting the value of \bar{V} at any node i as v_i , the approximation is:

$$\bar{V}_1' = 0 = \frac{1}{2h}(v_2 - v_0)$$

The equation can be solved to reveal that $v_0 = v_2$. The procedure can also be used at node N to show that $v_{N+1} = v_{N-1}$.

The conditions at the ends of the cross-section can be substituted into the finite difference equations for nodes 2, 3, $N-2$, and $N-1$. These can be reduced to give:

$$\bar{V}_2' = \frac{1}{2h}v_3$$

$$\bar{V}_2'' = \frac{1}{h^2}(v_3 - 2v_2)$$

$$\bar{V}_2''' = \frac{1}{2h^3}(v_4 - 2v_3 - v_2)$$

$$\bar{V}_2'''' = \frac{1}{h^4}(v_4 - 4v_3 + 7v_2)$$

$$\bar{V}_3' = \frac{1}{2h}(v_4 - v_2)$$

$$\bar{V}_3'' = \frac{1}{h^2}(v_4 - 2v_3 + v_2)$$

$$\bar{V}_3''' = \frac{1}{2h^3}(v_5 - 2v_4 + 2v_2)$$

$$\bar{V}_3'''' = \frac{1}{h^4}(v_5 - 4v_4 + 6v_3 - 4v_2)$$

$$\bar{V}_{N-2}' = \frac{1}{2h}(v_{N-1} - v_{N-3})$$

$$\bar{V}_{N-2}'' = \frac{1}{h^2}(v_{N-1} - 2v_{N-2} + v_{N-3})$$

$$\bar{V}_{N-2}''' = \frac{1}{2h^3}(-2v_{N-1} + 2v_{N-3} - v_{N-4})$$

$$\bar{V}_{N-2}'''' = \frac{1}{h^4}(-4v_{N-1} + 6v_{N-2} - 4v_{N-3} + v_{N-4})$$

$$\bar{V}_{N-1}' = \frac{1}{2h}(-v_{N-2})$$

$$\bar{V}_{N-1}'' = \frac{1}{h^2}(-2v_{N-1} + v_{N-2})$$

$$\bar{V}_{N-1}''' = \frac{1}{2h^3}(v_{N-1} + 2v_{N-2} - v_{N-3})$$

$$\bar{V}_{N-1}'''' = \frac{1}{h^4}(7v_{N-1} - 4v_{N-2} + v_{N-3})$$

From node 4 to node N-3, the central difference equations are used in the following form:

$$\bar{V}_i' = \frac{1}{2h}(v_{i+1} - v_{i-1})$$

$$\bar{V}_i'' = \frac{1}{h^2}(v_{i+1} - 2v_i + v_{i-1})$$

$$\bar{V}_i''' = \frac{1}{2h^3}(v_{i+2} - 2v_{i+1} + 2v_{i-1} - v_{i-2})$$

$$\bar{V}_i'''' = \frac{1}{h^4}(v_{i+2} - 4v_{i+1} + 6v_i - 4v_{i-1} + v_{i-2})$$

Since h is the equivalent distance between each node on the nondimensional perimeter length, it is nondimensional, and its value is $\bar{S}/(N - 1)$, so the preceding equations are unitless.

A.4 The Equations of Motion in Computer Form

The approximations for the derivatives, obtained in Section A.3, can be substituted into Eq. [A-14] for specific nodes. The terms in the point specific equations can then be sorted according to the v_i 's, and the set of equations can be placed in matrix form. In order to simplify the equations, Eq. [A-14] can be placed in the form:

$$0 = \bar{V}_i R1_i + \bar{V}_i' R2_i + \bar{V}_i'' R3_i + \bar{V}_i''' R4_i + \bar{V}_i'''' R5_i - \bar{\omega}^2 \bar{V}_i' R6_i - \bar{\omega}^2 \bar{V}_i'' R7_i - \bar{\omega}^2 \bar{V}_i R8_i$$

where $R1$ through $R8$ are the coefficients from Eq. (A-14), as shown below:

$$R1 = -p\bar{A}\bar{B} \sin \psi_0 - 2p\bar{A}^3 \cos \psi_0 - \bar{A}\bar{C}\bar{T}_1 + \bar{B}^2\bar{T}_1$$

$$R2 = \sin \psi_0 (-5p\bar{A}^{-2}\bar{B}^2 + 2p\bar{A}^{-1}\bar{C} - 2p\bar{A}^2) + 2p\bar{B} \cos \psi_0 + 8\bar{A}^{-3}\bar{B}^3\bar{T}_1 - 7\bar{A}^{-2}\bar{B}\bar{C}\bar{T}_1 + \bar{A}^{-1}\bar{D}\bar{T}_1 - \bar{A}\bar{B}\bar{T}_1$$

$$R3 = 5p\bar{A}^{-1}\bar{B} \sin \psi_0 - 2p\bar{A} \cos \psi_0 - 8\bar{A}^{-2}\bar{B}^2\bar{T}_1 + 3\bar{A}^{-1}\bar{C}\bar{T}_1 - \bar{A}^2\bar{T}_1$$

$$R4 = -2p \sin \psi_0 + 4\bar{A}^{-1}\bar{B}\bar{T}_1$$

$$R5 = -\bar{T}_1$$

$$R6 = -2\bar{A}^{-1}\bar{B}$$

$$R7 = 1$$

$$R8 = -\bar{A}^2$$

The substitution for the first point of interest, node 2, is illustrated below:

$$0 = v_2 R1_2 + \left(\frac{v_3}{2h}\right) R2_2 + \left(\frac{v_3 - 2v_2}{h^2}\right) R3_2 + \left(\frac{v_4 - 2v_3 - v_2}{2h^3}\right) R4_2 \\ + \left(\frac{v_4 - 4v_3 + 7v_2}{h^4}\right) R5_2 - \bar{\omega}^2 \left(\frac{v_3}{2h}\right) R6_2 - \bar{\omega}^2 \left(\frac{v_3 - 2v_2}{h^2}\right) R7_2 - \bar{\omega}^2 v_2 R8_2$$

When the v terms are collected, the equation of motion for the cross-section of the dam at node 2 becomes:

$$0 = \left(R1_2 - \frac{2R3_2}{h^2} - \frac{R4_2}{2h^3} + \frac{7R5_2}{h^4}\right) v_2 \\ + \left(\frac{R2_2}{2h} + \frac{R3_2}{h^2} - \frac{2R4_2}{2h^3} - \frac{4R5_2}{h^4}\right) v_3 \\ + \left(\frac{R4_2}{2h^3} + \frac{R5_2}{h^4}\right) v_4 \\ - \bar{\omega}^2 \left(-\frac{2R7_2}{h^2} + R8_2\right) v_2 \\ - \bar{\omega}^2 \left(\frac{R6_2}{2h} + \frac{R7_2}{h^2}\right) v_3$$

The equations of motion are found at all points on the cross-section in a manner similar to that illustrated for node 2. The simplified equation for each of the particular case nodes will be presented, as well as the general case equation, which is valid for the interior points from node 4 to node N-3. For node 3, the equation of motion is found to be:

$$\begin{aligned}
0 = & \left(-\frac{R2_3}{2h} + \frac{R3_3}{h^2} + \frac{2R4_3}{2h^3} - \frac{4R5_3}{h^4} \right) v_2 \\
& + \left(R1_3 - \frac{2R3_3}{h^2} + \frac{6R5_3}{h^4} \right) v_3 \\
& + \left(\frac{R2_3}{2h} + \frac{R3_3}{h^2} - \frac{2R4_3}{2h^3} - \frac{4R5_3}{h^4} \right) v_4 \\
& + \left(\frac{R4_3}{2h^3} + \frac{R5_3}{h^4} \right) v_5 \\
& - \bar{\omega}^2 \left(-\frac{R6_3}{2h} + \frac{R7_3}{h^2} \right) v_2 \\
& - \bar{\omega}^2 \left(-\frac{2R7_3}{h^2} + R8_3 \right) v_3 \\
& - \bar{\omega}^2 \left(\frac{R6_3}{2h} + \frac{R7_3}{h^2} \right) v_4
\end{aligned}$$

For node N-2, the equation of motion is found to be:

$$\begin{aligned}
0 = & \left(-\frac{R4_{N-2}}{2h^3} + \frac{R5_{N-2}}{h^4} \right) v_{N-4} \\
& + \left(-\frac{R2_{N-2}}{2h} + \frac{R3_{N-2}}{h^2} + \frac{2R4_{N-2}}{2h^3} - \frac{4R5_{N-2}}{h^4} \right) v_{N-3} \\
& + \left(R1_{N-2} - \frac{2R3_{N-2}}{h^2} + \frac{6R5_{N-2}}{h^4} \right) v_{N-2} \\
& + \left(\frac{R2_{N-2}}{2h} + \frac{R3_{N-2}}{h^2} - \frac{2R4_{N-2}}{2h^3} - \frac{4R5_{N-2}}{h^4} \right) v_{N-1} \\
& - \bar{\omega}^2 \left(-\frac{R6_{N-2}}{2h} + \frac{R7_{N-2}}{h^2} \right) v_{N-3} \\
& - \bar{\omega}^2 \left(-\frac{2R7_{N-2}}{h^2} + R8_{N-2} \right) v_{N-2} \\
& - \bar{\omega}^2 \left(\frac{R6_{N-2}}{2h} + \frac{R7_{N-2}}{h^2} \right) v_{N-1}
\end{aligned}$$

and for node N-1, the resulting equation of motion is:

$$\begin{aligned}
0 = & \left(-\frac{R4_{N-1}}{2h^3} + \frac{R5_{N-1}}{h^4} \right) v_{N-3} \\
& + \left(-\frac{R2_{N-1}}{2h} + \frac{R3_{N-1}}{h^2} + \frac{2R4_{N-1}}{2h^3} - \frac{4R5_{N-1}}{h^4} \right) v_{N-2} \\
& + \left(R1_{N-1} - \frac{2R3_{N-1}}{h^2} + \frac{R4_{N-1}}{2h^3} + \frac{7R5_{N-1}}{h^4} \right) v_{N-1} \\
& - \bar{\omega}^2 \left(-\frac{R6_{N-1}}{2h} + \frac{R7_{N-1}}{h^2} \right) v_{N-2} \\
& - \bar{\omega}^2 \left(-\frac{2R7_{N-1}}{h^2} + R8_{N-1} \right) v_{N-1}
\end{aligned}$$

In general, for the i -th node, the equation of motion for the cross-section may be presented in the form:

$$\begin{aligned}
0 = & \left(-\frac{R4_i}{2h^3} + \frac{R5_i}{h^4} \right) v_{i-2} \\
& + \left(-\frac{R2_i}{2h} + \frac{R3_i}{h^2} + \frac{2R4_i}{2h^3} - \frac{4R5_i}{h^4} \right) v_{i-1} \\
& + \left(R1_i - \frac{2R3_i}{h^2} + \frac{6R5_i}{h^4} \right) v_i \\
& + \left(\frac{R2_i}{2h} + \frac{R3_i}{h^2} - \frac{2R4_i}{2h^3} - \frac{4R5_i}{h^4} \right) v_{i+1} \\
& + \left(\frac{R4_i}{2h^3} + \frac{R5_i}{h^4} \right) v_{i+2} \\
& - \bar{\omega}^2 \left(-\frac{R6_i}{2h} + \frac{R7_i}{h^2} \right) v_{i-1} \\
& - \bar{\omega}^2 \left(-\frac{2R7_i}{h^2} + R8_i \right) v_i \\
& - \bar{\omega}^2 \left(\frac{R6_i}{2h} + \frac{R7_i}{h^2} \right) v_{i+1}
\end{aligned} \tag{A - 17}$$

where i represents any node from 4 to $N-3$.

Each of the four node-specific equations and the generalized equation of motion are used in the FORTRAN program, DYNAMIC. The correct equation of motion is used at each node

on the cross-section, and the resulting equations are placed in matrices, which form the characteristic equation of the structure:

$$[A - \lambda B] = 0$$

where A and B are matrices containing the multipliers of the various v 's, and $\lambda = \bar{\omega}^2$ are the eigenvalues to be found. The matrices in the DYNAMIC program are in slightly different notation due to the fact that it is easier to program a matrix with values from $i = 1$ to $N-2$ than one with values from $i = 2$ to $N-1$. The DYNAMIC program is presented as Appendix D.

Appendix B. The STATIC Computer Program

The STATIC program, written in the FORTRAN 77 computer language, is shown on the following pages. It calculates the shape of an air-inflated dam, loaded only with its own weight and the internal pressure, for the static case.

```

C
C
C           INFLATABLE DAM STATIC PROGRAM
C
C
C WRITTEN BY TONY D. FAGAN, AS PART OF RESEARCH FOR HIS MASTERS
C OF SCIENCE THESIS, USING PORTIONS OF A PROGRAM WRITTEN BY
C J. C. HSIEH [12], AND THE ZEROIN SUBROUTINE [8].
C MARCH 10, 1987
C
C PROGRAM DESCRIPTION:
C THE STATIC PROGRAM COMPUTES THE SHAPE OF AN INFLATABLE DAM FOR
C A GIVEN PERIMETER AND BASE LENGTH. THE TENSION CAN BE VARIED
C IN ORDER TO SATISFY THE BOUNDARY CONDITIONS, WHICH INCLUDE THE
C BASE LENGTH. WHEN THE REQUIRED BASE LENGTH MATCHES THE ACTUAL
C LENGTH FOR A PARTICULAR CASE, THE CORRECT SOLUTION IS OBTAINED.
C THE INITIAL ANGLE, ZA, IS FOUND BY A SHOOTING METHOD USING THE
C ZEROIN SUBROUTINE.
C
C VARIABLES ARE DEFINED, AND COMMON BLOCKS ARE ESTABLISHED.
C
EXTERNAL F
DIMENSION XA(103),YA(103),ZA(103),WA(103)
DOUBLE PRECISION A,B,Z,TOL2,ZEROIN,TN,P,SN
DOUBLE PRECISION DNMAX,T,STEP,F,BLENG,ERROR,XCENTR
DOUBLE PRECISION XEND,YEND,XA,YA,ZA,WA
DOUBLE PRECISION XSCAL,YSCAL,XAPI,XAP2,YAPI,YAP2
INTEGER SUM,I,J,ITOP,LIKE,ITYPE
REAL XTN,XP,TOP
COMMON /K1/TN,P
COMMON /K2/NMAX,ITER
COMMON /K3/T,STEP,ERROR,BLENG
COMMON /K4/XAPI,XAP2,YAPI,YAP2
COMMON /K5/XEND,YEND,XSCAL,YSCAL
COMMON /K6/XA,YA,ZA,WA,NX

NMAX = 41
DNMAX = NMAX*1.0D0

C THE MAXIMUM VALUES OF THE PLOTTED AXES, XEND AND YEND, THE
C PERIMETER LENGTH, SN, THE STEP SIZE, STEP, AND THE RANGE OF
C THE INITIAL ANGLES, A AND B, ARE ESTABLISHED.

XEND = 0.9D0
YEND = 0.5D0

SN = 1.0D0
STEP = SN/(DNMAX-1.0D0)
CALL PLOTS(0,0,50)
CALL PLOT(2.15,2.25,-3)

A = 0.30D0
B = 3.14D0

C TRIAL VALUES ARE ENTERED.
C NOTES: IF ITYPE = 0, THE UNMODIFIED VALUES ARE PRINTED.
C IF ITYPE > 0, THE VALUES ARE AVERAGED TO OBTAIN SYMMETRY.
C THE BASE LENGTH, BLENG, IS READ, ALONG WITH THE TRIAL VALUE OF
C THE TENSION AND OF THE WEIGHT.

READ(5,7) ITYPE
READ(5,8) XTN, BLENG

```

```

READ(5,9) XP
7 FORMAT(2X,I1)
8 FORMAT(2X,F10.8,2X,F16.13)
9 FORMAT(2X,F10.8)

TN = DBLE(XTN)
P = DBLE(XP)

ITER = 1
CALL NEWPEN(1)

C THE ZEROIN FUNCTION IS CALLED TO FIND THE CORRECT VALUE OF THE
C INITIAL ANGLE FOR THE CASE BEING TESTED. THE STATIC SHAPE IS
C PLOTTED WITH THE SHOW1 SUBROUTINE.

TOL2 = 2.5D-5
Z = ZEROIN(A,B,F,TOL2)
CALL SHOW1(XA,YA,NX)
DO 10 I=1,NMAX
  XA(I)=XA(I)/XSCAL
  YA(I)=YA(I)/YSCAL
10 CONTINUE

C IF THE CORRECT VALUE OF INITIAL TENSION IS KNOWN, THE COORDINATES
C ARE AVERAGED TO OBTAIN A SYMMETRICAL SHAPE ABOUT THE CENTER LINE
C OF THE STRUCTURE. IF THE VALUE IS NOT KNOWN, THE ERROR DISTANCE
C IS PRINTED.

TOP = NMAX/2.0
ITOP = NINT(TOP)
SUM = 0
IF (ITYPE.NE.0) THEN
DO 60 I=1,ITOP
  IF (I.NE.ITOP) THEN
    LIKE = NMAX-SUM
    XCENTR = ((XA(LIKE)-XA(I))/2.0D0)
    XA(I) = (BLENG/2.0D0)-XCENTR
    XA(LIKE) = (BLENG/2.0D0)+XCENTR
    YA(I) = ((YA(I)+YA(LIKE))/2.0D0)
    YA(LIKE) = YA(I)
    ZA(I) = ((ZA(I)-ZA(LIKE))/2.0D0)
    ZA(LIKE) = -ZA(I)
    WA(I) = ((WA(I)+WA(LIKE))/2.0D0)
    WA(LIKE) = WA(I)
  ELSE
    XA(I) = (BLENG/2.0D0)
    ZA(I) = 0.0D0
  ENDIF
  SUM = SUM + 1
60 CONTINUE
XA(1) = 0.0D0
XA(NMAX) = BLENG
YA(1) = 0.0D0
YA(NMAX) = 0.0D0
ELSE
  PRINT(2X,A,F10.8), 'ERROR = ', ERROR
ENDIF

C THE VALUES OF THE COORDINATES, XA AND YA, THE ANGLE, ZA, AND THE
C TENSION, WA, AT EACH POINT ARE PRINTED TO THE OUTPUT FILE, ALONG
C WITH THE MEMBRANE WEIGHT AND THE STRUCTURE'S BASE LENGTH.

```

```

PRINT'(2X,F16.13,4X,F16.14)', P, BLENG
DO 70 J=1,NMAX
  PRINT'(2X,4(F16.13,4X))', XA(J),YA(J),ZA(J),WA(J)
70 CONTINUE

```

```

51 CALL PLOT(12.,-2.,999)
50 STOP
END

```

DOUBLE PRECISION FUNCTION F(X)

C THE FUNCTION F SERVES AS THE SOLUTION DRIVER ROUTINE, BY CALLING
C DVERK.

```

EXTERNAL BUCK1
DIMENSION C(24),W(3,9)
DIMENSION Y(3),XA(103),YA(103),ZA(103),WA(103)
DOUBLE PRECISION X,Y,C,W,T,TOL,TOUT,STEP,TN,P
DOUBLE PRECISION XEND,YEND,XA,YA,ZA,WA,ERROR,BLENG
INTEGER N,IND,NW,IER
COMMON /K1/TN,P
COMMON /K2/NMAX,ITER
COMMON /K3/T,STEP,ERROR,BLENG
COMMON /K6/XA,YA,ZA,WA,NX

```

```

NW = 3
N = 3

```

```

TOL = 1.0D-5
IND = 1

```

C THE INITIAL BOUNDARY CONDITIONS ARE SET.

```

Y(1) = 0.0D0
Y(2) = 0.0D0
Y(3) = X
ITER = ITER + 1
T = 0.0D0

```

```

DO 100 NC = 1,NMAX
  XA(NC) = Y(1)
  YA(NC) = Y(2)
  ZA(NC) = Y(3)
  WA(NC) = P*Y(2) + TN

```

```

TOUT = T + STEP
CALL DVERK(N,BUCK1,T,Y,TOUT,TOL,IND,C,NW,W,IER)
IF((IND.LT.0.).OR.(IER.GT.0.)) GO TO 200

```

```

100 CONTINUE
NX = NMAX

```

C THE ERROR DISTANCE, F, IS COMPUTED.

```

F = SQRT(((ABS(BLENG-XA(NX)*1.0D0))**2)
$      + ((ABS(YA(NX)*1.0D0))**2))
ERROR = F
200 RETURN
END

```

SUBROUTINE BUCK1(N,T,Y,YPRIME)

C THE SUBROUTINE BUCK1 CONTAINS THE EQUATIONS OF EQUILIBRIUM FOR
C THE INFLATABLE DAM.

```

INTEGER N
DIMENSION Y(N),YPRIME(N)
DOUBLE PRECISION T,Y,YPRIME,TN,P
COMMON /K1/TN,P

YPRIME(1) = COS(Y(3))
YPRIME(2) = SIN(Y(3))
YPRIME(3) = ((-1 + P*COS(Y(3)))/(P*Y(2) + TN))
RETURN
END

```

```

SUBROUTINE SHOW1(XA,YA,NP)

```

```

C  SHOW1 IS THE PLOTTING ROUTINE WHICH PLOTS THE STATIC SHAPE OF
C  THE DAM.

```

```

DIMENSION XA(*),YA(*)
DOUBLE PRECISION XEND,YEND,XA,YA,ZA,WA,ERROR
DOUBLE PRECISION XSCAL,YSCAL,XAP1,XAP2,YAP1,YAP2
COMMON /K4/XAP1,XAP2,YAP1,YAP2
COMMON /K5/XEND,YEND,XSCAL,YSCAL

```

```

CALL FACTOR(1.1)
XA(NP+1) = 0.
XA(NP+2) = XEND/9.0
XAP1 = XA(NP+1)
XAP2 = XA(NP+2)
YA(NP+1) = 0.
YA(NP+2) = YEND/5.0
YAP1 = YA(NP+1)
YAP2 = YA(NP+2)

```

```

C  THE X AND Y AXES ARE DRAWN.

```

```

CALL AXIS(0.,0.,1HX,-1.9.,0.,XAP1,XAP2)
CALL AXIS(-1.0,0.,1HY,1.5.,90.,YAP1,YAP2)

```

```

C  THE COORDINATES ARE SCALED FOR PLOTTING, AND THE SHAPE IS DRAWN.

```

```

XSCAL = 9./XEND
YSCAL = 5./YEND
XEND1 = XEND*XSCAL
YEND1 = YEND*YSCAL
DO 10 I = 1, NP
  XA(I) = XA(I)*XSCAL
  YA(I) = YA(I)*YSCAL
10 CONTINUE

```

```

CALL PLOT(XA(1),YA(1),3)

```

```

DO 20 I = 2,NP
  CALL PLOT(XA(I),YA(I),2)
20 CONTINUE
CALL NEWPEN(1)

```

```

CALL FACTOR(1.)
RETURN
END

```

```

DOUBLE PRECISION FUNCTION ZEROIN(AX,BX,F,TOL)

```

C A ZERO OF THE FUNCTION F(X) IS COMPUTED IN THE INTERVAL AX, BX,
 C WHERE AX AND BX ARE THE MINIMUM AND MAXIMUM VALUES OF THE
 C POSSIBLE RANGE OF THE INITIAL ANGLE.

DOUBLE PRECISION AX,BX,F,TOL

DOUBLE PRECISION A,B,C,D,E,EPS,FA,FB,FC,TOL1,XM,P,Q,R,S

EPS = 1.0D0

10 EPS = EPS/2.0D0

TOL1 = 1.0D0 + EPS

IF (TOL1 .GT. 1.0D0) GO TO 10

A = AX

B = BX

FA = F(A)

FB = F(B)

20 C = A

FC = FA

D = B - A

E = D

30 IF (ABS(FC) .GE. ABS(FB)) GO TO 40

A = B

B = C

C = A

FA = FB

FB = FC

FC = FA

40 TOL1 = 2.0D0*EPS*ABS(B) + 0.5*TOL

XM = .5*(C - B)

IF (ABS(XM) .LE. TOL1) GO TO 90

IF (FB .EQ. 0.0D0) GO TO 90

IF (ABS(E) .LT. TOL1) GO TO 70

IF (ABS(FA) .LE. ABS(FB)) GO TO 70

IF (A .NE. C) GO TO 50

S = FB/FA

P = 2.0D0*XM*S

Q = 1.0D0 - S

GO TO 60

50 Q = FA/FC

R = FB/FC

S = FB/FA

P = S*(2.0D0*XM*Q*(Q - R) - (B - A)*(R - 1.0D0))

Q = (Q - 1.0D0)*(R - 1.0D0)*(S - 1.0D0)

60 IF (P .GT. 0.0D0) Q = -Q

P = ABS(P)

IF ((2.0D0*P) .GE. (3.0D0*XM*Q - ABS(TOL1*Q))) GO TO 70

IF (P .GE. ABS(0.5*E*Q)) GO TO 70

E = D

D = P/Q

GO TO 80

70 D = XM

E = D

```
80 A = B
   FA = FB
   IF (ABS(D) .GT. TOL1) B = B + D
   IF (ABS(D) .LE. TOL1) B = B + SIGN(TOL1, XM)
   FB = F(B)
   IF ((FB*(FC/ABS(FC))) .GT. 0.D0) GO TO 20
   GO TO 30

90 ZEROIN = B
   RETURN
   END
```

Appendix C. The ALPHA Program

The routine which calculates the first four derivatives of ψ_0 , denoted \bar{A} , \bar{B} , \bar{C} , and \bar{D} in the simplified notation of this work, is shown on the following pages. Written in the FORTRAN 77 programming language, the program, ALPHA, computes each of the derivatives at every interior node on the cross-section of the dam.

```

C
C
C   ALPHA PROGRAM FOR DERIVATIVES OF PSI BY FINITE DIFFERENCES
C
C
C   WRITTEN BY TONY D. FAGAN, AS PART OF THE RESEARCH FOR A MASTER
C   OF SCIENCE THESIS.
C   DATE: MARCH 10, 1987

C   PROGRAM DESCRIPTION:
C   THIS PROGRAM COMPUTES THE FIRST FOUR DERIVATIVES OF THE INITIAL
C   ANGLE PSI (SUB 0) AT EACH NODE BY USING FINITE DIFFERENCE
C   APPROXIMATIONS. FORWARD AND BACKWARD DIFFERENCES ARE USED AT
C   THE SECOND AND NEXT-TO-LAST POINTS, RESPECTIVELY, FOR THE THIRD
C   AND FOURTH DERIVATIVES, AND CENTRAL DIFFERENCES ARE USED FOR ALL
C   OTHER POINTS EXCEPT THE FIRST AND LAST WHICH ARE IGNORED SINCE
C   THEY DO NOT MOVE, AND ARE NOT USED IN THE DYNAMIC EVALUATION.
C   THE LETTERS A THROUGH D REPRESENT THE DERIVATIVES.

C   ASSIGNMENT OF VARIABLES

INTEGER NMAX,INMAX,NINMAX,J
PARAMETER (NMAX=41)
DOUBLE PRECISION A,B,C,D,PSI,H,DNMAX
DOUBLE PRECISION ANG0,ANG1,ANG2,ANG3,ANG4
DIMENSION A(NMAX),B(NMAX),C(NMAX),D(NMAX),PSI(NMAX)

C   THE DATA ARE ENTERED.

DNMAX = DBLE(NMAX)
READ(5,*) TRASH1, TRASH2
DO 10 J=1,NMAX
  READ(5,8) PSI(J)
8  FORMAT(42X,F16.13)
10 CONTINUE
  H = 1.0D0/(DNMAX-1.0D0)
  WRITE(6,15) H
15 FORMAT(2X,F16.13)
  INMAX = NMAX - 1
  NINMAX = INMAX - 1

C   THE FIRST DERIVATIVES, A(I)'S, ARE CALCULATED FOR ALL POINTS.

DO 20 J=2,INMAX
  ANG2 = PSI(J+1)
  ANG0 = PSI(J-1)
  A(J-1) = ((ANG2-ANG0)/(2*H))
20 CONTINUE

C   THE SECOND DERIVATIVES, B(I)'S, ARE CALCULATED FOR ALL POINTS.

DO 30 J=2,INMAX
  ANG2 = PSI(J+1)
  ANG1 = PSI(J)
  ANG0 = PSI(J-1)
  B(J-1) = ((ANG2-2.0D0*ANG1 + ANG0)/(H*H))
30 CONTINUE

C   THE THIRD DERIVATIVES, C(I)'S, ARE CALCULATED AT NODES (2)
C   AND (N-1), AND AT THE INTERIOR POINTS.

DO 40 J=2,INMAX

```

```

IF (J.EQ.2) THEN
  ANG3 = PSI(J+2)
  ANG2 = PSI(J+1)
  ANG1 = PSI(J)
  ANG0 = PSI(J-1)
  C(1) = ((ANG3-3.D0*ANG2+3.D0*ANG1-ANG0)/(H**3))
ELSE IF (J.EQ.INMAX) THEN
  ANG3 = PSI(J+1)
  ANG2 = PSI(J)
  ANG1 = PSI(J-1)
  ANG0 = PSI(J-2)
  C(J-1) = ((ANG3-3.D0*ANG2+3.D0*ANG1-ANG0)/(H**3))
ELSE
  ANG3 = PSI(J+2)
  ANG2 = PSI(J+1)
  ANG1 = PSI(J-1)
  ANG0 = PSI(J-2)
  C(J-1) = ((ANG3-2.D0*ANG2+2.D0*ANG1-ANG0)/(2*H**3))
ENDIF
40 CONTINUE

C THE FOURTH DERIVATIVES, D(I)'S, ARE CALCULATED AT NODES (2)
C AND (N-1), AND AT THE INTERIOR POINTS.

DO 50 J=2,INMAX
  IF (J.EQ.2) THEN
    ANG4 = PSI(J+3)
    ANG3 = PSI(J+2)
    ANG2 = PSI(J+1)
    ANG1 = PSI(J)
    ANG0 = PSI(J-1)
    D(1) = ((ANG4-4*ANG3+6*ANG2-4*ANG1+ANG0)/(H**4))
  ELSE IF (J.EQ.INMAX) THEN
    ANG4 = PSI(J+1)
    ANG3 = PSI(J)
    ANG2 = PSI(J-1)
    ANG1 = PSI(J-2)
    ANG0 = PSI(J-3)
    D(J-1) = ((ANG4-4*ANG3+6*ANG2-4*ANG1+ANG0)/(H**4))
  ELSE
    ANG4 = PSI(J+2)
    ANG3 = PSI(J+1)
    ANG2 = PSI(J)
    ANG1 = PSI(J-1)
    ANG0 = PSI(J-2)
    D(J-1) = ((ANG4-4*ANG3+6*ANG2-4*ANG1+ANG0)/(H**4))
  ENDIF
50 CONTINUE

C THE RESULTS OF A, B, C, AND D FOR NODES (2) THROUGH (N-1),
C AND THE SINE AND COSINE FOR EACH OF THESE POINTS ARE
C PRINTED TO AN OUTPUT FILE.

DO 70 J=1,NINMAX
  WRITE(6,65) A(J),B(J),C(J),D(J)
65  FORMAT(2X,4(F17.12,2X))
70 CONTINUE

STOP
END

```

Appendix D. The DYNAMIC Program

The node-specific equations of motion are entered in matrix form in the FORTRAN 77 program, DYNAMIC, and are solved using the eigenvalue solution subroutine, RGG [6]. The eigenvalues are used to find the normalized eigenvectors. The four lowest eigenvalues are chosen, and the matching eigenvectors are scaled, converted to displacements in the x and y directions, and used to find the first four mode shapes for the vibrating structure. The four mode shapes computed are plotted, along with the shape of the dam in the static condition for comparison purposes. The DYNAMIC program is presented on the following pages.

```

C
C
C           INFLATABLE DAM DYNAMIC PROGRAM
C
C
C WRITTEN BY TONY D. FAGAN, AS PART OF THE RESEARCH FOR A MASTER
C OF SCIENCE THESIS.
C DATE: MARCH 10, 1987
C
C PROGRAM DESCRIPTION:
C THIS PROGRAM CALCULATES AND PLOTS THE FORMS OF THE FIRST FOUR
C MODE SHAPES OF VIBRATION FOR AN AIR INFLATED DAM. THE MEMBRANE
C WEIGHT AND THE INTERNAL AIR PRESSURE ARE THE ONLY FORCES ACTING
C ON THE STRUCTURE.
C
C THE VARIABLES ARE ASSIGNED.
C
PARAMETER (NMAX = 41)
INTEGER INMAX,NINMAX,I,J,MATZ,IERR,IR
DOUBLE PRECISION A,B,C,D,XCOSIN,XSINE,AINVRS
DOUBLE PRECISION R1,R2,R3,R4,R5,R6,R7,R8
DOUBLE PRECISION H,P,BLENG,PSI,T1,S,T,X,Y
DOUBLE PRECISION ALFR,ALFI,BETA,Z,W
DIMENSION S(39,39),T(39,39),ALFR(39),ALFI(39),BETA(39)
DIMENSION Z(39,39),IR(39),AINVRS(39),W(39),PSI(39)
DIMENSION X(50),Y(50),XA(50),YA(50),UX(50),UY(50),SX(50),SY(50)
C
C THE STEP SIZE, H, AND THE MEMBRANE WEIGHT, P, ARE ENTERED.
C
READ(5,4) H
4 FORMAT(2X,F16.13)
READ(4,5) P, BLENG
5 FORMAT(2X,F16.13,4X,F16.14)
INMAX = NMAX-1
NINMAX = INMAX-1
C
C THIS LOOP READS THE COORDINATES, XA AND YA, THE ANGLE, PSI, AND
C THE TENSION, T1, FOR EACH NODE ON THE CROSS-SECTION. THE VALUES
C OF THE DERIVATIVES WITH RESPECT TO PSI ARE READ (COMPUTED IN
C ALPHA ROUTINE), AND THE CONSTANTS R1 THROUGH R9 ARE COMPUTED.
C FINALLY, THE ENTRIES IN THE MATRICES OF THE CHARACTERISTIC
C EQUATION ARE COMPUTED FOR EACH NODE, WHERE THE CHARACTERISTIC
C EQUATION IS OF THE FORM, [S - (LAMBDA) T] = 0.
C
DO 40 I= 1,NINMAX
  IF (I.EQ.1) THEN
    READ(4,6) XA(I),YA(I),PSI(I),T1
    6   FORMAT(/,2X,4(F16.13,4X))
  ELSE
    READ(4,7) XA(I),YA(I),PSI(I),T1
    7   FORMAT(2X,4(F16.13,4X))
  ENDIF
  UX(I+1) = XA(I)
  UY(I+1) = YA(I)
  XCOSIN = DCOS(PSI(I))
  XSINE = DSIN(PSI(I))
  READ(5,8) A, B, C, D
  8   FORMAT(2X,4(F17.12,2X))
  AINVRS(I) = (1/A)
  DO 10 J= 1,NINMAX
    S(I,J) = 0.0D0
    T(I,J) = 0.0D0
  
```

10 CONTINUE

C COMPONENTS OF EQUATION

$$R1 = -P*A*B*XSINE-2*P*(A**3)*XCOSIN-A*C*T1 + (B*B)*T1$$

$$\begin{aligned} R2 &= XSINE*(((-5*P*(B*B))/(A*A)) + ((2*P*C)/A) - (2*P*(A*A))) \\ S &+ 2*P*B*XCOSIN + ((8*(B**3)*T1)/(A**3)) \\ S &- ((7*B*C*T1)/(A*A)) + (D*T1/A) - A*B*T1 \end{aligned}$$

$$\begin{aligned} R3 &= (5*P*B*XSINE/A) - 2*P*A*XCOSIN - (8*(B*B)*T1/(A*A)) \\ S &+ (3*C*T1/A) - (A*A)*T1 \end{aligned}$$

$$R4 = -2*P*XSINE + (4*B*T1/A)$$

$$R5 = -T1$$

$$R6 = -2*B/A$$

$$R7 = 1$$

$$R8 = -(A*A)$$

IF (I.EQ.1) THEN

$$\begin{aligned} S(I,I) &= (R1 - (2*R3/(H*H)) - (R4/(2*(H**3))) + (7*R5/(H**4))) \\ S(I,I+1) &= ((R2/(2*H)) + (R3/(H*H)) - (2*R4/(2*(H**3)))) \\ S &- (4*R5/(H**4)) \\ S(I,I+2) &= ((R4/(2*(H**3))) + (R5/(H**4))) \end{aligned}$$

$$\begin{aligned} T(I,I) &= ((-2*R7/(H*H)) + R8) \\ T(I,I+1) &= ((R6/(2*H)) + (R7/(H*H))) \end{aligned}$$

ELSE IF (I.EQ.2) THEN

$$\begin{aligned} S(I,I-1) &= ((-R2/(2*H)) + (R3/(H*H)) + (2*R4/(2*(H**3)))) \\ S &- (4*R5/(H**4)) \\ S(I,I) &= (R1 - (2*R3/(H*H)) + (6*R5/(H**4))) \\ S(I,I+1) &= ((R2/(2*H)) + (R3/(H*H)) - (2*R4/(2*(H**3)))) \\ S &- (4*R5/(H**4)) \\ S(I,I+2) &= ((R4/(2*(H**3))) + (R5/(H**4))) \end{aligned}$$

$$\begin{aligned} T(I,I-1) &= ((-R6/(2*H)) + (R7/(H*H))) \\ T(I,I) &= ((-2*R7/(H*H)) + R8) \\ T(I,I+1) &= ((R6/(2*H)) + (R7/(H*H))) \end{aligned}$$

ELSE IF (I.EQ.(NMAX-3)) THEN

$$\begin{aligned} S(I,I-2) &= ((-R4/(2*(H**3))) + (R5/(H**4))) \\ S(I,I-1) &= ((-R2/(2*H)) + (R3/(H*H)) + (2*R4/(2*(H**3)))) \\ S &- (4*R5/(H**4)) \\ S(I,I) &= (R1 - (2*R3/(H*H)) + (6*R5/(H**4))) \\ S(I,I+1) &= ((R2/(2*H)) + (R3/(H*H)) - (2*R4/(2*(H**3)))) \\ S &- (4*R5/(H**4)) \end{aligned}$$

$$\begin{aligned} T(I,I-1) &= ((-R6/(2*H)) + (R7/(H*H))) \\ T(I,I) &= ((-2*R7/(H*H)) + R8) \\ T(I,I+1) &= ((R6/(2*H)) + (R7/(H*H))) \end{aligned}$$

ELSE IF (I.EQ.NINMAX) THEN

$$\begin{aligned} S(I,I-2) &= ((-R4/(2*(H**3))) + (R5/(H**4))) \\ S(I,I-1) &= ((-R2/(2*H)) + (R3/(H*H)) + (2*R4/(2*(H**3)))) \end{aligned}$$

```

$      -(4*R5/(H**4))
S(I,I) = (R1-(2*R3/(H*H))+(R4/(2*(H**3)))+(7*R5/(H**4)))

T(I,I-1) = ((-R6/(2*H))+(R7/(H*H)))
T(I,I) = ((-2*R7/(H*H))+R8)

```

ELSE

```

S(I,I-2) = ((-R4/(2*(H**3)))+(R5/(H**4)))
S(I,I-1) = ((-R2/(2*H))+(R3/(H*H))+(2*R4/(2*(H**3)))
$      -(4*R5/(H**4)))
S(I,I) = (R1-(2*R3/(H*H))+(6*R5/(H**4)))
S(I,I+1) = ((R2/(2*H))+(R3/(H*H))-(2*R4/(2*(H**3)))
$      -(4*R5/(H**4)))
S(I,I+2) = ((R4/(2*(H**3)))+(R5/(H**4)))

T(I,I-1) = ((-R6/(2*H))+(R7/(H*H)))
T(I,I) = ((-2*R7/(H*H))+R8)
T(I,I+1) = ((R6/(2*H))+(R7/(H*H)))

```

ENDIF

40 CONTINUE

C THE BOUNDARY CONDITIONS ARE ENTERED.

```

UX(1)=0.0
UX(NMAX)=(BLENG/1.0)
UY(1)=0.0
UY(NMAX)=0.0
ICOUNT=1
CALL PLOTS(0,0,50)
CALL PLOT(2.15,2.25,-3)

```

C THE COORDINATES OF THE STATIC FORM ARE STORED IN XA AND YA.

```

DO 50 I = 1,NMAX
  XA(I) = UX(I)
  YA(I) = UY(I)
50 CONTINUE

```

C THE EISPACK ROUTINE RGG [6] IS CALLED TO SOLVE THE
C CHARACTERISTIC EQUATION. IT RETURNS THE REAL PORTION OF THE
C NUMERATOR IN ALFR, AND THE DENOMINATOR IN BETA. ANY COMPLEX
C PORTION IS STORED IN ALFI. IF A COMPLEX PORTION IS RETURNED,
C THE PROGRAM TERMINATES. THE NORMALIZED EIGENVECTORS ARE STORED
C IN THE MATRIX Z.

```

MATZ=1
CALL RGG(NINMAX,NINMAX,S,T,ALFR,ALFI,BETA,MATZ,Z,IERR)
PRINT '(,2X,A,I10)', 'IERR = ', IERR
DO 250 I=1,NINMAX
  ALFR(I) = ALFR(I)/BETA(I)
  ALFI(I) = ALFI(I)/BETA(I)
  IR(I) = I
  IF (ALFI(I).NE.0) THEN
    PRINT '(2X,A)', ' ERROR! EIGENVALUES COMPLEX! PROGRAM ENDS'
    GOTO 888
  ENDIF
250 CONTINUE

```

C THE IMSL SUBROUTINE VSRTRD [14] ORDERS THE EIGENVALUES FROM
C SMALLEST TO LARGEST.

```

CALL VSRTRD(ALFR,NINMAX,IR)
PRINT '(,2X,A)', 'EIGENVALUES, FROM LOWEST TO HIGHEST'
DO 300 I=1,NINMAX
  PRINT '(2X,I3,4X,F16.6)', IR(I), ALFR(I)
300 CONTINUE
PRINT '(2X,A)', 'EIGENVECTORS (FIRST THROUGH FOURTH MODES)'
DO 400 I=1,NINMAX
  PRINT '(2X,4(F12.8,4X))', (Z(I,IR(J)), J=1,4)
400 CONTINUE

C   SINCE THE EIGENVECTORS ARE NORMALIZED, THEY MUST BE REDUCED BY
C   SOME FACTOR, SINCE THE NON-DIMENSIONALIZED COORDINATES ARE SMALL.
C   THE FOUR LOWEST MODES OF VIBRATION ARE CONSIDERED.

DO 600 J=1,4
  DO 450 I=1,NINMAX
    IF ((J.EQ.1).OR.(J.EQ.2)) THEN
      Z(I,IR(J))=Z(I,IR(J))/20.0D0
    ELSE
      Z(I,IR(J))=Z(I,IR(J))/50.0D0
    ENDIF
450  CONTINUE
  DO 460 I=1,50
    X(I)=0.0D0
    Y(I)=0.0D0
460  CONTINUE

C   THE EIGENVECTORS IN THEIR REDUCED FORM REPRESENT DISPLACEMENTS,
C   V, IN THE TANGENTIAL DIRECTION OF THE CROSS-SECTION. USING THE
C   RELATIONSHIP ( $W = A V$  (SUB S)), THE DISPLACEMENTS IN THE NORMAL
C   DIRECTION CAN BE FOUND. THEN, TRIGONOMETRY IS USED TO CONVERT
C   TANGENTIAL AND NORMAL DISPLACEMENTS INTO DISPLACEMENTS IN THE
C   X AND Y DIRECTIONS.

DO 500 I=1,NINMAX
  IF (I.EQ.1) THEN
    W(I)=AINVRS(I)*(Z((I+1),IR(J))/(2*H))
  ELSE IF (I.EQ.NINMAX) THEN
    W(I)=AINVRS(I)*(-Z((I-1),IR(J))/(2*H))
  ELSE
    W(I)=AINVRS(I)*((Z((I+1),IR(J))-Z((I-1),IR(J)))/(2*H))
  ENDIF

  X(I+1)=XA(I+1)+Z(I,IR(J))*DCOS(PHI(I))-W(I)*DSIN(PHI(I))
  Y(I+1)=YA(I+1)+Z(I,IR(J))*DSIN(PHI(I))+W(I)*DCOS(PHI(I))
500  CONTINUE
  X(1)=0.0D0
  X(NMAX)=BLENG
  Y(1)=0.0D0
  Y(NMAX)=0.0D0

C   THE X AND Y COORDINATES ARE PRINTED FOR THE DYNAMIC SHAPE FOR
C   EACH OF THE FIRST FOUR MODES. THE SUBROUTINE MODES IS CALLED
C   AND EACH OF THE MODES ARE PLOTTED, ALONG WITH THE STATIC SHAPE
C   AS A REFERENCE.

DO 530 I=1,NMAX
  PRINT '(2X,F16.10,4X,F16.10)', X(I), Y(I)
  SX(I) = XA(I)
  SY(I) = YA(I)
  UX(I) = X(I)
  UY(I) = Y(I)
530  CONTINUE

```

CALL MODES(UX,UY,SX,SY,NMAX,ICOUNT)

600 CONTINUE
CALL PLOT(12.,-2.,999)

888 STOP
END

SUBROUTINE MODES(X,Y,SX,SY,NP,ICOUNT)
DIMENSION X(*),Y(*),SX(*),SY(*)

CALL FACTOR(.4)
CALL NEWPEN(1)
X(NP+1) = 0.0
X(NP+2) = 0.1
XAP1 = X(NP+1)
XAP2 = X(NP+2)
Y(NP+1) = 0.0
Y(NP+2) = 0.1
YAP1 = Y(NP+1)
YAP2 = Y(NP+2)

C THE X AND Y AXES ARE PLOTTED FOR EACH OF THE FIRST FOUR MODE
C SHAPES. THE COORDINATES ARE SCALED TO FIT THE PLOTS.

IF (ICOUNT.EQ.1) THEN
CALL AXIS(0.,8.,1HX,-1,5.,0.,XAP1,XAP2)
CALL AXIS(-1.0,8.,1HY,1,5.,90.,YAP1,YAP2)
XSCAL = 10.0
YSCAL = 10.0
DO 10 I = 1,NP
X(I) = X(I)*XSCAL
Y(I) = Y(I)*YSCAL + 8.0
SX(I) = SX(I)*XSCAL
SY(I) = SY(I)*YSCAL + 8.0
10 CONTINUE
ELSE IF (ICOUNT.EQ.2) THEN
CALL AXIS(8.,8.,1HX,-1,5.,0.,XAP1,XAP2)
CALL AXIS(7.,8.,1HY,1,5.,90.,YAP1,YAP2)
XSCAL = 10.0
YSCAL = 10.0
DO 20 I = 1,NP
X(I) = X(I)*XSCAL + 8.0
Y(I) = Y(I)*YSCAL + 8.0
SX(I) = SX(I)*XSCAL + 8.0
SY(I) = SY(I)*YSCAL + 8.0
20 CONTINUE
ELSE IF (ICOUNT.EQ.3) THEN
CALL AXIS(0.,0.,1HX,-1,5.,0.,XAP1,XAP2)
CALL AXIS(-1.0,0.,1HY,1,5.,90.,YAP1,YAP2)
XSCAL = 10.0
YSCAL = 10.0
DO 30 I = 1,NP
X(I) = X(I)*XSCAL
Y(I) = Y(I)*YSCAL
SX(I) = SX(I)*XSCAL
SY(I) = SY(I)*YSCAL
30 CONTINUE
ELSE
CALL AXIS(8.,0.,1HX,-1,5.,0.,XAP1,XAP2)
CALL AXIS(7.,0.,1HY,1,5.,90.,YAP1,YAP2)
XSCAL = 10.0

```
YSCAL = 10.0
DO 40 I = 1, NP
  X(I) = X(I)*XSCAL + 8.0
  Y(I) = Y(I)*YSCAL
  SX(I) = SX(I)*XSCAL + 8.0
  SY(I) = SY(I)*YSCAL
40 CONTINUE
ENDIF
```

C THE STATIC SHAPE OF THE DAM IS PLOTTED.

```
CALL NEWPEN(3)
CALL PLOT(SX(1),SY(1),3)
DO 50 I = 2, NP
  CALL PLOT(SX(I),SY(I),2)
50 CONTINUE
```

C THE MODE SHAPE IS PLOTTED.

```
CALL NEWPEN(1)
CALL PLOT(X(1),Y(1),3)
DO 60 I = 2, NP
  CALL PLOT(X(I),Y(I),2)
60 CONTINUE
```

```
CALL FACTOR(1.)
ICOUNT = ICOUNT + 1
```

```
RETURN
END
```

The vita has been removed
from the scanned document